NACA TN 3459

NATIONAL ADVISORY COMMITTEE FOR AERONAUTICS

TECHNICAL NOTE 3459

JUN 27 1955

SIMPLIFIED PROCEDURES AND CHARTS FOR THE RAPID ESTIMATION

OF BENDING FREQUENCIES OF ROTATING BEAMS

By Robert T. Yntema

Langley Aeronautical Laboratory
Langley Field, Va.

NACA

Washington

June 1955

P

CONTENTS

NATIONAL ADVISORY COMMITTEE FOR AERONAUTICS

TECHNICAL NOTE 3459

SIMPLIFIED PROCEDURES AND CHARTS FOR THE RAPID ESTIMATION

OF BENDING FREQUENCIES OF ROTATING BEAMS[1]

By Robert T. Yntema

SUMMARY

A Rayleigh energy approach utilizing the bending mode of the nonrotating beam in the determination of the bending frequency of the rotating beam is evaluated and is found to give good practical results for helicopter blades.

Charts are presented for the rapid estimation of the first three bending frequencies for rotating and nonrotating cantilever and hinged beams with variable mass and stiffness distributions, as well as with root offsets from the axis of rotation. Some attention is also given to the case of rotating beams with a tip mass.

A more exact mode-expansion method used in evaluating the Rayleigh approach is also described. Numerous mode shapes and derivatives obtained in conjunction with the frequency calculations are presented in tabular form.

INTRODUCTION

Designers of helicopter rotor blades generally agree that accurate means are needed for estimating the natural bending frequencies of the rotating blades in order to obtain a blade design which is as free as possible from resonant or near-resonant excitation by the periodic loading on the rotor. Although numerous methods are available for determining the bending frequencies of rotating blades (see, for example, refs. 1 to 14), designers have expressed the need for a simplified, yet reasonably accurate, procedure for their determination, preferably in the form of a set of charts. With this need in mind, an investigation was undertaken which had a twofold purpose: (a) an evaluation to show whether a Rayleigh energy approach utilizing the mode shape of the nonrotating beam may be employed to obtain close approximations for the natural bending frequencies of the rotating beam and (b) a set of charts

---

[1]An amplified and extended version of NACA RM L54G02, 1954.

which would permit the rapid estimation of the first three bending frequencies of both nonrotating and rotating hinged and cantilever blades. The main purpose of this report is to present this evaluation and the frequency charts.

The Rayleigh energy approach was evaluated with respect to such items as various rotational speeds, higher modes, flapping-hinge or root offset, variable blade mass and stiffness distributions, and a large concentrated tip mass. The evaluation was made by comparing frequency results obtained by the Rayleigh method with results obtained by a more accurate mode-expansion method. The details of the mode-expansion method are given in appendix A.

The charts for frequency estimation were obtained by considering various families of beams with selected mass and stiffness distributions and were derived for both hinged and cantilever beams. The frequencies of both nonrotating and rotating cases may be estimated for (a) beams with and without offset which have mass and stiffness distributions which can be approximated by linear relations and (b) beams with uniform mass and stiffness distributions plus a concentrated mass at the tip.

If the bending frequencies of the nonrotating beams are known, a third set of charts permits the estimation of the bending frequencies of rotating beams with approximately linear stiffness distribution and arbitrary mass distribution.

As an adjunct to the Rayleigh approach utilizing the nonrotating-beam mode shapes, a method is presented in appendix B which permits a fairly accurate determination of the first bending mode and frequency of a rotating or nonrotating hinged beam with a tip mass from a knowledge of the first bending mode of the nonrotating beam without a tip mass.

The report also presents bending-mode results, obtained in conjunction with the frequency determination, which show the effect of the parameters on mode shape. Many of these mode shapes are tabulated in normalized form together with their first and second derivatives, or as mode coefficients (coefficients of an expansion in terms of uniform-beam modes). These results can be used in connection with the modified approach of appendix B or in other analyses.

In order to facilitate the further application of the mode-expansion method to the accurate determination of modes and frequencies of rotating beams with linear mass and stiffness distributions, concentrated tip mass, and offset different from those considered herein, certain integrals which have been evaluated are also presented in tabular form.

SYMBOLS

A_{n_q} mode coefficients for the nth rotating-beam mode (see eq. (A3))

a nonrotating-beam bending frequency coefficient, $\omega_{NR}\sqrt{\dfrac{m_o L^4}{EI_o}}$

b rotating-beam bending frequency coefficient, $\omega_R\sqrt{\dfrac{m_o L^4}{EI_o}}$

c beam-stiffness-distribution constant (see eq. (A12))

D_0 pendulum- or zeroeth-mode coefficient (see appendix B)

$EI(x)$ lengthwise bending stiffness distribution for beam

EI_o bending stiffness of beam at root

$\overline{EI}(\bar{x})$ nondimensional bending stiffness distribution for beam, $EI(\bar{x})/EI_o$

K Southwell coefficient (see eqs. (4) and (5))

K_0 zero-offset Southwell coefficient

K_1 offset-correction factor for Southwell coefficient

$K_0{}'$ zero-offset rotating-beam frequency coefficient; found to be essentially independent of beam mass distribution (see eq. (11))

k beam-mass-distribution constant (see eq. (A12))

L beam length, measured from point of root fixity to tip

$m(x)$ lengthwise mass distribution for beam (mass per unit length)

m_o mass per unit length of beam at root

$\bar{m}(\bar{x})$ nondimensional mass distribution for beam, $m(\bar{x})/m_o$

m_d part of beam mass distribution which is continuous (not concentrated)

M_t mass concentrated at tip of beam

r   nondimensional tip-mass ratio, $M_t / m_o L$

T   lengthwise distribution of tension force in beam, $T_1(x)\Omega^2$

T_1 lengthwise-distribution function for tension force
                               (see eq. (2))

x   spanwise coordinate along beam measured from root

$\bar{x}$ nondimensional spanwise coordinate, x/L

Y   bending mode shape of nonrotating beam

y   bending mode shape of rotating beam

$\delta(x-L)$ Dirac delta function

$\delta(\bar{x}-1)$ Dirac delta function in nondimensional coordinates

e   offset of hinge or point of fixity from axis of rotation

$\bar{e}$ nondimensional offset, e/L

$\eta, \bar{\eta}$ dummy variables for x and $\bar{x}$

θ characteristic number for nonrotating uniform beam with
                               mass at tip; identical to square root of nonrotating-
                               beam bending frequency coefficient

ϕ bending mode shape for nonrotating uniform beam normalized
                               at tip

Ω rotational speed of beam

ω_R natural bending frequency of rotating beam

ω_{NR} natural bending frequency of nonrotating beam

Subscripts:

n   integral number designating natural bending mode of beam

F   beam cantilevered or fixed at root

t   tip of beam

    Primes mean differentiation with respect to x or $\bar{x}$ unless
indicated otherwise.

THE RAYLEIGH APPROACH APPLIED TO A ROTATING BEAM

Description

The problem being treated in this report is a rotating beam vibrating freely in one of its natural bending modes. By equating the kinetic energy at zero displacement to the potential energy of both the bending and centrifugal forces at maximum displacement, the following frequency equation for vibration perpendicular to the plane of rotation can easily be derived:

$$\omega_{R_n}^2 = \frac{\int_0^L EI y_n''^2 dx}{\int_0^L m y_n^2 dx} + \frac{\int_0^L T_1 y_n'^2 dx}{\int_0^L m y_n^2 dx} \Omega^2 \tag{1}$$

where n refers to the mode under consideration and

$$T_1 = \int_x^L (\eta + e) m \, d\eta \tag{2}$$

Equation (1) yields an exact value for the nth bending frequency of a beam rotating at any rotational speed Ω if the nth natural bending mode shape of the rotating beam is known for this value of Ω. Unfortunately, the mode shape is usually just as much of an unknown as the frequency is. An estimation of the frequency may be made, however, by making use of the well-known Rayleigh principle; that is, a mode shape which is consistent with the constraints of the system is assumed and is used to evaluate the energy integrals which, in turn, give an approximate value for the frequency. In this report the nonrotating-beam mode shape is chosen as the approximation for the rotating-beam mode shape, and an evaluation is made to show whether the use of such a shape yields close approximations to the exact frequencies of the rotating beam.

If the nth mode shape of the nonrotating beam Y_n is substituted into equation (1), the first term becomes exactly the square of the bending frequency of the nonrotating beam. By denoting the ratio in the second term by K_n, a Southwell coefficient, the frequency equation takes the following simplified form:

$$\omega_{R_n}^2 = \omega_{NR_n}^2 + K_n \Omega^2 \tag{3}$$

where

$$K_n = \frac{\int_0^L Y_n'^2 dx \int_x^L (\eta + e)m \, d\eta}{\int_0^L mY_n^2 dx} \qquad (4)$$

This expression for K_n can be subdivided into two independent parts as follows:

$$K_n = K_{0_n} + K_{1_n} e \qquad (5)$$

where both K_{0_n} and K_{1_n} are independent of the offset e and are defined as follows:

$$\left. \begin{aligned} K_{0_n} &= \frac{\int_0^L Y_n'^2 dx \int_x^L \eta m \, d\eta}{\int_0^L mY_n^2 dx} \\[3em] K_{1_n} &= \frac{\int_0^L Y_n'^2 dx \int_x^L m \, d\eta}{\int_0^L mY_n^2 dx} \end{aligned} \right\} \qquad (6)$$

In the remainder of this report K_{0_n} is referred to as the zero-offset Southwell coefficient and K_{1_n} is referred to as the offset-correction factor for the Southwell coefficient.

It is convenient to write $\omega_{NR_n}^2$ in terms of a nonrotating-beam frequency coefficient a_n and the mass and stiffness of the beam at the root as

$$\omega_{NR_n}^2 = a_n^2 \frac{EI_o}{m_o L^4} \tag{7}$$

By means of equations (5) and (7), equation (3) may be written as

$$\omega_{R_n}^2 = a_n^2 \frac{EI_o}{m_o L^4} + \left(K_{O_n} + K_{1_n} e \right) \Omega^2 \tag{8}$$

Equation (8) with K_{O_n}, K_{1_n}, and e in nondimensional form serves as the basis for the charts for rapid frequency estimation to be presented subsequently in this report. These charts provide values of a_n, K_{O_n}, and K_{1_n} which, in conjunction with the mass and stiffness of the beam at the root, the length of the beam, the hinge offset, and the rotational speed, permit rapid estimation of the first three bending frequencies of rotating or nonrotating beams.

If the mass distribution of the blade is given by a simple analytic function, the integral expression for T_1 (eq. (2)) can usually be evaluated exactly; for arbitrary mass distribution, however, numerical-integration methods such as are given in reference 15 must be employed. Because of the nature of the numerical-integration procedure used in the present paper, a slightly different form of the expression for K_n was found to be useful. This form can be obtained by performing an integration by parts on the numerator of equation (4), and in nondimensional form the result appears as

$$\bar{K}_n = \frac{\displaystyle\int_0^1 (\bar{x} + \bar{e}) \bar{m} \, d\bar{x} \int_0^{\bar{x}} Y_n'^2 \, d\bar{\eta}}{\displaystyle\int_0^1 \bar{m} Y_n^2 \, d\bar{x}} \tag{9}$$

whence the definitions for $\bar{K}_{O_n}$ and $\bar{K}_{1_n}$ are evident.

An additional form of equation (3) is now presented for use in subsequent sections of this report. Dividing equation (3) by $\omega_{NR_n}^2$ yields

the expansion; for the hinged beams, a pendulum mode was included in addition to five hinged-beam bending modes.

The cases studied by both methods are shown in figure 1. Both cantilever and hinged beams are considered for the following cases:

(a) Uniform beams with 0- and 10-percent root offset

(b) Beams with mass and stiffness distributions varying linearly from the root value to zero at the tip and with 0- and 10-percent root offset

(c) Uniform beams with a mass at the tip.

The results for all the cases treated were obtained in nondimensional form and are presented in plots in which the variation of bending frequencies with rotational speed as predicted by the exact method of appendix A and by the Rayleigh approach may be compared. In each of the figures introduced in this section the abscissa is the squared nondimensional rotational-speed parameter (the squared ratio of rotational speed to the first bending frequency of the nonrotating beam) and the ordinate is the squared nondimensional frequency parameter (the squared ratio of the nth bending frequency of the rotating beam to the nth bending frequency of the nonrotating beam).

The range of the rotational-speed parameter in each case corresponds roughly to that encountered in current helicopters with some latitude for new design. Since the first bending frequency of a hinged beam is roughly four times the first bending frequency of the same beam fixed at the root, widely different scales result for the hinged and cantilever beams. The abscissa range also varied with tip mass because the fundamental frequency of a nonrotating beam decreases with increase in tip mass. For the uniform cantilever beam with a tip mass, this variation is large and thus results in a greatly expanded abscissa scale with each increase in tip mass. For the uniform hinged beam with a tip mass, the effect of tip mass on the nonrotating frequency is relatively small and thus the abscissa range was not extended appreciably with each increase in tip mass.

Hinged beams without tip mass.- The variation of bending frequency with rotational speed for a uniform hinged beam is shown in figure 2 for offsets of 0 and 10 percent. For this case the Rayleigh approach may be seen to be very accurate for all three modes throughout the entire rotational-speed range covered. The maximum error is about 3 percent in the frequency squared and thus only about $1\frac{1}{2}$ percent in the frequency.

This maximum error occurs at the highest rotational speed and is roughly the same for all three modes.

Frequency results for the hinged beams with linear mass and stiffness distributions are shown in figure 3 for offsets of 0 and 10 percent. From this figure it is evident that the results obtained by the Rayleigh method for this case are very accurate, even for the highest rotational speeds shown.

A comparison of the exact frequency results for the uniform and "linear" hinged beams is presented in figure 4 for the case of zero offset. The difference between the results for the two beams is very marked, particularly for the first mode. One of the most important things to be noted in this comparison is the large difference in slope between the two curves for the first mode. The average slope of each of these lines is directly proportional to the Southwell coefficient for the first mode (see eq. (10)), and the large difference in slope indicates that a single value of this coefficient could not adequately predict the first-mode-frequency variations for both beams. This result contradicts the often made assumption that the Southwell coefficient is largely independent of beam mass and stiffness distribution.

For the higher modes the slope of each of the lines (fig. 4) is also proportional to the Southwell coefficient, but unfortunately each beam has a different constant of proportionality. Thus, it cannot be observed directly from this figure that the Southwell coefficient for the higher modes also varies appreciably with beam characteristics; this fact, however, is evident from the charts for frequency determination to be presented subsequently.

Cantilever beams without tip mass.- The frequency of rotating cantilever beams as well as of hinged beams is of interest in the analysis of a teetering rotor because both symmetrical (cantilever) modes and anti-symmetrical (hinged) modes may be excited. Consequently, in the following paragraphs the Rayleigh approach employed in the present report is evaluated for cantilever beams.

Frequency results for uniform cantilever beams are presented in figure 5. The Rayleigh results are in good agreement with the more exact results for the second and third modes. For the first mode, however, the maximum error is somewhat larger, about 5 percent in the frequency. Nevertheless, the effect of offset on the frequency variation is predicted fairly accurately for all three modes.

For comparison, the results of approximating the first cantilever mode by the pendulum mode of a hinged beam are also given in figure 5. Frequency results based on this shape are seen to be always less than the exact values. As the rotational-speed parameter increases, these results become more and more accurate; for the lower rotational speeds, however, the use of the nonrotating-beam first mode shape yields the most accurate results. The effects of root offset on frequency are predicted by the use of either the pendulum mode or the first cantilever bending mode.

The variation of bending frequency with rotational speed is shown in figure 6 for a cantilever beam with linear mass and stiffness distribution and with offsets of 0 and 10 percent. As is the case for the uniform cantilever, the Rayleigh frequency results, based on the nonrotating-beam cantilever mode, are very accurate for the second and third modes, but are not so accurate for the first mode at the higher values of the rotational-speed parameter; however, the effect of the offset is again predicted fairly accurately.

The Rayleigh results based on a pendulum mode, which are also shown in figure 6, are again seen to be always less than the exact values and to increase in accuracy as the rotational-speed parameter increases. At the lower rotational speeds, however, these results are again appreciably less accurate than those based on the first cantilever bending mode shape. As was the case for the uniform beam, both the pendulum mode and the first cantilever mode predict the effects of the offset equally well.

A comparison of the frequency results for the uniform and "linear" cantilever beams with zero offset is given in figure 7. From the figure it is evident that there is only a small difference in the slope of the exact first-mode frequency curves and thus in the Southwell coefficient for the two beams. This small difference, however, is predicted, although not too accurately, by the Rayleigh approach based on the nonrotating-beam mode shape; whereas, if a pendulum-mode approximation had been used, no difference could have been predicted.

For the higher modes, the effects of mass and stiffness distribution on frequency are more pronounced and lead again to the conclusion that, in general, a single value of the Southwell coefficient cannot accurately predict the frequency variations for beams with appreciably different mass and stiffness distributions.

The error in the first-mode-frequency results obtained by the Rayleigh approach (fig. 7) is almost the same for both beams. Thus, this error apparently is independent of beam mass and stiffness distribution; this observation suggests the possibility of applying a correction, based on the known errors for these particular beams, to the Rayleigh results obtained for cantilever beams with other mass and stiffness distributions.

Cantilever beams with tip mass.- For beams with a mass at the tip, the results for the cantilever case suggest certain simplifications which may be carried over to the hinged beams; thus the cantilever results are discussed first.

The variation of bending frequency with rotational speed for a uniform cantilever beam with a concentrated mass at the tip and zero offset

is given in figure 8. Results are presented for two cases: tip mass
equal to the beam mass and tip mass equal to one-half the beam mass.
Figure 8 shows that the Rayleigh results are of the same order of accu-
racy as for the beam without tip mass - very accurate for the second and
third modes but relatively less accurate for the first mode.

It is of interest to note that for each mode the variation of the
frequency parameter with the rotational-speed parameter is almost identi-
cal for the two values of tip mass considered. In fact, if these results
are compared with those for the beam with zero tip mass in figure 5, the
variation for all three cases is seen to be practically identical.

The foregoing observations create the impression that the zero-
offset Southwell coefficient for each mode is independent of the value
of the tip mass. This assumption is true for the first mode but is mis-
leading for the higher modes as is evident from equation (10) where it
can be seen that a constant of proportionality $\left(\omega_{NR_1} \big/ \omega_{NR_n}\right)^2$, which varies
with tip mass, is involved. Nonetheless, inasmuch as this constant of
proportionality is defined by a ratio of nonrotating-beam frequencies, a
new rotating-beam frequency coefficient, or modified Southwell coeffi-
cient $K_{O_n}{}'$ can be defined (see eq. (11)) which is essentially indepen-
dent of tip mass and, as will be shown subsequently, of beam mass distri-
bution as well.

Hinged beams with tip mass.- The variation of bending frequency with
rotational speed for a uniform hinged beam with a concentrated mass at
its tip and zero offset is given in figure 9. Results are given for two
cases: tip mass equal to beam mass and tip mass equal to one-half the
beam mass. The Rayleigh results are very accurate for all three modes
over the entire range of variables investigated, and it may be inferred,
particularly for the first mode, that the Rayleigh procedure will yield
reasonably accurate results for appreciably larger values of the
rotational-speed parameter and tip mass.

From figure 9 the frequency variation can readily be seen to be con-
siderably different for the two values of tip mass, unlike the cantilever
results of figure 8, for which the frequency variation is essentially
independent of tip mass. In an attempt to explain this difference between
the two cases, the results of figure 9 were replotted in figure 10 as a
function of the rotational-speed parameter used for the cantilever cases,
that is, the squared ratio of rotational speed to the bending frequency
of the beam in the first cantilever mode. From figure 10 the frequency
variation with this rotational-speed parameter may be seen to be essen-
tially independent of tip mass, as was noted for the cantilever. Conse-
quently, a new constant which is insensitive to the mass distribution of
the beam is suggested. For hinged beams this constant is also defined by
equation (11). The invariance of this constant with beam mass distribu-
tion is discussed subsequently in this report.

Rotating and Nonrotating Beams Without Tip Mass

In order to provide a means for the rapid, yet reasonably accurate, estimation of rotor-blade bending frequencies, nonrotating-beam frequency coefficients, zero-offset Southwell coefficients, and offset-correction factors for the Southwell coefficients have been computed for a series of beams with linear mass and stiffness distributions and have been compiled in chart form. The range of mass and stiffness distributions was selected to encompass variations found in currently manufactured blades with some latitude for new design. All the constants are based on the mode shapes of the nonrotating beam, which were obtained by standard numerical-iteration procedures. (See section entitled "Results for Bending Modes" for more details regarding these procedures.)

The form of the Rayleigh energy equation which is used in conjunction with the charts to obtain bending frequencies is equation (8) with K_{O_n}, K_{1_n}, and e in nondimensional form:

$$\omega_{R_n}^2 = a_n^2 \frac{EI_o}{m_o L^4} + \left(\bar{K}_{O_n} + \bar{K}_{1_n} \bar{e} \right) \Omega^2 \qquad (12)$$

where $\bar{K}_{O_n} = K_{O_n}$ and $\bar{K}_{1_n} = K_{1_n} L$. The charts for frequency determination are presented in figures 11 to 16. In each chart, the abscissa is the ratio of the beam mass per unit length at the tip of the beam to the mass per unit length at the root; 1.0 represents a constant-mass beam and 0 a beam in which the mass varies linearly to zero at the tip. Curves are presented for three different stiffness variations: the solid curves for beams with constant stiffness, the long-dash curves for beams where the stiffness drops linearly to half the root value at the tip, and the long-dash, short-dash curves for beams which have zero stiffness at the tip.

Each of these curves is faired through only three points, one at each end and one at the middle; for the Southwell coefficients and offset-correction factors, this procedure should involve little error because, in most cases, the variation is nearly linear, but for the frequency coefficients the fairing may appear to be questionable. However, the fairing of these curves was not entirely arbitrary. The fundamental bending frequency of cantilever beams with linear mass and stiffness distributions is given in reference 16 for cases in which the mass and stiffness variations are proportional, that is, where

$$\frac{EI_t}{EI_o} = \frac{m_t}{m_o}$$

Two of the cases considered in this reference, namely, the ones where both ratios equal 0 and 1, are identical to cases treated in this report and the results for these are in good agreement. The other cases treated in reference 16, namely, those for which this ratio is 0.2, 0.4, and 0.6, were used in fairing the curves of a_1 for the cantilever case. The other curves for the frequency coefficient for cantilever and hinged beams were then faired by using this first set of curves as a guide.

Charts which permit the rapid estimation of nonrotating-beam frequency coefficients, zero-offset Southwell coefficients, and offset-correction factors for the Southwell coefficients are presented in figures 11 to 13 for beams hinged at the root and in figures 14 to 16 for beams fixed at the root.

Since the zero-offset Southwell coefficient for the pendulum mode is always unity regardless of the mass and stiffness distribution of the beam, it is not included in figure 12. However, the offset-correction factor for this mode is not independent of mass distribution but is independent of stiffness distribution, as indicated in figure 13. The pendulum-mode results in figure 13 are also given in reference 4.

As was mentioned in the section of this report entitled "Evaluation of Rayleigh Approach," the zero-offset Southwell coefficients for the first cantilever mode (given in fig. 15) will yield accurate rotational frequencies only at relatively low values of the rotational-speed parameter and must be corrected in accordance with the results of figure 5 or 6 at higher values of this parameter. A fixed-percentage correction cannot be given because the error is a function of the rotational-speed parameter.

The effect of root fixity on the Southwell coefficients can be noted by comparing the curves of figure 12 with those of figure 15. The first-mode results for the cantilever beams should be compared with the pendulum-mode Southwell coefficient for the hinged beam which is always unity for the case of zero offset. Likewise, the second-mode curves of figure 15 should be compared with the first-mode curves of figure 12, and so forth for the higher modes. From this comparison it is seen that the effects of root fixity on the Southwell coefficients are fairly small and can probably be neglected for rough approximations in all cases, except for the first cantilever mode. With this assumption, the results of figure 12 for the third bending mode can be used as reasonable approximations for the fourth cantilever mode.

The variation of the Southwell coefficient may be seen from figures 12, 13, 15, and 16 to be relatively insensitive to beam stiffness distribution, particularly for cantilever beams but also for the hinged beams. This observation, coupled with the facts that frequency is proportional to the square root of the Southwell coefficient and that the influence of the Southwell coefficient decreases for higher modes (for constant rotational

speed), leads to the conclusion that fairly good approximations to the
Southwell coefficients for beams with other than linear stiffness distri-
butions may also be obtainable from this set of charts. The examples
presented in the following section appear to bear out this conclusion.

Application of charts to several actual helicopter blades.- To illus-
trate the use and the type of accuracy which can be expected from the
frequency charts of figures 11 to 16 and to demonstrate that the charts
work well even when the mass and stiffness distributions of the beams are
not exactly linear, bending frequencies have been estimated for the first
three modes of four existing helicopter blades, all of which are hinged.
The following procedure, which may be made clearer by reference to the
sketches in table I, was used in the estimation:

(a) Straight lines were faired through the mass and stiffness dis-
tributions for the blade; large values near the root were ignored.

(b) From these fairings, the effective root values m_0 and EI_0
and the necessary tip-root ratios were obtained.

(c) By using these ratios, values of a_n, K_0, and $\bar{K}_1$ were
obtained from the appropriate charts (figs. 11 to 16).

(d) Substitution of these constants and $\bar{e}$ into the Rayleigh equa-
tion (eq. (12)) yielded the bending frequencies at zero and the rated rotor
speed.

The mass and stiffness distributions for the blades considered are
shown on the left side of table I. The actual distribution is given by
the solid lines, and the linear approximation, selected to represent this
variation, is given by the dashed lines. These linear approximations
used in estimating the frequencies were the initial ones selected, and
no attempt was made to improve them in order to obtain the best agreement
for all modes. The frequencies shown as "exact" in table I are values
furnished by the manufacturer.

A comparison of the exact and estimated results given in table I for
these blades indicates that the estimated results are very accurate when
the crudeness of the linear approximations used is considered.

Although no comparisons have been made for cantilever blades because
sufficient information regarding such blades was not available, even more
accurate results should be obtainable for this end condition since large
values of root stiffness can be taken into account more accurately by con-
sidering the blade to be cantilevered at the outboard edge of the stiff
region and then using the offset-correction factor for the Southwell
coefficients.

Beams With a Mass at the Tip

Uniform cantilever beam.- Expressions defining the bending frequencies and mode shapes of nonrotating uniform cantilever beams with a tip mass equal to a fraction r of the beam mass are given in reference 17. These expressions, in somewhat simpler form, are the following: the defining relation for the frequencies is

$$1 + \cos \theta \cosh \theta - r\theta(\sin \theta \cosh \theta - \cos \theta \sinh \theta) = 0 \qquad (13)$$

where

$$\omega_{NR_n} = \theta_n^2 \sqrt{\frac{EI}{mL^4}}$$

and the mode shapes are

$$y_n(x) = \sinh x - \sin x + (\cos x - \cosh x)\frac{\sinh \theta_n + \sin \theta_n}{\cosh \theta_n + \cos \theta_n} \qquad (14)$$

In addition to the defining relation for the frequency, reference 17 also gives values of θ_n for the first three modes of cantilevers and for several values of r. Some of these results, which are pertinent to helicopter blades, are plotted in figure 17. Values of θ_n^2 rather than θ_n are plotted, because θ_n^2 is directly proportional to frequency and corresponds to the nonrotating frequency coefficients a_n presented previously.

For larger values of r fairly accurate values of θ_n^2 can be obtained from the following approximate expression:

$$\theta_n^2 \approx \left(\theta_n^2\right)_{r=0} \sqrt{\frac{1}{1 + \kappa_n r}} \qquad (15)$$

where κ_n is a constant for each mode which can be determined from the frequency results for the largest value of r - in this case, 2. Equation (15) can also be used for nonuniform beams and for hinged as well as cantilever beams.

The variation of the Southwell zero-offset coefficient with tip mass is given in figure 18 for the first three modes of a uniform cantilever beam. These results were computed by using the mode shape of the nonrotating beam presented in equation (14); the integrations were performed analytically. Although only three points were used to establish each curve of figure 18, the fairing should be quite accurate since the variations shown are almost linear.

The Southwell coefficients of figure 18, in conjunction with the nonrotating-beam frequency coefficients of figure 17, should permit very accurate estimates for the bending frequencies of rotating uniform beams with a tip mass except possibly for the first mode, for which a correction may be made in accordance with results given in figure 8 for large values of the rotational-speed parameter.

The effect of root offset has not been studied for this case, but offset-correction factors can be obtained from the mode shapes defined by equation (14).

Uniform hinged beam.- By using the method of reference 17, expressions defining the bending frequencies and mode shapes of nonrotating uniform hinged beams with a mass at the tip have been determined. The defining relation for the frequency is

$$2r\theta + \coth \theta - \cot \theta = 0 \tag{16}$$

and the mode shapes are given by

$$y_n(x) = \sinh x + \frac{\sinh \theta_n}{\sin \theta_n} \sin x \tag{17}$$

Values of θ_n have been determined for several values of r; these results are given in figure 19 as frequency coefficients θ_n^2, together with the frequency coefficients for the case of zero tip mass.

By using the nonrotating-beam mode shape, given by equation (17), values for the zero-offset Southwell coefficient have been determined for hinged beams with a tip mass and are given in figure 20. For the pendulum mode, K_0 is always unity and therefore is not shown. The results in figures 19 and 20 together permit the rapid estimation of the bending frequencies of rotating uniform hinged beams with a mass at the tip.

Pendulum-mode results for hinged beams with linear mass distribu-
tions.- The zero-offset Southwell coefficient for the pendulum mode of
a hinged beam is equal to unity, regardless of the mass or stiffness
distribution of the beam. For the case of hinge offset, however, the
Southwell coefficient is independent of stiffness distribution but varies
considerably with beam mass distribution and with the tip mass. A chart
(see fig. 21) has been prepared which permits the rapid estimation of the
offset-correction factor to the Southwell coefficient for hinged beams
with an approximately linear mass distribution plus a mass at the tip.

First bending mode frequency of nonuniform hinged beam.- A simple
method is indicated in appendix B for obtaining an approximate first
mode shape for any beam with a tip mass from a knowledge of the beam
mode shape without a tip mass. Once such a shape is determined, the
fundamental bending frequencies of the rotating and nonrotating beams
can be determined very easily by application of the Rayleigh frequency
equation (eq. (1)).

Rotating Beams With Nonlinear Mass Distribution and

Approximately Linear Stiffness Distribution

In the section of this report concerned with the evaluation of the
Rayleigh approach, a modified form of the zero-offset Southwell coeffi-
cient K_{O_n}' was shown to be insensitive to variations in beam tip mass.
This coefficient is defined for both cantilever and hinged beams by equa-
tion (11).

In order to determine whether this new coefficient is also insensi-
tive to other variations in beam mass distribution, all values of K_{O_n}
presented in the charts for rapid frequency estimation were converted to
K_{O_n}'. For each stiffness distribution K_{O_n}' was found to be almost con-
stant for each mode, the differences being of the same order of magnitude
as the errors inherent in the Rayleigh approach used herein.

To facilitate the estimation of bending frequencies for rotating
beams with large tip masses or possibly other nonlinear mass distribu-
tions, values of K_{O_n}' for all the beams treated in the present report
are plotted in figure 22(a) for cantilever beams and in figure 22(b) for
hinged beams. Curves have been faired through the points to give average
values for K_{O_n}' and thus for K_{O_n} for beams with approximately linear
stiffness distributions and with any mass distribution. In analyzing

these results, the facts that frequency is a function of the square root of K_{O_n} and that the influence of K_{O_n} on frequency decreases with increase in mode number should be kept in mind.

From equation (11) it is apparent that the first bending frequency of the nonrotating beam cantilevered at the root and the nth bending frequency of the nonrotating beam with its actual end fixity are required to determine K_{O_n} (and thus the bending frequency of the rotating beam) from a knowledge of K_{O_n}'. In spite of this complication, however, the charts presented should be useful in design studies involving rotating beams with nonlinear mass distributions but with approximately linear stiffness distributions. It should be emphasized at this point that the constancy of K_{O_n}' has been demonstrated for only a limited variety of mass distributions, and thus application to blades having mass distributions radically different from those considered in this report should be made with caution.

<p style="text-align:center">Rotating Beams With Mass and Stiffness Distributions</p>

<p style="text-align:center">Not Representable by Foregoing Approximations</p>

The charts presented in this report permit the rapid estimation of bending frequencies for rotating beams with a mass and stiffness distribution each of which can be reasonably approximated by a straight line and for uniform beams with a tip mass; also the charts facilitate the estimation of bending frequencies for rotating beams with fairly arbitrary mass distributions and approximately linear stiffness distributions. For other cases, for example, beams in which the stiffness varies irregularly all along the blade, the basic Rayleigh energy method utilizing the modes of the nonrotating beam may be used. Although this method has been evaluated in this report only for linear distributions of mass and stiffness and concentrated tip mass, there is no reason to believe that it will not work equally well for other distributions. All that is required in this approach is the frequency and mode of the nonrotating beam, which can be determined by methods such as are described in references 2 and 15. (A method which gives directly the required first derivative of the mode as well as the mode shape itself is preferable.) With such results the integrals of equation (1) can be evaluated readily by accurate numerical methods such as those of reference 15, and values can be obtained for the Southwell coefficient from which the bending frequencies at any rotational speed can be determined with little effort.

Mode-Expansion Method

A more accurate mode-expansion method for determining the bending frequencies and modes of a rotating or nonrotating beam has been developed in appendix B and has been used as a yardstick in the evaluation of the Rayleigh approach. In this approach the lowest three bending modes and frequencies are obtained by the solution of a fifth-order determinantal equation for cantilever beams and a sixth-order equation for hinged beams. In order to facilitate the further application of this method to the accurate determination of the modes and frequencies of rotating and nonrotating beams, certain integrals which have been evaluated are presented in table II. These results permit the setting up of frequency determinants for beams with any combination of linear mass and stiffness distribution, concentrated tip mass, offset, and rotational speed (including many combinations not treated herein). With the evaluation of additional integrals (some of which are given in ref. 18), these results can be used to determine the bending frequencies and modes for rotating and nonrotating beams with concentrated mass at other locations or with higher order mass and stiffness distributions. If practice dictates the necessity of additional charts for other combinations of linear mass and stiffness distribution and tip mass or for parabolic beam mass and stiffness distributions, it might be advantageous to use this method to set up such charts if high-speed computing machines suitable for solving the determinantal equations are available.

Vibration in Planes Other Than Those Perpendicular

to Plane of Rotation

The frequency charts and procedures for frequency determination of this report have all been directed toward the determination of frequencies for uncoupled bending vibrations perpendicular to the plane of rotation. In cases where the principal axis of the blade cross sections (axis about which the stiffness is a minimum) is not parallel to the plane of rotation, natural bending vibrations having the lowest frequency will take place perpendicular to the chord. An extreme case of such vibrations would occur if the blade chord were perpendicular to the plane of rotation, in which case, blade vibrations would take place in the plane of rotation.

Frequencies of vibration, when the blade chord is inclined at any angle ψ with the plane of rotation, can be determined from the frequencies of vibration perpendicular to the plane of rotation by means of a simple formula proposed in reference 19: namely,

$$\omega_{R_\psi}{}^2 = \omega_{R_L}{}^2 - \Omega^2 \sin^2 \psi$$

where ω_{R_L} is the frequency of bending vibrations perpendicular to the plane of rotation and ω_{R_ψ} is the frequency for bending vibrations in a plane making an angle ψ with the axis of rotation.

At large angles of attack, the indicated correction may be significant for the lower modes. However, inasmuch as $\omega_{R_L}^2$ is usually 5 to 10 times as large as Ω^2 for the lowest bending mode of helicopter blades and even larger for the higher modes, in most cases the angle of attack of the blade will have little effect on bending frequency and may be disregarded. This fact is significant since it indicates that blade frequency will not change appreciably during each revolution because of cyclic-pitch changes and thus may be assumed to be constant.

RESULTS FOR BENDING MODES

In the process of obtaining the frequency results presented in the preceding sections of this paper, a large number of mode shapes of both rotating and nonrotating beams with various mass and stiffness distributions were determined. These results are presented in tabular form in order to make them more useful in analytical studies and are compared in this section with each other in order to show the effect of the various parameters on mode shape.

Nonrotating Beams

The first three mode shapes for nine nonrotating cantilever and nine nonrotating hinged beams with different combinations of linear mass and stiffness distributions are given in tables III and IV, together with their first and second derivatives. These results were obtained by standard numerical-iteration procedures. For the cantilever beams (table III), the procedure of reference 15 was used with 10 stations; step-integration procedures were used for the first mode, and equivalent-load methods were used for the second and third modes. For the hinged beams (table IV), a matrix-iteration procedure using weighted integration matrices similar to those given in reference 21 was employed with 15 stations. More stations were needed for the hinged beams than for the cantilever beams because the third hinged mode has one more loop or node than the third cantilever mode.

In order to illustrate the accuracy of the nonrotating mode shapes computed by this method, the exact results given for the uniform beam in reference 20 are also included in tables III and IV. A comparison of the results indicates that the error of the present results is less than 1 percent. Nonrotating mode shapes are shown for the hinged beams in figure 23 and for the cantilever beams in figure 24.

Rotating Beams

The mode and frequency results for rotating beams were obtained in the present paper by the method of appendix A. This method yields mode coefficients which, when multiplied by the mode shapes of nonrotating uniform beams normalized to positive tip values and summed, give the mode shapes of the rotating beam. These coefficients can also be used in conjunction with the spanwise derivatives of the uniform-beam mode shapes to obtain similar derivatives for the rotating beams. The required uniform-beam modes and derivatives are given in reference 20, but they are not all normalized to positive tip deflections and thus certain sign modifications are necessary. These modes and the first two derivatives are also given in tables III and IV with the proper signs and tip deflections.

All the mode coefficients for rotating beams obtained in the present investigation are given in tables V and VI. These coefficients have been normalized in such a manner that the modes obtained by using them will have the same tip deflection as the uniform-beam modes used in the computation. Table V contains the results for the hinged beams, whereas table VI contains those for the cantilever beams.

Comparison of Rotating and Nonrotating Beams

Hinged beams.- The mode shapes of a uniform hinged beam for zero rotational speed and a rotational speed Ω equal to the first bending frequency ω_{NR_1} are shown in figure 25. A comparison of these shapes indicates that although some differences between the modes exist, they are relatively small, particularly for the higher modes.

A similar comparison is given in figure 26 for hinged beams with linear mass and stiffness distributions, both zero at the tip. For this case the difference in mode shapes is very small for all three modes; this undoubtedly accounts for the fact that the Rayleigh approach was found to be very accurate for this case. (See fig. 3.)

By comparing the results of figures 25 and 26, a large disagreement may be noted between the mode shapes of the two beams; this disparity apparently accounts for the substantial differences in the Southwell coefficients for the two beams.

The calculated mode shapes have not been plotted in a form which shows the effect of offset on the mode shapes of rotating beams; but by comparing the mode coefficients for 0- and 10-percent offsets in table V, the effect may be seen to be small.

Cantilever beams.- The modes of rotating and nonrotating uniform cantilever beams are shown in figure 27. From the figure the mode shapes, particularly those for the first and second modes, may be seen to change appreciably with rotational speed.

A similar comparison can be made for cantilever beams with linear mass and stiffness distributions on the basis of the results shown in figure 28. The mode shapes vary in about the same manner with rotational speed for this type of beam as for the uniform beam.

If the mode coefficients for 0- and 10-percent offsets in table VI are compared, the effect of offset on mode shape is again seen to be very small for both beams.

Beams with a mass at tip.- Bending mode shapes for a rotating and a nonrotating uniform hinged beam with a mass at the tip equal to the beam mass are shown in figure 29. The differences in mode shape are very small for all three modes. This similarity apparently accounts for the excellent accuracy of the Rayleigh approach for this configuration.

Similar results for a uniform cantilever beam with a mass at the tip equal to the beam mass are presented in figure 30. For this case, results are given for three values of the rotational-speed parameter, namely, $\frac{\Omega}{\omega_{NR_1}}$ = 0, 10.43, and 14.76, and also for the nonrotating uniform beam without tip mass. From this figure the rotating-beam mode shapes may be seen to be only slightly different from each other but considerably different from the nonrotating shape, particularly for the first and second modes, and vastly different from the mode shape of the beam without a tip mass.

Mode coefficients for rotating uniform hinged and cantilever beams with a mass at the tip are listed in tables V and VI. Mode shapes for nonrotating uniform beams with a mass at the tip have not been tabulated but can be calculated by means of equations (14) and (17) for any value of tip mass.

CONCLUDING REMARKS

A Rayleigh energy approach, which utilizes the mode shape of the nonrotating beam as an approximation for the mode shape of the rotating beam in the determination of the bending frequencies of the rotating beam, has been evaluated. The evaluation led to the conclusion that this approach yields reasonably accurate bending frequencies for rotating hinged and cantilever beams with arbitrary stiffness and mass distributions, including concentrated masses, at least within the limits of the

rotational speeds currently encountered by helicopter blades. The evaluation also showed that the Southwell coefficients vary appreciably with beam mass distribution and, to a less extent, with beam stiffness distribution. A modified form of the zero-offset Southwell coefficient, which involves the nonrotating-beam frequencies, was found to be insensitive to changes in beam mass distribution.

By using the Rayleigh approach as a basis, several groups of charts and associated procedures have been presented, which permit the rapid estimation of the first three bending frequencies for a variety of rotating and nonrotating hinged and cantilever beams. Since the charts are not applicable to all beams, practice may dictate the need for additional charts which may be set up by using the methods described. The charts and associated procedures presented in this report are summarized below, the most easily applied being listed first:

(a) Charts are presented which permit the rapid estimation of bending frequencies of rotating and nonrotating beams with mass and stiffness distributions, each of which can be approximated by a linear relation. In example applications, this procedure has been shown to give good results for the bending frequencies of several actual helicopter blades with mass and stiffness distributions appreciably different from linear.

(b) Charts are presented for rapidly estimating the effects of tip mass on the rotating and nonrotating bending frequencies of uniform beams.

(c) A chart is presented which permits the rapid estimation of the effects of offset on the pendulum frequency of hinged beams with any stiffness distribution, an approximately linear mass distribution, and a concentrated tip mass.

(d) A simplified procedure is presented for estimating the first bending mode and frequency of a rotating or nonrotating hinged beam with a tip mass from a knowledge of the first mode shape of the nonrotating beam without a tip mass.

(e) Charts for a modified Southwell coefficient, which appears to be insensitive to changes in beam mass distribution, are presented; these charts permit the rapid estimation of the first three bending frequencies of rotating beams with approximately linear stiffness distributions from a knowledge of the bending frequencies of the nonrotating beam.

(f) Bending frequencies for beams with unusual mass and stiffness distributions which cannot be estimated by using the charts can be determined directly from the Rayleigh energy equation by first calculating the bending frequencies and associated mode shapes of the nonrotating beams. This approach can be expected to yield results which are in error by less (usually much less) than 3 percent, except for the first cantilever frequency which may be in error by as much as 5 percent but which can easily

be corrected to give a much more accurate result. The method has the
advantage over other simplified approaches of improved accuracy and
wider applicability and over more exact approaches of simplicity and
flexibility.

A more accurate mode-expansion method for determining the bending
frequencies and modes of a rotating or a nonrotating beam has been devel-
oped and has been used to evaluate the Rayleigh approach. In order to
facilitate the further application of this method to the accurate deter-
mination of modes and frequencies of rotating and nonrotating beams with
combinations of linear mass and stiffness distribution and concentrated
tip mass different from those considered herein, certain integrals which
have been evaluated are presented in tabular form.

In conjunction with obtaining the frequency results which comprise
the greater part of this report, bending mode shapes were determined for
a wide variety of hinged and cantilever beams. These results show the
effect of rotational speed, mass and stiffness distributions, offset,
root fixity, and other parameters on bending mode shape; they have been
tabulated in normalized form together with their first and second deriva-
tives or as mode coefficients which, in conjunction with tabulated modes
and derivatives of uniform beams, permit the rapid determination of the
mode shape and higher derivatives as well. The tabulated results should
prove useful in other analyses, for example, in the simplified approach
presented in an appendix.

Langley Aeronautical Laboratory,
      National Advisory Committee for Aeronautics,
            Langley Field, Va., February 24, 1955.

APPENDIX A

SOLUTION OF DIFFERENTIAL EQUATION FOR ROTATING BEAM

BY EXPANSION IN TERMS OF NORMAL MODES OF

UNIFORM NONROTATING BEAM

Solution by Galerkin Method

The equation of motion which defines the bending vibrations perpendicular to the plane of rotation of a rotating beam with a concentrated mass at its tip can be written as

$$\frac{d^2}{dx^2}\left(EI\ \frac{d^2 y_n}{dx^2}\right) = m\omega_{R_n}^2 y_n + M_t \omega_{R_n}^2 y_n(L)\delta(x-L) + \frac{d}{dx}\left(T\ \frac{dy_n}{dx}\right) \tag{A1}$$

where

$$\delta(x-L) = 0 \qquad (x \neq L)$$

$$\delta(x-L) = \frac{1}{L} \qquad (x = L)$$

and

$$T = \Omega^2 \left[\int_x^L (\eta + e)m\ d\eta + M_t(L + e)\right]$$

or, in nondimensional form,

$$\frac{d^2}{d\bar{x}^2}\left(\overline{EI}\ \frac{d^2 y_n}{d\bar{x}^2}\right) = b_n^2 \bar{m} y_n + r b_n^2 \delta(\bar{x}-1) y_n(1) + \left(\frac{\Omega}{\omega_{NR_1}}\right)^2 a_1^2\ \frac{d}{d\bar{x}}\left(\overline{T}_1\ \frac{dy_n}{d\bar{x}}\right) \tag{A2}$$

where

$$\delta(\bar{x}-1) = 0 \qquad (\bar{x} \neq 1)$$

$$\delta(\bar{x}-1) = 1 \qquad (\bar{x} = 1)$$

and

$$\bar{T}_1 = \int_{\bar{x}}^{1} (\bar{\eta} + \bar{e})\bar{m}(\bar{\eta})d\bar{\eta} + r(1 + \bar{e})$$

$$b_n^{\,2} = \omega_{R_n}^{\,2}\frac{m_oL^4}{EI_o}$$

Each normal mode of the rotating beam can be expanded in terms of the modes of a uniform nonrotating beam with the same end restraints as follows:

$$y_n = \sum_{q=0}^{\infty} A_{n_q}\phi_q \tag{A3}$$

where the quantities ϕ_q are the normalized bending mode shapes of a stationary uniform beam, and the coefficients A_{n_q} are undetermined.

Substituting this expansion into equation (A2) gives

$$\frac{d^2}{d\bar{x}^2}\left[\overline{EI}\,\frac{d^2}{d\bar{x}^2}\left(\sum_{q=0}^{\infty} A_{n_q}\phi_q\right)\right] - b_n^{\,2}\bar{m}\sum_{q=0}^{\infty} A_{n_q}\phi_q - rb_n^{\,2}\delta(\bar{x}-1)\sum_{q=0}^{\infty} A_{n_q}\phi_q(1) -$$

$$\left(\frac{\Omega}{\omega_{NR_1}}\right)^2 a_1^{\,2}\,\frac{d}{d\bar{x}}\left[\bar{T}_1\,\frac{d}{d\bar{x}}\left(\sum_{q=0}^{\infty} A_{n_q}\phi_q\right)\right] = 0 \tag{A4}$$

One way of determining the coefficients A_{n_q} from this equation is the Galerkin procedure which consists in multiplying the equation by ϕ_p and integrating over the length of the beam. Thus,

$$\int_0^1 \phi_p \frac{d^2}{d\bar{x}^2}\left[\overline{EI}\frac{d^2}{d\bar{x}^2}\left(\sum_{q=0}^{\infty} A_{n_q}\phi_q\right)\right]d\bar{x} - b_n^2 \int_0^1 \bar{m}\phi_p \sum_{q=0}^{\infty} A_{n_q}\phi_q \, d\bar{x} -$$

$$rb_n^2\phi_p(1)\sum_{q=0}^{\infty} A_{n_q}\phi_q(1) - \left(\frac{\Omega}{\omega_{NR_1}}\right)^2 a_1^2 \int_0^1 \phi_p \frac{d}{d\bar{x}}\left[\overline{T}_1 \frac{d}{d\bar{x}}\left(\sum_{q=0}^{\infty} A_{n_q}\phi_q\right)\right]d\bar{x} = 0$$

$$(A5)$$

Integrating the first term in equation (A5) by parts twice and the last term by parts once and making use of the known boundary conditions gives for either a cantilever or a hinged beam:

$$\int_0^1 \phi_p''\overline{EI}\sum_{q=0}^{\infty} A_{n_q}\phi_q'' \, d\bar{x} - b_n^2 \int_0^1 \bar{m}\phi_p \sum_{q=0}^{\infty} A_{n_q}\phi_q \, d\bar{x} -$$

$$rb_n^2\phi_p(1)\sum_{q=0}^{\infty} A_{n_q}\phi_q(1) + \left(\frac{\Omega}{\omega_{NR_1}}\right)^2 a_1^2 \int_0^1 \phi_p'\overline{T}_1 \sum_{q=0}^{\infty} A_{n_q}\phi_q' \, d\bar{x} = 0 \qquad (A6)$$

where the primes designate differentiations with respect to $\bar{x}$. Interchanging the order of integration and summation yields:

$$\sum_{q=0}^{\infty} A_{n_q} \int_0^1 \overline{EI}\phi_p''\phi_q'' \, d\bar{x} - b_n^2 \sum_{q=0}^{\infty} A_{n_q} \int_0^1 \bar{m}\phi_p\phi_q \, d\bar{x} -$$

$$rb_n^2\phi_p(1)\sum_{q=0}^{\infty} A_{n_q}\phi_q(1) + \left(\frac{\Omega}{\omega_{NR_1}}\right)^2 a_1^2 \sum_{q=0}^{\infty} A_{n_q} \int_0^1 \overline{T}_1\phi_p'\phi_q' \, d\bar{x} = 0 \qquad (A7)$$

Equation (A7) can be rewritten as

$$\sum_{q=0}^{\infty} A_{n_q}\left[I_{qp} - b_n^2\left(M_{qp} + R_{qp}\right) + \left(\frac{\Omega}{\omega_{NR_1}}\right)^2 a_1^2 S_{qp}\right] = 0 \qquad (A8)$$

in terms of a new set of constants: namely,

$$\left.\begin{aligned} I_{qp} &= \int_0^1 \overline{EI}\phi_p''\phi_q'' \ d\bar{x} \\[2em] M_{qp} &= \int_0^1 \bar{m}\phi_p\phi_q \ d\bar{x} \\[2em] R_{qp} &= r\phi_p(1)\phi_q(1) \\[2em] S_{qp} &= \int_0^1 \bar{T}_1\phi_p'\phi_q' \ d\bar{x} \end{aligned}\right\} \qquad (A9)$$

These coefficients are symmetric; that is, $I_{qp} = I_{pq}$, and so forth.

For practical purposes, the expansion must be limited to a finite number of nonrotating uniform-beam modes.   In this case the summation goes from $q = 0$ to m and equation (A8) yields $m + 1$ equations of the form

$$\sum_{q=0}^{\infty} A_{n_q} B_{qp} = 0$$

where

$$B_{qp} = I_{qp} - b_n^2\left(M_{qp} + R_{qp}\right) + \left(\frac{\Omega}{\omega_{NR_1}}\right)^2 a_1^2 S_{qp} \qquad (A10)$$

so that the coefficients B_{qp} are also symmetric.

The modes and frequencies of the system represented by this group of equations can be obtained for any value of the rotational-speed parameter Ω/ω_{NR_1} by equating the following determinant of the multipliers B_{qp} of the mode coefficients A_{n_q} to zero:

$$
\begin{vmatrix}
B_{00} & B_{01} & B_{02} & \cdots & B_{0m} \\
B_{10} & B_{11} & B_{12} & \cdots & B_{1m} \\
B_{20} & B_{21} & B_{22} & \cdots & B_{2m} \\
\cdot & \cdot & \cdot & \cdots & \cdot \\
\cdot & \cdot & \cdot & \cdots & \cdot \\
\cdot & \cdot & \cdot & \cdots & \cdot \\
B_{m0} & B_{m1} & B_{m2} & \cdots & B_{mm}
\end{vmatrix} = 0 \qquad\qquad (A11)
$$

This determinantal equation can be solved by trial and error, with any method of evaluating determinants, such as Crout's, to obtain the frequency coefficients b_n and subsequently the associated mode coefficients A_{n_q} for a rotating beam. The resonant frequencies for 1p, 2p, or np resonant conditions can also be obtained directly from the determinant. For small values of Ω/ω_{NR_1} less than about 0.8, solutions can also be obtained by the matrix-iteration procedure; for larger values, however, convergence is poor, and undesired negative values of the frequency squared (imaginary frequencies) may be encountered before the desired positive values are obtained. In the present investigation the frequency determinants (eq. (A11)) were solved by trial-and-error methods with automatic computing machines of the punchcard type.

For the case of a beam without a tip mass, $r = 0$, and thus R_{qp} is not needed and S_{qp} is simplified slightly. If, in addition, the beam is uniform, I_{qp} and M_{qp} are zero by orthogonality for $q \neq p$; thus for this case the unknown frequency coefficients b_n occur only on the principal diagonal. If the determinantal equation is divided by $(\Omega/\omega_{NR_1})^2$, then for this case the rotational-speed parameter also appears only in the terms on the principal diagonal.

Evaluation of the Integrals I_{qp}, M_{qp}, R_{qp}, and S_{qp}

The integrals I_{qp}, M_{qp}, R_{qp}, and S_{qp} may be evaluated numerically by a method such as that given in reference 15, or, if the mass and stiffness distributions of the beams are defined by analytical expressions, they can sometimes be evaluated in closed form. (See ref. 1, pp. 333-336, for instance.) In some cases integrals already evaluated and tabulated in reference 18 can be employed; these results, converted to the coordinate system and tip deflection of the present paper, were employed wherever possible in the present study. In this report all integrals for the uniform rotating beams with and without a tip mass were evaluated by exact methods. Some were also evaluated by numerical methods in order to determine how many stations were required to obtain good accuracy. By this procedure about 25 stations were found to be required for some of the integrals involving the fourth and fifth modes.

For the nonuniform rotating beams, I_{qp}, M_{qp}, and R_{qp} were evaluated both exactly and numerically, but S_{qp} was evaluated only numerically because of the effort involved in evaluating this integral exactly. All the integrations performed in this report are based on mode shapes normalized to unity at the tip. Where numerical integrations were made, the mode shapes and derivatives were obtained from reference 20, but the results were modified to correspond to shapes with a unit positive tip deflection.

The remainder of this appendix is devoted to the presentation of results (in both numerical and analytical form) for I_{qp}, M_{qp}, R_{qp}, and S_{qp} which were obtained in connection with the present study but which are also applicable to cases not treated in this report.

Numerical results for beams with linear mass and stiffness distributions with or without tip mass and offset.- If only linear variations in beam mass and stiffness are considered and if they are expressed as

$$
\left.
\begin{aligned}
m &= m_0(1 - k\bar{x}) \\
\\
EI &= EI_0(1 - c\bar{x})
\end{aligned}
\right\}
\tag{A12}
$$

then the various integrals can be evaluated expeditiously by splitting them up as indicated in the following equations:

$$S_{pq} = S_{pq_O} - kS_{pq_k} + \bar{e}\left(S_{pq_e} - kS_{pq_{ke}}\right) + r(1 + \bar{e})S_{pq_t}$$

$$I_{qp} = I_{qp_O} - cI_{qp_c}$$

$$M_{qp_k} = M_{qp_O} - kM_{qp_k}$$ (A13)

$$R_{qp} = r$$

where, in turn,

$$S_{pq_O} = \frac{1}{2} \int_0^1 \left(1 - \bar{x}^2\right)\phi_p'\phi_q' \, d\bar{x}$$

$$S_{pq_k} = \frac{1}{3} \int_0^1 \left(1 - \bar{x}^3\right)\phi_p'\phi_q' \, d\bar{x}$$

$$S_{pq_e} = \int_0^1 (1 - \bar{x})\phi_p'\phi_q' \, d\bar{x}$$

$$S_{pq_{ke}} = S_{pq_O}$$

$$S_{pq_t} = \int_0^1 \phi_q'\phi_p' \, d\bar{x}$$ (A14)

$$I_{qp_O} = \int_0^1 \phi_q''\phi_p'' \, d\bar{x}$$

$$I_{qp_c} = \int_0^1 \bar{x}\phi_p''\phi_q'' \, d\bar{x}$$

$$M_{qp_O} = \int_0^1 \phi_q\phi_p \, d\bar{x}$$

$$M_{qp_k} = \int_0^1 \bar{x}\phi_q\phi_p \, d\bar{x}$$

All these integrals are obviously symmetric in p and q. Numerical
values for them are given in table II for values of p and q from
0 to 5 for hinged beams and 1 to 5 for cantilever beams. As may be seen
from equations (A13), these results permit the rapid calculation of the
terms of a frequency determinant for a rotating beam with any combina-
tion of the following parameters: (a) linear mass distribution,
(b) linear stiffness distribution, (c) any offset (including large
values), and (d) any tip mass. In addition, the results can be used
in conjunction with values of additional integrals to set up similar
determinants for beams with higher order mass and stiffness distribu-
tions and beams with concentrated masses at other locations.

Integrals for uniform beams with tip mass.- In order to facilitate
the extension of the results for the uniform rotating beams to higher
modes, the exact expressions for integrals pertinent to such cases are
included herein.

The integrals for the cases where p = q can also be used to
determine values for Southwell coefficients for modes higher than the
third. The integrals were evaluated by the method of reference 1 or
taken from reference 18 and transformed into the notation of this report.
The expressions are given in terms of the parameters α_s, β_s, and γ_s;
values of the first two can be obtained from reference 20 for values
of s from 1 to 5. For s > 5, $\alpha_s = 1$ for all practical purposes
and β_s can be obtained from the appropriate frequency equation for the
nonrotating uniform beam. The square of β_s is the frequency coeffi-
cient for the nonrotating beam a_s for the sth bending mode of a uniform
beam. Values of γ_s are not required for the cantilever beams; for
hinged beams, $\gamma_s = 1$ for s > 3; the values for $s \leq 3$ are given in
the following table:

s	γ_s
1	1.02827
2	1.00121
3	1.00005

Tension integrals S_{qp} for cantilever beams:

If $p \neq q$,

$$S_{qp} = \frac{\beta_q{}^2\beta_p{}^2}{\beta_q{}^4 - \beta_p{}^4}\left(\left[\frac{1}{2}(-1)^{p+q}\left(\alpha_p\beta_p - \alpha_q\beta_q\right) - \frac{4\beta_q{}^2\beta_p{}^2}{\beta_q{}^4 - \beta_p{}^4}\right] + \right.$$

$$\bar{e}\left\{(-1)^{p+q}\left[\alpha_p\beta_p - \alpha_q\beta_q + \frac{2\left(\beta_q{}^4 + \beta_p{}^4\right)}{\beta_q{}^4 - \beta_p{}^4}\right] - \frac{4\beta_q{}^2\beta_p{}^2}{\beta_q{}^4 - \beta_p{}^4}\right\}\right) +$$

$$\frac{r(1 + \bar{e})}{\beta_q{}^4 - \beta_p{}^4}\left\{\alpha_p\beta_p\left[\beta_q{}^4 + (-1)^{p+q}\beta_p{}^2\beta_q{}^2\right] - \alpha_q\beta_q\left[\beta_p{}^4 + (-1)^{p+q}\beta_p{}^2\beta_q{}^2\right]\right\}$$

If $p = q$,

$$S_{qq} = \alpha_q\beta_q\left(\frac{\alpha_q\beta_q}{12} - \frac{1}{8}\right) + \frac{5}{16} + \bar{e}\left[\alpha_q\beta_q\left(\frac{\alpha_q\beta_q}{8} + \frac{1}{4}\right) + \frac{1}{2}\right] +$$

$$r(1 + \bar{e})\left(\frac{1}{4}\,\alpha_q{}^2\beta_q{}^2 + \frac{1}{2}\,\alpha_q\beta_q\right)$$

Tension integrals S_{qp} for hinged beams:

If $p \neq q \neq 0$,

$$S_{qp} = -\frac{4\beta_q^4\beta_p^4}{\left(\beta_q^4 - \beta_p^4\right)^2} - \frac{\bar{e}}{\beta_q^4 - \beta_p^4}\left[\frac{4\beta_q^4\beta_p^4}{\beta_q^4 - \beta_p^4} - (-1)^{p+q}\frac{\beta_p\beta_q^3}{2\gamma_p}\left(1 + \frac{4\beta_p^4}{\beta_q^4 - \beta_p^4}\right) + \right.$$

$$\left.(-1)^{p+q}\frac{\beta_q\beta_p^3\gamma_p}{2\gamma_q}\left(1 - \frac{4\beta_q^4}{\beta_q^4 - \beta_p^4}\right)\right] + \frac{r(1 + \bar{e})}{\beta_q^4 - \beta_p^4}\left(\beta_p\alpha_p\beta_q^4 - \beta_q\alpha_q\beta_p^4\right)$$

If $p \neq q$, but $p = 0$,

$$S_{q0} = \bar{e}(-1)^q\frac{\gamma_q}{\beta_q\sqrt{2}} + r(1 + \bar{e})$$

If $p = q \neq 0$,

$$S_{qq} = \frac{1}{12}\beta_q^2\alpha_q^2 + \frac{5}{16} + \frac{\bar{e}}{8}\left(\beta_q^2\alpha_q^2 + 3\right) + r(1 + \bar{e})\left(\frac{1}{4}\beta_q^2\alpha_q^2 + \frac{3}{4}\beta_q\alpha_q\right)$$

If $p = q = 0$,

$$S_{00} = \frac{1}{3} + \frac{\bar{e}}{2} + r(1 + \bar{e})$$

Stiffness integrals I_{qp} for cantilever or hinged beams:

If $q \neq p$,

$$I_{qp} = 0$$

If $p = q \neq 0$,

$$I_{qq} = \frac{\beta_q^4}{4}$$

If $p = q = 0$,

$$I_{00} = 0$$

Mass integrals M_{qp} for cantilever or hinged beams:

If $p \neq q$,

$$M_{qp} = 0$$

If $p = q \neq 0$,

$$M_{qq} = \frac{1}{4}$$

If $p = q = 0$,

$$M_{00} = \frac{1}{3}$$

Tip-mass integrals for cantilever or hinged beams:

If $p = q$, or $p \neq q$,

$$R_{qp} = r$$

APPENDIX B

AN APPROXIMATE METHOD OF OBTAINING FIRST BENDING MODE OF

HINGED BEAM WITH TIP MASS FROM FIRST BENDING MODE OF

BEAM WITHOUT TIP MASS

The vibration modes of a rotating hinged beam must satisfy the following equation, which expresses the condition of zero moment at the root:

$$\omega_R^2 \int_0^L mxy \, dx - \Omega^2 \int_0^L (x + e)my \, dx = 0 \tag{B1}$$

or, in dimensionless form,

$$\left(\frac{\omega_R}{\Omega}\right)^2 \int_0^1 \bar{m}\bar{x}y \, d\bar{x} - \int_0^1 (\bar{x} + \bar{e})\bar{m}y \, d\bar{x} = 0 \tag{B2}$$

For any given beam the mode shapes of the nonrotating beam can readily be shown to satisfy this criterion exactly if e is zero and very closely if e is small; therefore, the nonrotating-beam mode shapes are good approximations to the rotating-beam mode shapes, regardless of the mass distribution of the beam. However, the nonrotating-beam mode shape must be that of the beam with the same mass distribution; the purpose of the present derivation is to go a step further and to obtain an approximate first mode shape for a nonrotating beam with tip mass in terms of the first mode of the same beam without tip mass. In view of the preceding argument, the mode shape obtained in this manner should serve as a good approximation to the first mode of the rotating or nonrotating beam with the same tip mass and when used in conjunction with the Rayliegh approach (eq. (1)) should yield a good approximation for the first bending frequency of a rotating or nonrotating hinged beam.

In deriving such a relation the assumption is made that the second derivative or curvature of the beam remains unchanged in the two configurations. Thus, the mode shape for the beam with tip mass is assumed to be of the form

$$y_1{}^* \approx y_1 + D_0\bar{x} \approx Y_1 + D_0\bar{x} \tag{B3}$$

where the first mode of the rotating beam without tip mass y_1 is assumed to be approximately equal to the nonrotating-beam first mode shape Y_1. With this mode shape, the criterion of equation (B2) becomes

$$\left(\frac{\omega_R}{\Omega}\right)^2 \int_0^1 \bar{m}\bar{x}(Y_1 + D_0\bar{x})d\bar{x} - \int_0^1 \bar{m}(\bar{x} + \bar{e})(Y_1 + D_0\bar{x})d\bar{x} = 0 \qquad (B4)$$

If, now, the mass distribution is considered to be made up of the continuous distributed mass of the beam m_d plus a concentrated tip mass, equation (B4) can be written as

$$\left(\frac{\omega_R}{\Omega}\right)^2 \int_0^1 \bar{m}_d\bar{x}(Y_1 + D_0\bar{x})d\bar{x} + \left(\frac{\omega_R}{\Omega}\right)^2 r\left[Y_1(1) + D_0\right] -$$

$$\int_0^1 \bar{m}_d(\bar{x} + \bar{e})(Y_1 + D_0\bar{x})d\bar{x} - r(1 + \bar{e})\left[Y_1(1) + D_0\right] = 0 \qquad (B5)$$

Inasmuch as Y_1 and $\bar{x}$ (the pendulum mode shape) are mode shapes of the hinged beam with mass distribution m_d, they must satisfy the orthogonality condition for normal modes for such a beam, namely,

$$\int_0^1 \bar{m}_d\bar{x}Y_1 \, d\bar{x} = 0$$

and, hence, equation (B5) becomes

$$\left(\frac{\omega_R}{\Omega}\right)^2 D_0 \int_0^1 \bar{m}_d\bar{x}^2 d\bar{x} + \left(\frac{\omega_R}{\Omega}\right)^2 r\left[Y_1(1) + D_0\right] - D_0 \int_0^1 \bar{m}_d\bar{x}^2 d\bar{x} -$$

$$\bar{e} \int_0^1 \bar{m}_d Y_1 \, d\bar{x} - \bar{e}D_0 \int_0^1 \bar{m}_d\bar{x} \, d\bar{x} - r(1 + \bar{e})\left[Y_1(1) + D_0\right] = 0 \qquad (B6)$$

When this equation is solved for D_0, the result is

$$D_0 = \frac{\bar{e}\int_0^1 \bar{m}_d Y_1\, d\bar{x} + \bar{e}r Y_1(1) - \left[\left(\frac{\omega_R}{\Omega}\right)^2 - 1\right]r Y_1(1)}{\left[\left(\frac{\omega_R}{\Omega}\right)^2 - 1\right]\int_0^1 \bar{m}_d \bar{x}^2 d\bar{x} + \left[\left(\frac{\omega_R}{\Omega}\right)^2 - 1\right]r - \bar{e}\int_0^1 \bar{m}_d \bar{x}\, d\bar{x} - \bar{e}r} \tag{B7}$$

If the offset $\bar{e}$ is zero, equation (B7) takes the much simpler form

$$D_0 = \frac{-r Y_1(1)}{\int_0^1 \bar{m}_d \bar{x}^2 d\bar{x} + r} \tag{B8}$$

or, with Y_1 normalized to unity at the tip,

$$D_0 = \frac{-1}{1 + \dfrac{\displaystyle\int_0^1 m_d \bar{x}^2 d\bar{x}}{r}} \tag{B9}$$

By comparing the relative values of the terms of equation (B7) and by considering the overall influence of terms containing $\bar{e}$, small offsets can be shown to have a negligible influence on the value of D_0 for values of the rotational-speed parameter encountered in helicopters. Also, for nonrotating beams, $\bar{e}$ does not enter the problem and, hence, can be set equal to zero; thus, as mentioned before, the mode shape, based on the result of equation (B9), obtained in the following paragraphs, should serve as a good approximation for both rotating and nonrotating beams with and without offset.

Upon substituting the value of D_0 in equation (B9) into equation (B3), the desired first mode shape of the beam with a mass at the tip is obtained as

$$y_1{}^* = Y_1 - \frac{1}{1 + \dfrac{\displaystyle\int_0^1 \bar{m}_d \bar{x}^2 d\bar{x}}{r}}\, \bar{x} \tag{B10}$$

and the slope $\left(y_1{}^*\right)'$ and curvature $\left(y_1{}^*\right)''$ of this mode shape are then given by

$$\left(y_1{}^*\right)' = Y_1{}' - \frac{1}{1 + \dfrac{\displaystyle\int_0^1 \bar{m}_d \bar{x}^2 d\bar{x}}{r}} \tag{B11}$$

$$\left(y_1{}^*\right)'' = Y_1{}'' \tag{B12}$$

(Eq. (B12), of course, expresses nothing more than the assumed equality of the second derivatives.) If the mode shape of a beam with a particular mass and stiffness distribution (but without tip mass) is known, expressions (B10) to (B12) thus permit the determination of an approximate mode shape for the same beam with any concentrated mass at the tip and can be used to evaluate the integrals of the basic Rayleigh equation (eq. (1)) by numerical methods; reasonably accurate values can easily be obtained in this manner for ω_{NR_1} and for K_{0_1} and K_{1_1}, from which the bending frequency at any rotational speed can be determined directly.

Beams With Linear Mass Distribution Plus Tip Mass

For the particular case of beams with a linear mass distribution plus a tip mass, $\bar{m}_d = 1 - k\bar{x}$ and

$$\int_0^1 \bar{m}_d \bar{x}^2 d\bar{x} = \int_0^1 \bar{x}^2 d\bar{x} - k \int_0^1 \bar{x}^3 d\bar{x}$$

$$= \frac{1}{3} - \frac{k}{4}$$

Thus

$$D_0 = \frac{-1}{1 + \dfrac{4 - 3k}{12r}} \tag{B13}$$

This result can be used in conjunction with the first mode shape given for hinged beams with linear mass and stiffness distributions in table IV to obtain mode and frequency results for such beams.

Beams With Uniform Mass Distribution Plus Tip Mass

For the case of beams with a uniform mass distribution plus a tip mass, $\bar{m}_d = 1$ and thus

$$D_0 = \frac{-1}{1 + \dfrac{1}{3r}} \tag{B14}$$

Uniform Beam With Tip Mass

For the case of a uniform beam with an arbitrary tip mass,

$$\bar{m}_d = 1$$

and

$$\overline{EI} = 1$$

Thus, D_0 is the same as for the preceding case. In this special case the integrals of the Rayleigh equation (eq. (1)), which permit the determination of ω_{NR} and K and thus of ω_R, can be evaluated exactly by the methods of reference 1 or 18. The results are

$$\int_0^1 \bar{m}\left(y_1{}^*\right)^2 d\bar{x} = \frac{1}{4} + \frac{r}{3r + 1} \tag{B15a}$$

$$\int_0^1 \overline{EI}\left[\left(y_1{}^*\right)''\right]^2 d\bar{x} = \frac{\beta_1{}^4}{4} \tag{B15b}$$

$$\int_0^1 \bar{T}_1 \left[(y_1{}^*)' \right]^2 d\bar{x} = \frac{\beta_1{}^2}{12} + \frac{5}{16} + \frac{r\beta_1}{4}(\beta_1 + 3) + r\left(\frac{1}{1 + \frac{1}{3r}} \right) +$$

$$\left(\frac{1}{1 + \frac{1}{3r}} \right)^2 \left(\frac{1}{12} + \frac{r}{4} \right) \tag{B15c}$$

$$\int_0^1 \bar{T}_{1_e} \left[(y_1{}^*) \right]^2 d\bar{x} = \frac{\bar{\bar{e}}}{4} \left[\left(\frac{1}{2} + r\beta_1 \right)(\beta_1 + 3) - 2\left(\frac{1}{1 + \frac{1}{3r}} \right)\left(4r - \frac{\sqrt{2}}{\beta_1} \right) + \right.$$

$$\left. \left(\frac{1}{1 + \frac{1}{3r}} \right)^2 \left(\frac{1}{2} + r \right) \right] \tag{B15d}$$

where $\beta_1 = 3.9266$, from the results given in reference 20. In the preceding integrations α_n (ref. 20) has been taken equal to unity; this assumption introduces a small error of less than 0.1 percent.

Equations (B15) are based on Y_1 rather than $y_1{}^*$ normalized to unity at the tip. To obtain equivalent formulas for $y_1{}^*$ normalized to unity at the tip, these results must be divided by the factor $\left(\frac{2}{3r + 1} \right)^2$.

Nonrotating- and rotating-beam frequencies obtained by this method for the uniform beam are compared with more accurate results in the section of this paper entitled "Charts for Bending-Frequency Determination."

REFERENCES

1. Timoshenko, S.: Vibration Problems in Engineering. Second ed.,
     D. Van Nostrand Co., Inc., 1937.

2. Myklestad, N. O.: Vibration Analysis. McGraw-Hill Book Co., Inc.,
     1944.

3. Houbolt, John C.: Coupled Bending and Torsional Deformations of
     Twisted Rotating Blades Under Arbitrary Loading. Preprint No. 539,
     S.M.F. Fund Preprint, Inst. Aero. Sci., Inc., Jan. 1955.

4. Prewitt, R. H., and Wagner, R. A.: Frequency and Vibration Problems
     of Rotors. Jour. Aero. Sci., vol. 7, no. 10, Aug. 1940, pp. 444-450.

5. Morduchow, Morris: A Theoretical Analysis of Elastic Vibrations of
     Fixed-Ended and Hinged Helicopter Blades in Hovering and Vertical
     Flight. NACA TN 1999, 1950.

6. Horvay, Gabriel: Chordwise and Beamwise Bending Frequencies of Hinged
     Rotor Blades. Jour. Aero. Sci., vol. 15, no. 8, Aug. 1948,
     pp. 497-502.

7. Theodorsen, T.: Propeller Vibrations and the Effect of the Centrifugal
     Force. NACA TN 516, 1935.

8. Liebers, F.: Contribution to the Theory of Propeller Vibrations.
     NACA TM 568, 1930.

9. Liebers, Fritz: Resonance Vibrations of Aircraft Propellers. NACA
     TM 657, 1932.

10. Liebers, F.: Analysis of the Three Lowest Bending Frequencies of a
     Rotating Propeller. NACA TM 783, 1936.

11. Berry, Arthur: On the Vibrations of a Uniform Rod Rotating Uniformly
     About One End, Which Is Encastré. R. & M. No. 488, British ACA,
     Sept. 1918.

12. Webb, H. A., and Swain, Lorna M.: Vibration Speeds of Airscrew Blades.
     R. & M. No. 626, British ACA, May 1919.

13. Prohl, M. A.: A General Method for Calculating Critical Speeds of
     Flexible Rotors. Jour. Appl. Mech., vol. 12, no. 3, Sept. 1945,
     pp. A-142 - A-148.

14. Den Hartog, J. P.: Mechanical Vibrations. Second ed., McGraw-Hill
     Book Co., Inc., 1940.

15. Houbolt, John C., and Anderson, Roger A.: Calculation of Uncoupled Modes and Frequencies in Bending or Torsion of Nonuniform Beams. NACA TN 1522, 1948.

16. Ono, Akimasa: Lateral Vibrations of Tapered Bars. Jour. Soc. Mech. Engineers, vol. 28, no. 99, July 1925, pp. 429-441.

17. Stowell, Elbridge Z., Schwartz, Edward B., Houbolt, John C., and Schmieder, Albert K.: Bending and Shear Stresses Developed by the Instantaneous Arrest of the Root of a Cantilever Beam With a Mass at Its Tip. NACA WR L-586, 1944. (Formerly NACA MR L4K30.)

18. Felgar, Robert P., Jr.: Formulas for Integrals Containing Characteristic Functions of a Vibrating Beam. Cir. No. 14, Bur. Eng. Res., Univ. of Texas, 1950.

19. Lo, Hsu, and Renbarger, Jack L.: Bending Vibrations of a Rotating Beam. Proc. First U. S. Nat. Cong. Appl. Mech. (Chicago, Ill., 1951), A.S.M.E., 1952, pp. 75-79.

20. Young, Dana, and Felgar, Robert P., Jr.: Tables of Characteristic Functions Representing Normal Modes of Vibration of a Beam. Univ. of Texas Pub. No. 4913, Eng. Res. Ser. No. 44, Bur. Eng. Res., July 1, 1949.

21. Benscoter, Stanley U., and Gossard, Myron L.: Matrix Methods for Calculating Cantilever-Beam Deflections. NACA TN 1827, 1949.

TABLE I
EXACT AND ESTIMATED FREQUENCIES FOR SEVERAL MANUFACTURED BLADES

m   EI

TRUE
FAIRED

MODE	ω_{NR}, RADIANS/SEC		ω_{R}, RADIANS/SEC	
	EXACT	ESTIMATED	EXACT	ESTIMATED
1st	17.3	17.4	49.2	47.7
2nd	48.5	50.0	86.8	85.7
3rd	95.5	101.0	137.0	137.8

MODE	EXACT	ESTIMATED	EXACT	ESTIMATED
1st	21.6	21.1	50.6	49.2
2nd	58.9	60.5	92.4	92.2
3rd	112.1	122.0	148.0	154.0

MODE	EXACT	ESTIMATED	EXACT	ESTIMATED
1st	21.9	21.1	74.0	78.3
2nd	63.7	59.5	132.0	134.4
3rd	126.0	125.5	200.0	207.5

MODE	EXACT	ESTIMATED	EXACT	ESTIMATED
1st	13.4	14.6	37.9	37.8
2nd	43.7	41.6	71.0	70.3
3rd	94.9	94.5	125.0	124.0

ROOT   TIP ROOT   TIP

TABLE II

VALUES FOR INTEGRALS IN THE MODE-EXPANSION METHOD OF APPENDIX A

p	q	S_{pq_o}	S_{pq_e}	S_{pq_k}	S_{pq_t}	I_{pq_o}	I_{pq_c}	M_{pq_o}	M_{pq_k}	R_{pq_t}
				Hinged beams with linear mass and stiffness distributions						
0	0	1/3	1/2	1/4	1	0	0	1/3	1/4	r
	1	0	-0.18517	-0.05578	1	0	0	0	0.05577	r
	2	0	.09992	-.00165	1	0	0	0	.00165	r
	3	0	-.06926	-.00320	1	0	0	0	.00321	r
	4	0	.05296	-.00024	1	0	0	0	.00025	r
	5	0	-.04287	-.00075	1	0	0	0	.00077	r
1	1	1.59938	2.30532	1.26052	6.80791	59.43015	25.63938	1/4	.14214	r
	2	-.46528	-1.22263	-.18122	3.59935	0	30.97991	0	.05286	r
	3	-.09145	.20921	-.09117	3.78925	0	-4.62284	0	.00288	r
	4	-.03037	-.21872	-.02260	3.85869	0	7.13092	0	.00531	r
	5	-.01293	.12567	-.01258	3.88921	0	-3.32571	0	.00082	r
2	2	4.47610	6.62225	3.43015	17.79273	624.12075	299.60439	1/4	.12999	r
	3	-1.54866	-3.43733	-.80926	6.13170	0	239.3184	0	.05202	r
	4	-.37008	.28431	-.37093	6.53295	0	-15.99519	0	.00182	r
	5	-.14453	-.52531	-.12984	6.73955	0	48.63946	0	.00582	r
3	3	8.99985	-13.40607	6.82541	33.71970	2716.90000	1332.5410	1/4	.12741	r
	4	-3.15890	-6.67345	-1.76094	8.57761	0	892.5356	0	.05144	r
	5	-.80708	.31838	-.81443	9.12863	0	-30.36181	0	.00130	r
4	4	15.16836	22.65800	11.44593	54.58150	7945.0300	3931.674	1/4	.12652	r
	5	-5.27717	-10.91717	-2.97035	10.98707	0	2319.820	0	.05001	r
5	5	22.98186	34.37920	17.25665	80.37810	18500.2025	9629.3965	0	.12710	r
				Cantilever beams with linear mass and stiffness distributions						
1	1	0.29833	0.39272	0.23958	1.16194	3.09056	0.59789	1/4	0.20163	r
	2	.17146	.10558	.18630	1.84496	0	2.97335	0	.03838	r
	3	-.19809	-.26802	-.13341	.98538	0	-1.10249	0	.00508	r
	4	.13660	.21828	.09267	1.64834	0	.93662	0	.00220	r
	5	-.11352	-.19058	-.07526	1.14799	0	-.67480	0	.00094	r
2	2	1.61955	2.16178	1.31905	8.10433	121.37958	49.26172	1/4	.14854	r
	3	-.04235	-.47251	.12583	5.58811	0	64.85774	0	.04771	r
	4	-.72797	-.91085	-.53287	3.39561	0	-13.73693	0	.00514	r
	5	.47229	.76571	.30697	5.70988	0	18.98574	0	.00430	r
3	3	4.46488	6.23803	3.50050	19.32474	951.63772	444.99392	1/4	.13308	r
	4	-.81857	-2.08457	-.29328	8.91208	0	367.5131	0	.04928	r
	5	-1.53861	-1.78527	-1.18157	5.04050	0	-40.74667	0	.00317	r
4	4	9.01387	12.86480	6.94974	35.72554	3654.3173	1765.9083	1/4	.12905	r
	5	-2.14253	-4.75477	-1.05264	12.17992	0	1209.091	0	.05007	r
5	5	15.20032	21.94810	11.63995	57.03349	9985.9627	4870.7227	1/4	.12687	r

TABLE III

MODE RESULTS FOR NONROTATING CANTILEVER BEAMS WITH LINEAR

MASS AND STIFFNESS DISTRIBUTIONS

Station	$Y_1 \equiv \phi_1$	$Y_1' \equiv \phi_1'$	$Y_1'' \equiv \phi_1''$	$Y_2 \equiv \phi_2$	$Y_2' \equiv \phi_2'$	$Y_2'' \equiv \phi_2''$	$Y_3 \equiv \phi_3$	$Y_3' \equiv \phi_3'$	$Y_3'' \equiv \phi_3''$
$m = m_0$; $EI = EI_0$ (exact solution, ref. 20)									
0	0	0	3.5160	0	0	-22.0345	0	0	61.6972
1	.0168	.3274	3.0332	-.0926	-1.6776	-11.5406	.2281	3.7655	14.0984
2	.0639	.6065	2.5508	-.3011	-2.3240	-1.5432	.6045	3.1181	24.3627
3	.1365	.8378	2.0775	-.5261	-2.0351	6.9860	.7562	-.3551	-40.5613
4	.2299	1.0226	1.6214	-.6835	-1.0114	12.9888	.5259	-4.0599	29.2300
5	.3395	1.1631	1.1938	-.7137	.4531	15.7253	.0197	-5.5520	1.2145
6	.4611	1.2627	.8083	-.5895	2.0194	15.0599	-.4738	-3.7912	32.4481
7	.5959	1.3266	.4799	-.3171	3.3709	11.5931	-.6574	.3568	46.6579
8	.7255	1.3612	.2246	.0700	4.2876	6.6336	-.3949	4.7354	37.2963
9	.8624	1.3745	.0590	.5238	4.7095	2.0411	.2285	7.3385	14.0713
10	1.0000	1.3765	0	1.0000	4.7808	0	1.0000	7.8487	0
$m = m_0$; $EI = EI_0$									
0	0		3.5104	0		-22.0247	0		61.7316
		0.1695			-0.9051			2.2608	
1	.0169		3.0282	-.0925		-11.5367	.2261		14.2680
		.4723			-2.0829			3.7628	
2	.0642		2.5482	-.3008		-1.5444	.6024		-24.1735
		.7271			-2.2495			1.5296	
3	.1369		2.0760	-.5257		6.9810	.7553		-40.5000
		.9347			-1.5725			-2.2914	
4	.2304		1.6207	-.6830		12.9814	.5262		-29.3314
		1.0968			-.3015			-5.0647	
5	.3400		1.1937	-.7131		15.7169	.0197		1.0704
		1.2162			1.2418			-4.9503	
6	.4617		.8087	-.5890		15.0516	-.4753		32.4148
		1.2970			2.7236			-1.8512	
7	.5914		.4806	-.3166		11.5857	-.6604		46.7572
		1.3451			3.8698			2.6262	
8	.7259		.2253	.0704		6.6278	-.3978		37.3956
		1.3676			4.5356			6.2482	
9	.8626		.0595	.5239		2.0377	.2270		14.0565
		1.3736			4.7607			7.7299	
10	1.0000		0	1.0000		0	1.0000		0

TABLE III.- Continued

MODE RESULTS FOR NONROTATING CANTILEVER BEAMS WITH LINEAR

MASS AND STIFFNESS DISTRIBUTIONS

$m = m_0$; $EI = EI_0\left(1 - \dfrac{\bar{x}}{2}\right)$

Station	Y_1	Y_1'	Y_1''	Y_2	Y_2'	Y_2''	Y_3	Y_3'	Y_3''
0	0		3.0852	0		-17.9825	0		49.0088
		0.1508			-0.7779			1.8715	
1	.0151		2.8044	-.0778		-10.5955	.1871		14.8158
		.4312			-1.8336			3.3746	
2	.0582		2.4942	-.2612		-2.7533	.5246		-16.8271
		.6807			-2.1111			1.8048	
3	.1263		2.1551	-.4723		4.8322	.7053		-34.9664
		.8962			-1.6386			-1.5083	
4	.2159		1.7910	-.6361		11.1252	.5543		-31.1090
		1.0753			-.5456			-4.4456	
5	.3234		1.4102	-.6907		15.0784	.1097		-6.4431
		1.2163			.9362			-5.0240	
6	.4450		1.0259	-.5971		15.9132	-.3927		26.1221
		1.3189			2.5002			-2.5050	
7	.5769		.6580	-.3470		13.4617	-.6432		47.5240
		1.3847			3.8252			2.0377	
8	.7154		.3350	.0355		8.4741	-.4394		43.8272
		1.4182			4.6675			6.2401	
9	.8572		.0967	.5022		2.8758	.1846		18.6063
		1.4278			4.9778			8.1542	
10	1.0000		0	1.0000		0	1.0000		0

$m = m_0$; $EI = EI_0(1 - \bar{x})$

Station	Y_1	Y_1'	Y_1''	Y_2	Y_2'	Y_2''	Y_3	Y_3'	Y_3''
0	0		2.5176	0		-11.4951	0		26.4729
		0.1247			-0.5178			1.0789	
1	.0125		2.4201	-.0518		-7.8970	.1079		11.4265
		.3667			-1.3001			2.2098	
2	.0491		2.2996	-.1818		-3.5774	.3289		-5.0368
		.5966			-1.6530			1.7288	
3	.1088		2.1512	-.3471		1.3316	.5018		-18.7863
		.8117			-1.5179			-.0799	
4	.1900		1.9705	-.4989		6.4680	.4938		-24.1585
		1.0088			-.8741			-2.3871	
5	.2908		1.7531	-.5863		11.2476	.2551		-16.5097
		1.1841			.2412			-3.9249	
6	.4093		1.4955	-.5622		14.8933	-.1374		4.6998
		1.3337			1.7135			-3.3940	
7	.5426		1.1943	-.3908		16.4929	-.4768		33.2025
		1.4531			3.3378			-.1303	
8	.6879		.8469	-.0570		15.0877	-.4899		54.9056
		1.5378			4.8142			5.1385	
9	.8417		.4513	.4244		9.7945	.0240		49.9675
		1.5829			5.7561			9.7602	
10	1.0000		0	1.0000		0	1.0000		0

TABLE III.- Continued

MODE RESULTS FOR NONROTATING CANTILEVER BEAMS WITH LINEAR

MASS AND STIFFNESS DISTRIBUTIONS

$$m = m_0\left(1 - \frac{x}{2}\right); \quad EI = EI_0$$

Station	Y_1	Y_1'	Y_1''	Y_2	Y_2'	Y_2''	Y_3	Y_3'	Y_3''
0	0		3.5961	0		-20.5149	0		56.8179
		0.1733			-0.8526			2.0307	
1	.0173		3.0782	-.0853		-10.2793	.2031		10.7772
		.4812			-1.8857			3.1960	
2	.0654		2.5638	-.2738		-.6581	.5227		-24.7575
		.7375			-1.9658			.9179	
3	.1392		2.0614	-.4704		7.2497	.6145		-36.5657
		.9437			-1.2637			-2.5205	
4	.2336		1.5835	-.5968		12.4090	.3624		-22.1859
		1.1020			-.0501			-4.6174	
5	.3438		1.1442	-.6018		14.2921	-.0993		6.8125
		1.2164			1.3533			-3.9663	
6	.4654		.7580	-.4665		13.0765	-.4960		32.2249
		1.2922			2.6423			-.8880	
7	.5946		.4391	-.2022		9.6161	-.5848		40.3627
		1.3362			3.5963			2.9901	
8	.7283		.1999	.1574		5.2513	-.2857		29.5511
		1.3562			4.1269			5.8749	
9	.8639		.0509	.5701		1.5398	.3018		10.3404
		1.3613			4.2990			6.9825	
10	1.0000		0	1.0000		0	1.0000		0

$$m = m_0\left(1 - \frac{x}{2}\right); \quad EI = EI_0\left(1 - \frac{x}{2}\right)$$

Station	Y_1	Y_1'	Y_1''	Y_2	Y_2'	Y_2''	Y_3	Y_3'	Y_3''
0	0		3.1688	0		-16.8561	0		45.1241
		0.1546			-0.7222			1.6861	
1	.0155		2.8585	-.0722		-9.5343	.1686		11.7757
		.4404			-1.6728			2.8950	
2	.0595		2.5168	-.2395		-1.8680	.4581		-17.8557
		.6921			-1.8638			1.2361	
3	.1287		2.1467	-.4259		5.2897	.5817		-32.3125
		.9068			-1.3480			-1.8134	
4	.2194		1.7557	-.5607		10.8679	.4004		-24.9765
		1.0823			-.2821			-4.1661	
5	.3276		1.3563	-.5889		13.9363	-.0162		-.2658
		1.2180			1.0866			-4.1669	
6	.4493		.9647	-.4802		14.0175	-.4330		27.5563
		1.3144			2.4651			-1.5214	
7	.5808		.6034	-.2337		11.3083	-.5851		42.1923
		1.3748			3.5808			2.5189	
8	.7183		.2979	.1244		6.7837	-.3333		35.4166
		1.4046			4.2586			5.9375	
9	.8587		.0836	.5502		2.1918	-.2605		13.9636
		1.4129			4.4978			7.3951	
10	1.0000		0	1.0000		0	1.0000		1.0000

TABLE III.- Continued

MODE RESULTS FOR NONROTATING CANTILEVER BEAMS WITH LINEAR

MASS AND STIFFNESS DISTRIBUTIONS

Station	Y_1	Y_1'	Y_1''	Y_2	Y_2'	Y_2''	Y_3	Y_3'	Y_3''
			$m = m_0\left(1 - \dfrac{\bar{x}}{2}\right)$; $EI = EI_0(1 - \bar{x})$						
0	0		2.5984	0		-11.0011	0		25.2707
		0.1284			-0.4911			1.0099	
1	.0128		2.4797	-.0491		-7.2927	.1010		9.7964
		.3764			-1.2146			1.9826	
2	.0505		2.3338	-.1706		-2.8931	.2992		-6.5750
		.6098			-1.5002			1.3592	
3	.1115		2.1566	-.3206		1.9575	.4352		-18.9042
		.8255			-1.3046			-1.4506	
4	.1940		1.9455	-.4511		6.7820	.3901		-21.5881
		1.0200			-.6320			-2.5029	
5	.2960		1.6994	-.5143		10.9396	.1398		-11.5213
		1.1899			.4505			-3.5647	
6	.4150		1.4185	-.4692		13.7170	-.2167		9.3586
		1.3318			1.8050			-2.6041	
7	.5482		1.1048	-.2887		14.4325	-.4771		33.1815
		1.4423			3.2265			.6360	
8	.6924		.7609	.0339		12.5408	-.4135		47.5995
		1.5184			4.4562			5.2112	
9	.8443		.3911	.4796		7.7223	.1077		39.7770
		1.5575			5.2043			8.9234	
10	1.0000		0	1.0000		0	1.0000		0
			$m = m_0(1 - \bar{x})$; $EI = EI_0$						
0	0		4.0558	0		-15.2162	0		35.5410
		0.1939			-0.6069			1.1740	
1	.0194		3.3450	-.0607		-6.2023	.1174		2.2191
		.5284			-1.2348			1.4916	
2	.0722		2.6451	-.1842		1.8823	.2666		-19.6272
		.7929			-1.0659			-.2901	
3	.1515		1.9813	-.2908		7.6453	.2375		-19.7496
		.9911			-.3292			-2.1229	
4	.2506		1.3838	-.3237		10.2183	.0253		-2.7888
		1.1294			.6672			-2.3870	
5	.3636		.8803	-.2570		9.7358	-.2135		15.9480
		1.2175			1.6238			-.8834	
6	.4853		.4904	-.0946		7.2110	-.3018		23.7445
		1.2665			2.3397			1.3851	
7	.6120		.2218	.1394		4.0543	-.1633		18.8323
		1.2887			2.7503			3.2238	
8	.7408		.0680	.4144		1.5122	.1591		8.5833
		1.2955			2.9121			4.1081	
9	.8704		.0068	.7056		.2282	.5699		1.4574
		1.2962			2.9437			4.3010	
10	1.0000		0	1.0000		0	1.0000		0

TABLE III.- Concluded

MODE RESULTS FOR NONROTATING CANTILEVER BEAMS WITH LINEAR

MASS AND STIFFNESS DISTRIBUTIONS

$$m = m_0(1 - \bar{x}); \quad EI = EI_0\left(1 - \frac{\bar{x}}{2}\right)$$

Station	Y_1	Y_1'	Y_1''	Y_2	Y_2'	Y_2''	Y_3	Y_3'	Y_3''
0	0		3.6228	0		-12.6640	0		28.6145
		0.1752			-0.5212			0.9900	
1	.0175		3.1505	-.0521		-5.9369	.0990		3.6038
		.4903			-1.1148			1.3986	
2	.0666		2.6356	-.1636		.8058	.2389		-15.6241
		.7539			-1.0442			-.0314	
3	.1419		2.0961	-.2680		6.3475	.2357		-18.9598
		.9635			-.4288			-1.7917	
4	.2383		1.5602	-.3109		9.5678	.0566		-6.0124
		1.1195			.5049			-2.3466	
5	.3502		1.0620	-.2604		10.0140	-.1781		12.4980
		1.2257			1.4867			-1.1598	
6	.4728		.6358	-.1118		8.1088	-.2941		23.4526
		1.2893			2.2874			1.0759	
7	.6017		.3106	.1170		4.9844	-.1865		21.2750
		1.3203			2.7856			3.1346	
8	.7338		.1034	.3955		2.0367	.1270		10.8683
		1.3307			2.9997			4.2345	
9	.8668		.0113	.6955		.3379	.5504		2.0489
		1.3318			3.0448			4.4958	
10	1.0000		0	1.0000		0	1.0000		0

$$m = m_0(1 - \bar{x}); \quad EI = EI_0(1 - \bar{x})$$

Station	Y_1	Y_1'	Y_1''	Y_2	Y_2'	Y_2''	Y_3	Y_3'	Y_3''
0	0		3.0750	0		-8.9963	0		18.1439
		0.1507			-0.3854			0.6710	
1	.0151		2.8299	-.0385		-4.9931	.0671		4.1930
		.4337			-.8801			1.0985	
2	.0584		2.5321	-.1266		-.4387	.1769		-8.8006
		.6869			-.9247			.2793	
3	.1271		2.1832	-.2190		4.0280	.2049		-14.5066
		.9052			-.5297			-1.0798	
4	.2176		1.7937	-.2720		7.5634	.0969		-9.2434
		1.0846			-.2128			-1.9343	
5	.3261		1.3813	-.2507		9.4334	-.0965		4.3850
		1.2227			1.1393			-1.4924	
6	.4484		.9705	-.1368		9.2835	-.2458		18.4222
		1.3198			2.0523			.2825	
7	.5803		.5903	.0684		7.3013	-.2175		24.3923
		1.3788			2.7735			2.6264	
8	.7182		.2735	.3458		4.2407	.0451		18.9564
		1.4061			3.1987			4.4100	
9	.8589		.0547	.6657		1.3128	.4861		6.8571
		1.4116			3.3434			5.1389	
10	1.0000		1.0000	1.0000		0	1.0000		0

TABLE IV

MODE RESULTS FOR NONROTATING HINGED BEAMS WITH LINEAR MASS AND STIFFNESS DISTRIBUTIONS

Station	$Y_1 \equiv \phi_1$	$Y_1' \equiv \phi_1'$	$Y_1'' \equiv \phi_1''$	$Y_2 \equiv \phi_2$	$Y_2' \equiv \phi_2'$	$Y_2'' \equiv \phi_2''$	$Y_3 \equiv \phi_3$	$Y_3' \equiv \phi_3'$	$Y_3'' \equiv \phi_3''$
				$m = m_0$; $EI = EI_0$ (exact solution, ref. 20)					
0	0	-2.7002	0	0	5.0043	0	0	-7.2193	0
1									
2									
3	-.4830	-1.8617	7.9756	.7001	.7950	-34.8133	-.6299	3.2792	65.6943
4									
5									
6	-.6620	.1938	11.6061	.2257	-4.7026	-10.5596	.5732	4.2548	-59.5223
7									
8									
9	-.3973	2.3756	9.3030	-.6005	-2.0600	32.9576	.1190	-7.0448	-10.6536
10									
11									
12	.2274	3.6749	3.5134	-.2940	4.9033	26.8434	-.6076	2.8935	76.8702
13									
14									
15	1.0000	3.9297	0	1.0000	7.0686	0	1.0000	10.2102	0
				$m = m_0$; $EI = EI_0$					
0	0		0	0		0	0		0
		-2.6675			4.8253			-6.5137	
1	.1778		2.9017	.3217		-16.1228	-.4342		43.4748
		-2.4751			3.7708			-3.7078	
2	-.3428		5.6183	.5731		-28.5821	-.6814		69.7829
		-2.1026			1.9000			.7747	
3	-.4830		7.9748	.6997		-34.8100	-.6298		64.4864
		-1.5737			-.3784			4.9212	
4	-.5879		9.8240	.6745		-33.4256	-.3017		30.1462
		-.9222			-2.5660			6.8673	
5	-.6494		11.0559	.5034		-24.7037	.1561		-17.7598
		-.1890			-4.1825			5.7417	
6	-.6620		11.6059	.2246		-10.5043	.5389		-57.7175
		.5809			-4.8692			2.0541	
7	-.6233		11.4610	-.1000		6.1398	.6758		-71.7578
		1.3413			-4.4659			-2.5328	
8	-.5339		10.6619	-.3977		21.7025	.5070		-53.4956
		2.0490			-3.0431			-5.9464	
9	-.3973		9.3030	-.6006		32.9430	.1106		-10.8931
		2.6669			-.8832			-6.6245	
10	-.2195		7.5279	-.6595		37.6597	-.3311		37.3827
		3.1679			1.5878			-4.2021	
11	-.0083		5.5239	-.5667		35.2256	-.6112		70.4947
		3.5357			3.9028			.3507	
12	.2274		3.5133	-.2935		26.7997	-.5878		75.1702
		3.7713			5.6720			5.2169	
13	.4788		1.7444	.0847		15.2316	-.2400		52.3442
		3.8904			6.6930			8.6477	
14	.7382		.4821	.5309		4.6639	.3365		18.2343
		3.9269			7.0367			9.9528	
15	1.0000		0	1.0000		0	1.0000		0

TABLE IV.- Continued

MODE RESULTS FOR NONROTATING HINGED BEAMS WITH LINEAR MASS AND STIFFNESS DISTRIBUTIONS

Station	Y_1	Y_1'	Y_1''	Y_2	Y_2'	Y_2''	Y_3	Y_3'	Y_3''
$m = m_0$; $EI = EI_0\left(1 - \dfrac{\bar{x}}{2}\right)$								
0	0		0	0		0	0		0
		-2.4011			4.2349			-5.7084	
1	-.1601		2.1968	.2823		-12.1633	-.3806		32.8485
		-2.2545			3.4337			-3.5718	
2	-.3104		4.4128	.5112		-22.5509	-.6187		57.1675
		-1.9610			1.9512			.0330	
3	-.4411		6.5121	.6413		-29.0968	-.6118		59.0998
		-1.5283			.0414			3.8918	
4	-.5430		8.3585	.6441		-30.1375	-.3523		36.3014
		-.9732			-1.9342			6.2024	
5	-.6079		9.8221	.5151		-24.9921	.0612		-3.3443
		-.3211			-3.5700			5.9598	
6	-.6293		10.7894	.2771		-14.2022	.4585		-43.9333
		.3949			-4.4964			3.1149	
7	-.6030		11.1731	-.0227		.4449	.6662		-67.5091
		1.1363			-4.4618			-1.2129	
8	-.5272		10.9231	-.3201		16.1636	.5843		-61.8610
		1.8610			-3.3977			-5.1621	
9	-.4031		10.0375	-.5466		29.6539	.2385		-26.7887
		2.5269			-1.4512			-6.8767	
10	-.2347		8.5728	-.6433		37.8479	-.2199		24.2333
		3.0959			1.0303			-5.2857	
11	-.0283		6.6547	-.5747		38.6874	-.5723		68.7554
		3.5382			3.5665			-.8435	
12	.2076		4.4883	-.3369		31.8978	-.6286		85.5398
		3.8377			5.6618			4.6710	
13	.4635		2.3693	.0406		19.5720	-.3172		66.4744
		3.9981			6.9620			8.9872	
14	.7300		.6982	.5047		6.4608	.2820		25.3995
		4.0501			7.4296			10.7702	
15	1.0000		0	1.0000		0	1.0000		0
$m = m_0$; $EI = EI_0(1 - \bar{x})$								
0	0		0	0		0	0		0
		-1.8612			2.8391			-3.4482	
1	-.1241		1.2599	.1893		-6.0403	-.2299		13.9649
		-1.7765			2.4377			-2.5277	
2	-.2425		2.6412	.3518		-11.8108	-.3984		27.3446
		-1.6000			1.6557			-.7583	
3	-.3492		4.0919	.4622		-16.5435	-.4489		33.6311
		-1.3272			.5632			1.4065	
4	-.4377		5.5538	.4997		-19.2804	-.3552		29.5841
		-.9572			-.7071			3.2949	
5	-.5015		6.9600	.4526		-19.1626	-.1335		14.6758
		-.4940			-1.9666			4.2065	
6	-.5344		8.2356	.3215		-15.6121	.1449		-7.9710
		.0539			-2.9887			3.6496	
7	-.5308		9.2994	.1222		-8.4580	.3882		-31.5748
		.6722			-3.5362			1.5779	
8	-.4860		10.0650	-.1135		1.9007	.4934		-46.9233
		1.3411			-3.3992			-1.4555	
9	-.3966		10.4435	-.3402		14.3995	.3964		-44.9846
		2.0346			-2.4389			-4.3171	
10	-.2609		10.3457	-.5027		27.2556	.1086		-20.5659
		2.7212			-.6351			-5.5508	
11	-.0795		9.6854	-.5451		38.0134	-.2615		23.7570
		3.3634			1.8695			-3.8912	
12	.1447		8.3825	-.4204		43.7041	-.5209		74.7164
		3.9182			4.7359			1.0372	
13	.4059		6.3673	-.1047		41.1267	-.4517		108.0221
		4.3385			7.4140			8.0094	
14	.6951		3.5845	.3896		27.2670	.0822		92.3208
		4.5730			9.1568			13.7667	
15	1.0000		0	1.0000		0	1.0000		0

TABLE IV.- Continued

MODE RESULTS FOR NONROTATING HINGED BEAMS WITH LINEAR MASS AND STIFFNESS DISTRIBUTIONS

$$m = m_0\left(1 - \frac{\bar{x}}{2}\right); \quad EI = EI_0$$

Station	Y_1	Y_1'	Y_1''	Y_2	Y_2'	Y_2''	Y_3	Y_3'	Y_3''
0	0		0	0		0	0		0
		-2.3363			4.0912			-5.5947	
1	-.1558		2.8306	.2727		-15.4147	-.3730		43.3868
		-2.1488			3.0857			-2.8156	
2	-.2990		5.4383	.4785		-26.8339	-.5607		65.7475
		-1.7886			1.3335			1.3899	
3	-.4182		7.6302	.5674		-31.5958	-.4680		55.0307
		-1.2830			-.7308			4.9171	
4	-.5038		9.2606	.5186		-28.7323	-.1402		17.6072
		-.6693			-2.6093			6.0537	
5	-.5484		10.2394	.3447		-19.1453	.2634		-27.5745
		.0096			-3.8621			4.2957	
6	-.5478		10.5356	.0872		-5.2516	.5497		-58.9163
		.7083			-4.2068			.5225	
7	-.5005		10.1773	-.1932		9.6994	.5846		-62.3944
		1.3836			-3.5727			-3.4830	
8	-.4083		9.2456	-.4314		22.4495	.3524		-37.4169
		1.9975			-2.1027			-5.8934	
9	-.2751		7.8663	-.5716		30.4780	-.0405		3.9909
		2.5203			-.1044			-5.6463	
10	-.1071		6.1992	-.5787		32.5262	-.4169		43.5972
		2.9330			2.0318			-2.8473	
11	.0884		4.4254	-.4431		28.8072	-.6068		65.5174
		3.2285			3.9288			1.3765	
12	.3037		2.7358	-.1812		20.8910	-.5150		62.9664
		3.4124			5.3124			5.4594	
13	.5312		1.3192	.1730		11.3644	-.1510		40.7963
		3.5029			6.0784			8.1471	
14	.7647		.3538	.5782		3.3416	.3921		13.4256
		3.5298			6.3271			9.1186	
15	1.0000		0	1.0000		0	1.0000		0

$$m = m_0\left(1 - \frac{\bar{x}}{2}\right); \quad EI = EI_0\left(1 - \frac{\bar{x}}{2}\right)$$

Station	Y_1	Y_1'	Y_1''	Y_2	Y_2'	Y_2''	Y_3	Y_3'	Y_3''
0	0		0	0		0	0		0
		-2.1075			3.5959			-4.8668	
1	-.1405		2.1650	.2937		-11.7139	-.3245		32.6840
		-1.9632			2.8262			-2.7515	
2	-.2714		4.3162	.4281		-21.3762	-.5079		53.5102
		-1.6764			1.4247			.6587	
3	-.3831		6.2980	.5231		-26.7516	-.4640		50.6902
		-1.2583			-.3274			3.9138	
4	-.4670		7.9670	.5013		-26.4102	-.2030		24.6040
		-.7296			-2.0558			5.4909	
5	-.5157		9.2014	.3642		-20.1587	.1630		-13.7307
		-.1191			-3.3735			4.6057	
6	-.5236		9.9102	.1393		-9.1019	.4700		-47.2762
		.5384			-3.9664			1.5683	
7	-.4877		10.0412	-.1251		4.5670	.5746		-60.4825
		1.2046			-3.6638			-2.3134	
8	-.4074		9.5875	-.3694		18.0105	.4204		-46.3612
		1.8407			-2.4809			-5.2843	
9	-.2847		8.5912	-.5347		28.3717	.0681		-9.9582
		2.4110			-.6194			-5.9149	
10	-.1240		7.1455	-.5760		33.4411	-.3262		33.4867
		2.8856			1.5746			-3.7545	
11	.0684		5.3954	-.4711		32.2076	-.5765		65.2075
		3.2447			3.6896			.4454	
12	.2847		3.5362	-.2251		25.2411	-.5468		71.5806
		3.4812			5.3528			5.0645	
13	.5168		1.8125	.1318		14.7929	-.2092		51.3484
		3.6044			6.3407			8.4144	
14	.7571		.5182	.5545		4.6798	.3517		18.4557
		3.6433			6.6828			9.7239	
15	1.0000		0	1.0000		0	1.0000		0

TABLE IV.- Continued

MODE RESULTS FOR NONROTATING HINGED BEAMS WITH LINEAR MASS AND STIFFNESS DISTRIBUTIONS

Station	Y_1	$Y_1{}'$	$Y_1{}''$	Y_2	$Y_2{}'$	$Y_2{}''$	Y_3	$Y_3{}'$	$Y_3{}''$
$m = m_0\left(1 - \frac{\bar{x}}{2}\right);\ EI = EI_0(1 - \bar{x})$									
0	0		0	0		0	0		0
		-1.6543			3.4651			-3.0051	
1	-.1103		1.2820	.1643		-6.0465	-.2003		14.3350
		-1.5682			2.0642			-2.0645	
2	-.2148		2.6679	.3020		-11.6724	-.3380		26.9253
		-1.3902			1.2932			-.3264	
3	-.3075		4.0886	.3882		-15.9371	-.3597		31.1310
		-1.1178			.2431			1.6735	
4	-.3500		5.4721	.4044		-17.8592	-.2482		24.3216
		-.7536			-.9314			3.2227	
5	-.4323		6.7435	.3423		-16.7340	-.0333		7.4502
		-.3051			-2.0293			3.6744	
6	-.4526		7.8273	.2070		-12.2504	.2116		-14.6474
		.2153			-2.8297			2.6991	
7	-.4383		8.6503	.0184		-4.6272	.3916		-34.2032
		.7902			-3.1264			.4730	
8	-.3856		9.1450	-.1901		5.3591	.4231		-42.7143
		1.3977			-2.7646			-2.2779	
9	-.2924		9.2516	-.3744		16.3886	.2712		-33.8828
		2.0120			-1.6775			-4.4252	
10	-.1583		8.9210	-.4862		26.6827	-.0238		-6.5779
		2.6041			.0846			-4.7776	
11	.0153		8.1173	-.4806		34.1999	-.3423		33.1451
		3.1425			2.3363			-2.5501	
12	.2248		6.8194	-.3248		36.8503	-.5123		71.8610
		3.5944			4.7546			2.1574	
13	.4645		5.0225	-.0078		32.7806	-.3684		90.9456
		3.9265			6.8945			8.0186	
14	.7262		2.7389	.4518		20.6465	.1667		71.1259
		4.1066			8.2232			12.4991	
15	1.0000		0	1.0000		0	1.0000		0
$m = m_0(1 - \bar{x});\ EI = EI_0$									
0	0		0	0		0	0		0
		-1.5091			2.1411			-2.5582	
1	-.1006		2.6772	.1427		-11.3779	-.1705		27.6738
		-1.3324			1.4053			-.8148	
2	-.1894		5.0299	.2364		-18.6533	-.2249		36.4609
		-1.0003			.1972			1.4862	
3	-.2561		6.8123	.2496		-19.5232	-.1258		20.8593
		-.5501			-1.0696			2.8127	
4	-.2928		7.8813	.1783		-14.1242	.0617		-7.4162
		-.0288			-1.9884			2.3549	
5	-.2947		8.2013	.0457		-4.5930	.2187		-30.0183
		.5141			-2.2893			.4591	
6	-.2604		7.8349	-.1069		5.9348	.2493		-34.1493
		1.0334			-1.9048			-1.7115	
7	-.1916		6.9215	-.2339		14.4825	.1352		-19.1967
		1.4928			-.9611			-2.9417	
8	.0920		5.6493	-.2980		19.1285	-.0409		5.1045
		1.8686			.2897			-2.6244	
9	.0325		4.2248	-.2787		19.3997	-.2358		25.9492
		2.1505			1.5634			-.9652	
10	.1759		2.8430	-.1744		16.1429	-.3002		34.8202
		2.3411			2.6292			1.2810	
11	.3320		1.6634	.0008		11.0251	-.2148		30.8241
		2.4537			3.3640			3.2917	
12	.4956		.7904	.2251		5.8786	.0047		19.3206
		2.5083			3.7635			4.5778	
13	.6628		.2606	.4760		2.1146	.3098		7.7297
		2.5274			3.9154			5.1208	
14	.8313		.0359	.7370		.3109	.6512		1.2214
		2.5308			3.9444			5.2315	
15	1.0000		0	0		0	1.0000		0

TABLE IV.- Concluded

MODE RESULTS FOR NONROTATING HINGED BEAMS WITH LINEAR MASS AND STIFFNESS DISTRIBUTIONS

$$m = m_o(1 - \bar{x}); \quad EI = EI_o\left(1 - \frac{\bar{x}}{2}\right)$$

Station	Y_1	Y_1'	Y_1''	Y_2	Y_2'	Y_2''	Y_3	Y_3'	Y_3''
0	0		0	0		0	0		0
		-1.3685			1.8817			-2.2572	
1	-.0912		2.1268	.1254		-8.8479	-.1505		21.7677
		-1.2273			1.3053			-.8715	
2	-.1731		4.1481	.2125		-15.2839	-.2086		30.8281
		-.9526			.3843			1.0885	
3	-.2366		5.8470	.2332		-17.1710	-.1360		21.1573
		-.5655			-.8044			2.4377	
4	-.2743		7.0565	.1796		-13.8954	.0265		-1.3903
		-.0984			-1.7075			2.3568	
5	-.2808		7.6765	.0658		-6.4412	.1836		-23.3985
		.4100			-2.1257			.8750	
6	-.2535		7.6819	-.0759		3.0165	.2419		-32.2246
		.9190			-1.9280			-1.1742	
7	-.1922		7.1221	-.2045		11.8656	.1637		-23.1981
		1.3913			-1.1527			-2.6558	
8	-.0995		6.1118	-.2813		17.8750	-.0134		-1.5876
		1.7972			.0165			-2.7629	
9	.0203		4.8141	-.2802		19.8367	-.1976		21.2899
		2.1176			1.3170			-1.4052	
10	.1615		3.4186	-.1924		17.8332	-.2913		34.8049
		2.3460			2.4906			.8298	
11	.3179		2.1148	-.0264		13.0866	-.2359		34.5490
		2.4884			3.3583			3.0677	
12	.4838		1.0648	.1975		7.4790	-.0314		23.7284
		2.5613			3.8625			4.6312	
13	.6545		.3729	.4550		2.8817	.2773		10.2935
		2.5883			4.0667			5.3430	
14	.8271		.0547	.7261		.4541	.6335		1.7510
		2.5934			4.1079			5.4972	
15	1.0000		0	1.0000		0	1.0000		0

$$m = m_o(1 - \bar{x}); \quad EI = EI_o(1 - \bar{x})$$

Station	Y_1	Y_1'	Y_1''	Y_2	Y_2'	Y_2''	Y_3	Y_3'	Y_3''
0	0		0	0		0	0		0
		-1.1222			1.3728			-1.5560	
1	-.0748		1.4218	.0915		-5.2011	-.1037		11.8732
		-1.0267			1.0305			-.7877	
2	-.1433		2.8943	.1602		-9.6016	-.1562		18.9034
		-1.2587			.4020			.4284	
3	-.1989		4.2872	.1878		-11.9049	-.1277		16.7673
		-.5499			-.3755			1.5050	
4	-.2356		5.4778	.1620		-11.2941	-.0274		5.7258
		-.1864			-1.1116			1.8722	
5	-.2480		6.3621	.0879		-7.6441	.0975		-9.3345
		.2356			-1.6078			1.2737	
6	-.2323		6.8635	-.0193		-1.5725	.1824		-21.0490
		.6908			-1.7061			-.0748	
7	-.1862		6.9403	-.1331		5.6793	.1774		-23.0546
		1.1511			-1.3297			-1.5500	
8	-.1095		6.5903	-.2216		12.5389	.0741		-13.1568
		1.5883			-.5045			-2.3886	
9	-.0036		5.8531	-.2553		17.4785	-.0852		5.3345
		1.9768			.6438			-2.0398	
10	.1282		4.8088	-.2124		19.3913	-.2212		24.8731
		2.2964			1.9177			-.4364	
11	.2813		3.5747	-.0846		17.9102	-.2503		37.0753
		2.5345			3.0957			1.9527	
12	.4502		2.2986	.1218		13.5472	-.1201		36.7275
		2.6884			3.9904			4.3263	
13	.6275		1.1517	.3878		7.6745	.1683		24.6765
		2.7669			4.5050			5.9419	
14	.8139		.3206	.6882		2.3373	.5645		8.3232
		2.7912			4.6775			6.5395	
15	1.0000		0	1.0000		0	1.0000		0

TABLE V

MODE COEFFICIENTS FOR ROTATING BEAMS HINGED AT THE ROOT

$$\left[y_n = \sum_{q=0}^{5} A_{n_q} \phi_q \right]$$

n	q	A_{n_q}						
		Uniform mass and stiffness distributions					Linear mass and stiffness distributions $\left(m_t = EI_t = 0 \right)$	
		$\Omega/\omega_{NR_1} = 1$		$\Omega/\omega_{NR_1} = 1.02$	$\Omega/\omega_{NR_1} = 1.36$	$\Omega/\omega_{NR_1} = 1.44$	$\Omega/\omega_{NR_1} = 1$	
		$\bar{e} = 0\%$	$\bar{e} = 10\%$	$\bar{e} = 0\%$			$\bar{e} = 0\%$	$\bar{e} = 10\%$
		r = 0		r = 0.1	r = 0.5	r = 1	r = 0	
1	0	0	-0.00676	-2.99989	-1.50000	-3.00000	0.38847	0.38042
	1	.90279	.88995	3.59557	2.19920	3.57296	.57936	.57921
	2	.08290	.09482	.30674	.22694	.32128	.02942	.03739
	3	.01170	.01223	.06637	.05056	.07153	.00226	.00234
	4	.00209	.00150	.02200	.01656	.02408	.00053	.00071
	5	.00052	.00827	.00920	.00673	.01011	-.00003	-.00007
2	0	0	.00111	-3.00008	-1.50000	-3.00000	.21916	.21681
	1	-.08920	-.10460	-5.12037	-2.72581	-5.17981	.31280	.30752
	2	.95499	.95733	7.59936	4.20150	7.51089	.43608	.43748
	3	.11344	.13274	1.08367	.73215	1.18259	.02899	.03480
	4	.01745	.02015	.31287	.21113	.34805	.00216	.00241
	5	.00332	-.00672	.12455	.08096	.13835	.00082	.00098
3	0	0	-.00028	-3.00002	-1.50000	-3.00000	.15969	.15854
	1	-.00209	.00029	-4.11650	-2.04984	-4.10909	.21031	.20886
	2	-.12027	-.14548	-6.70530	-3.73548	-6.98322	.23822	.23474
	3	.99297	1.02956	12.14772	6.54922	12.06709	.36653	.36824
	4	.11228	.13716	2.01361	1.31803	2.27887	.02448	.02874
	5	.01711	-.02126	.66071	.41804	.74647	.00077	.00089

TABLE VI

MODE COEFFICIENTS FOR ROTATING CANTILEVER BEAMS

$$y_n = \sum_{q=1}^{5} A_{nq}\phi_q$$

n	q	A_{nq} Uniform mass and stiffness distributions												Linear mass and stiffness distributions ($m_t = EI_t = 0$)			
		$\Omega/\omega_{NR_1} = 2$		$\Omega/\omega_{NR_1} = 3$		$\Omega/\omega_{NR_1} = 4$		$\Omega/\omega_{NR_1} = 6$		$\Omega/\omega_{NR_1} = 7.37$	$\Omega/\omega_{NR_1} = 10.43$	$\Omega/\omega_{NR_1} = 10.42$	$\Omega/\omega_{NR_1} = 14.76$	$\Omega/\omega_{NR_1} = 1.97$		$\Omega/\omega_{NR_1} = 5.91$	
		$\bar{e}=0\%$	$\bar{e}=10\%$	$\bar{e}=0\%$	$\bar{e}=10\%$	$\bar{e}=0\%$	$\bar{e}=10\%$	$\bar{e}=0\%$	$\bar{e}=10\%$	$\bar{e}=0\%$	$\bar{e}=0\%$	$\bar{e}=0\%$	$\bar{e}=0\%$	$\bar{e}=0\%$	$\bar{e}=10\%$	$\bar{e}=0\%$	$\bar{e}=10\%$
		$r=0$								$r=0.5$	$r=1$	$r=0.5$	$r=1$	$r=0$			
1	1	1.04097	1.04089	1.06395	1.06197	1.07930	1.07532	1.09529	1.08853	1.10074	1.10782	1.10942	1.11411	1.03214	1.03585	1.08425	1.06814
	2	-.04833	-.04894	-.07740	-.07629	-.09825	-.09511	-.12241	-.11612	-.12739	-.13759	-.14118	-.14791	-.04119	-.04395	-.11831	-.10205
	3	.00871	.00955	.01624	.01732	.02318	.02415	.03332	.03361	.03361	.03803	.04038	.04345	.01013	.00911	.03656	.03537
	4	-.00204	-.00230	-.00445	-.00486	-.00713	-.00756	-.01177	-.01195	-.01235	-.01501	-.01645	.01863	-.00217	-.00190	-.01081	-.01003
	5	.00069	.00080	.00165	.00187	.00290	.00320	.00557	.00593	.00538	.00676	.00783	.00899	.00109	.00088	.00832	.00858
2	1	.04394	.04433	.06651	.06533	.08100	.07815	.09573	.09055	-1.52892	-3.09047	-1.48611	-3.03164	.45247	.45453	.47752	.46764
	2	.94669	.94331	.91470	.91041	.89001	.88517	.85678	.85126	2.46260	4.10283	2.44348	4.08961	.52469	.52591	.48967	.48853
	3	.00269	.00501	.00581	.01007	.00935	.01538	.01593	.02443	-.04590	-.20169	-.08323	-.26294	.01908	.01627	.01733	.02711
	4	.00864	.00957	.01669	.01827	.02505	.02708	.03951	.04180	.13421	.24787	.16179	.28779	.00461	.00390	.02109	.02216
	5	-.00197	-.00222	-.00372	-.00409	-.00541	-.00578	-.00796	-.00805	-.02198	-.05853	.03593	-.08283	-.00085	-.00062	-.00561	-.00544
3	1	-.00837	-.00927	-.01519	-.01646	-.02116	-.02251	-.02918	-.03024	-2.20034	-4.37577	-2.22531	-4.40523	.26764	.26961	.25087	.24559
	2	-.00253	.00497	-.00554	-.01020	-.00925	-.01605	-.01695	-.02690	-2.10654	-3.87354	-2.02987	-3.71664	.29081	.29247	.28773	.28096
	3	.98895	.98801	.97492	.97254	.95671	.95254	.91636	.90939	4.63597	8.28092	4.54906	8.16877	.41432	.41420	.38838	.38889
	4	.01395	.01729	.02882	.03526	.04586	.05527	.07897	.09244	.32641	.31370	.28756	.19255	.02430	.02151	.04932	.05888
	5	.00802	.00894	.01699	.01887	.02783	.03075	.05079	.05531	.34450	.65469	.41856	.76055	.00292	.00222	.02369	.02569

Uniform

"Linear"

Hinged beams
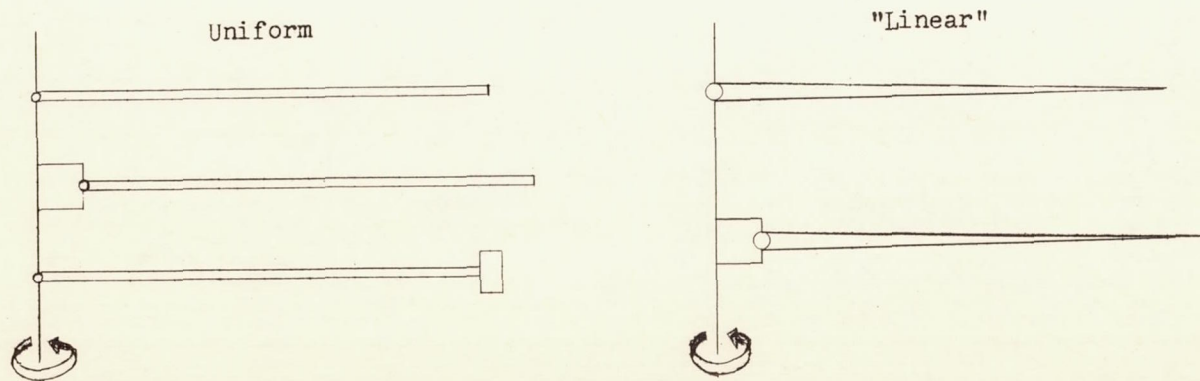
Uniform

"Linear"

Figure 1.- Beams treated by both the "exact" and Rayleigh methods.
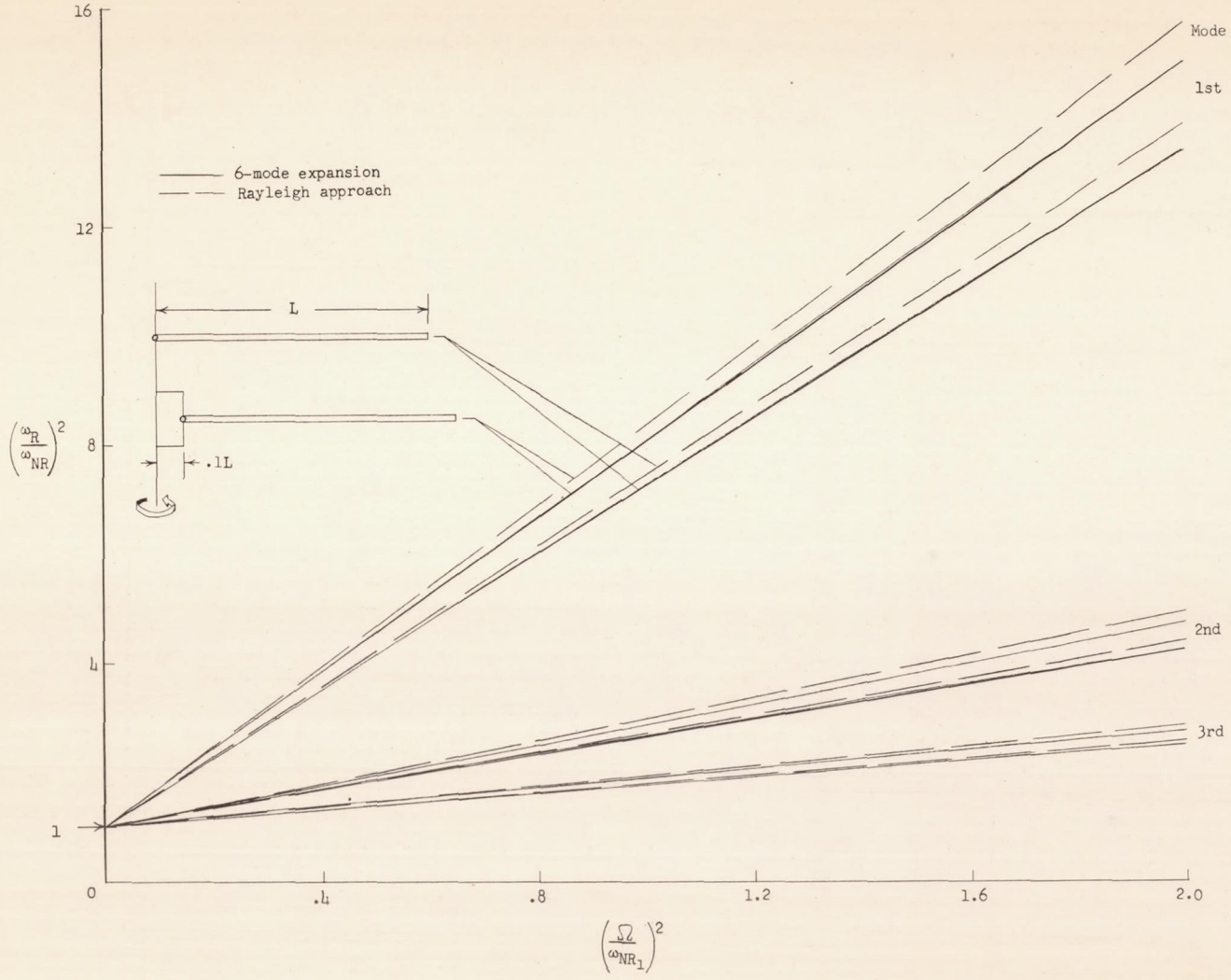
Figure 2.- Effect of rotational speed on the bending frequencies of a uniform hinged beam.
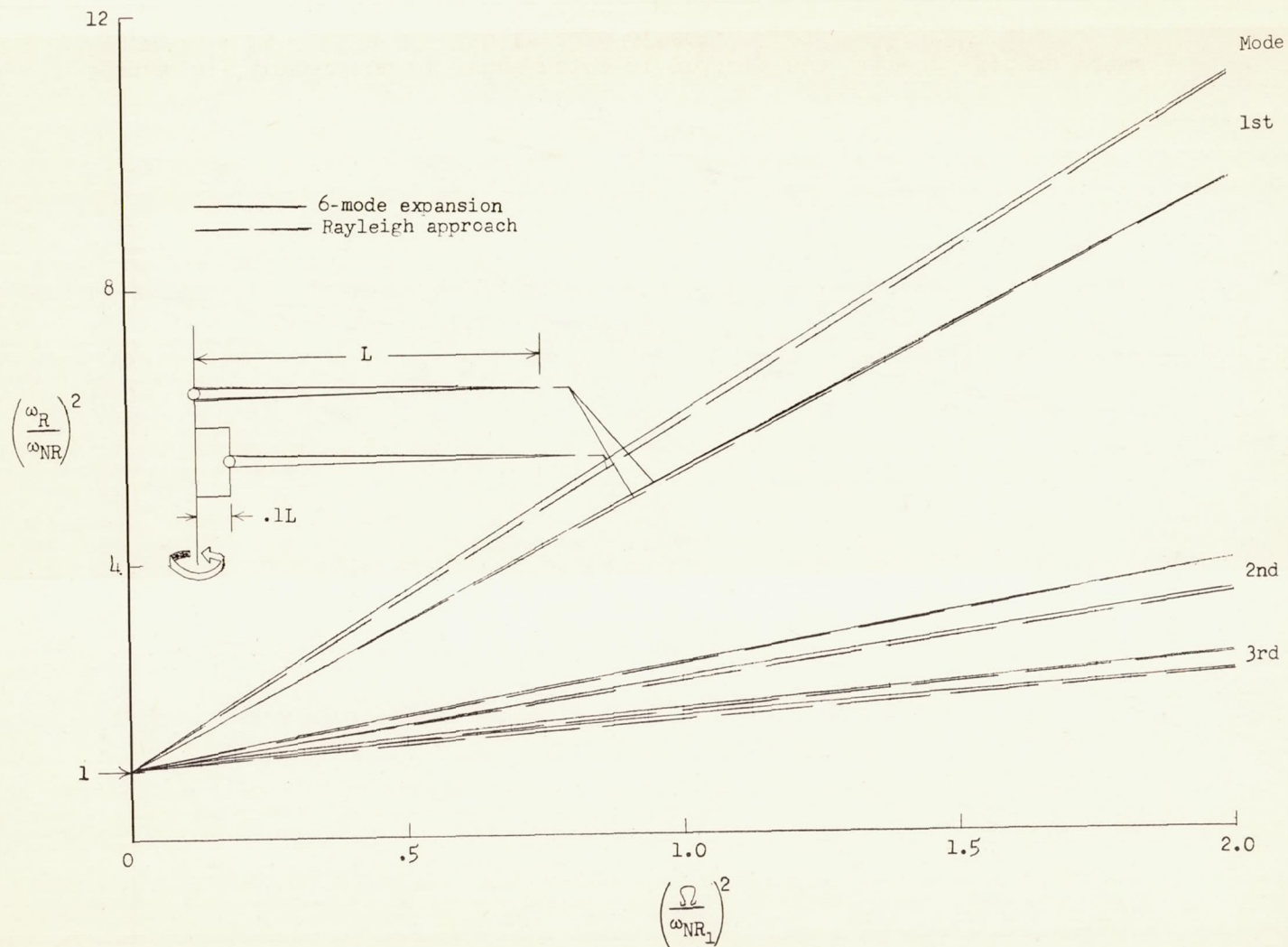
Figure 3.- Effect of rotational speed on the bending frequencies of a
hinged beam with linear mass and stiffness distribution.
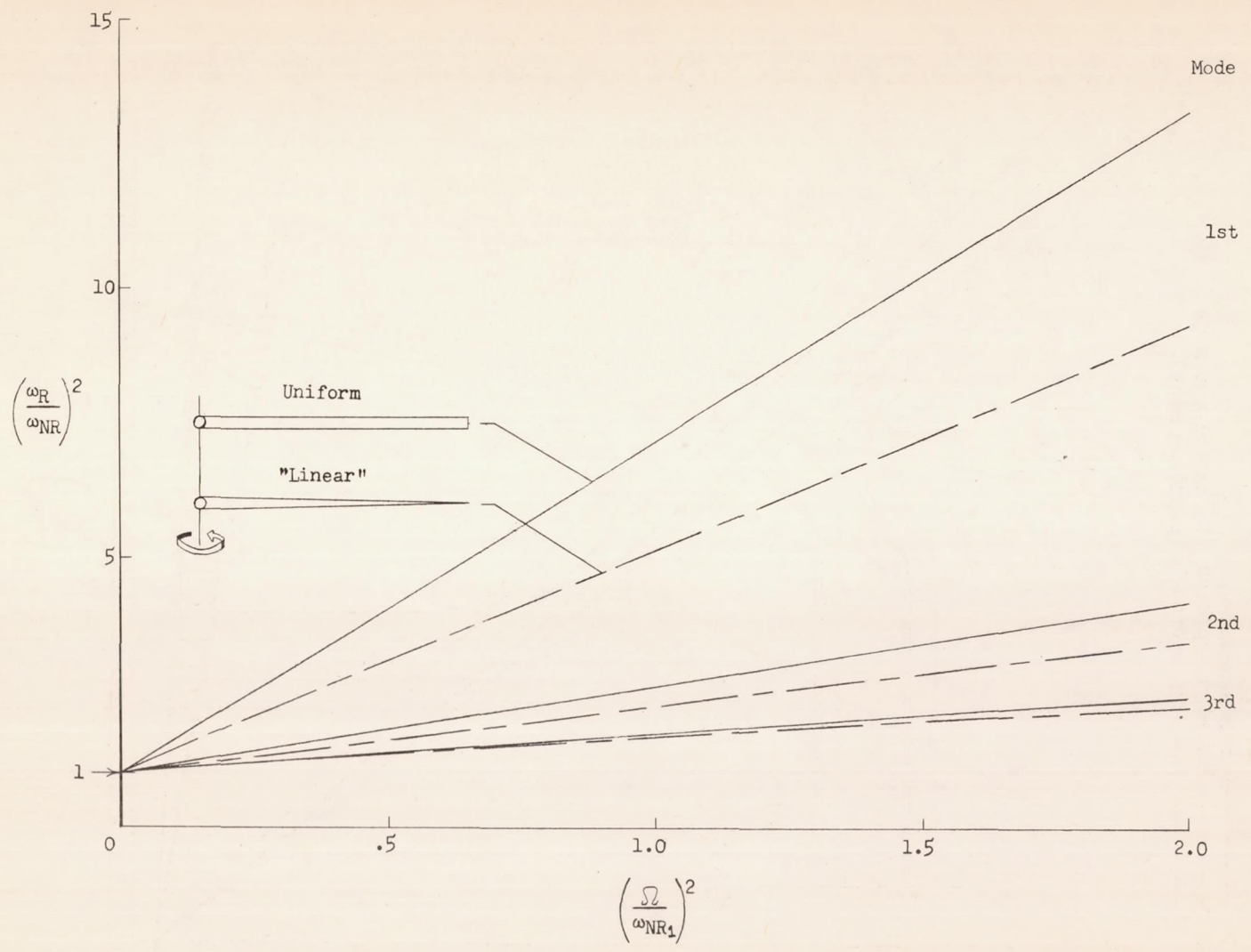
Figure 4.- Comparison of frequencies of uniform and "linear" hinged beams with zero offset.
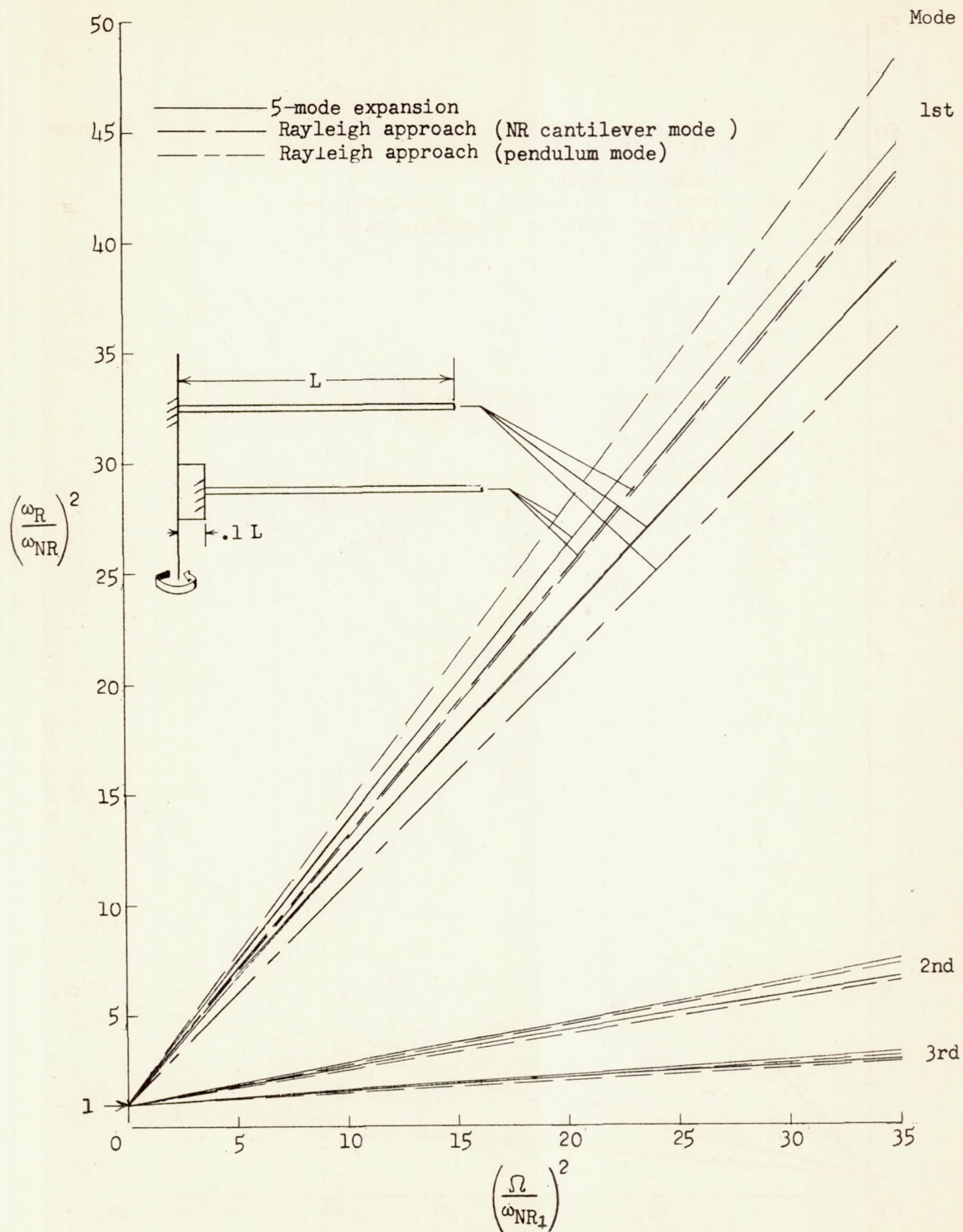
Figure 5.- Effect of rotational speed on the bending frequencies of a
uniform cantilever beam.
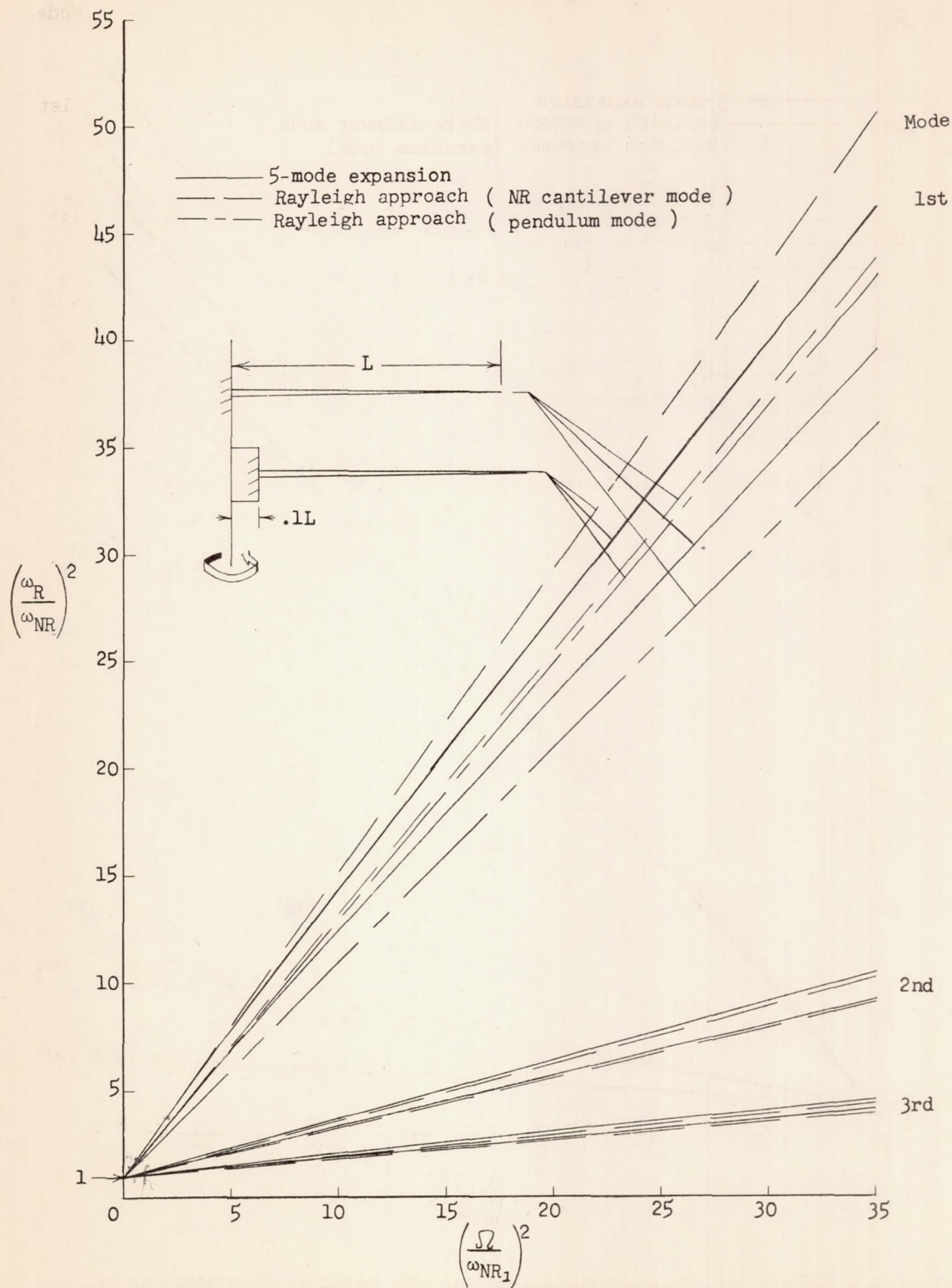
Figure 6.- Effect of rotational speed on the bending frequencies of a
cantilever beam with linear mass and stiffness distribution.
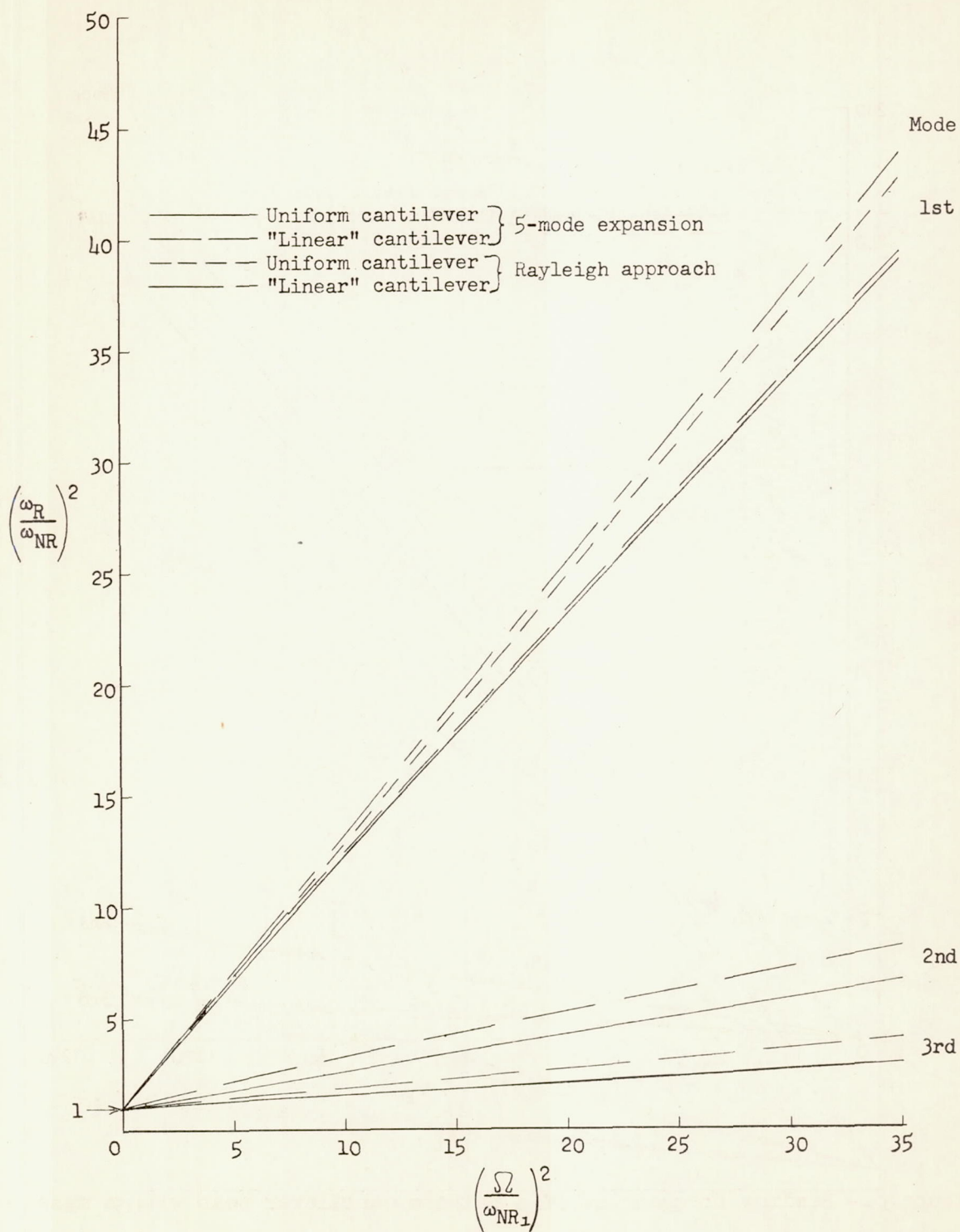
Figure 7.- Comparison of frequencies of uniform and "linear" cantilever
beams with zero offset.
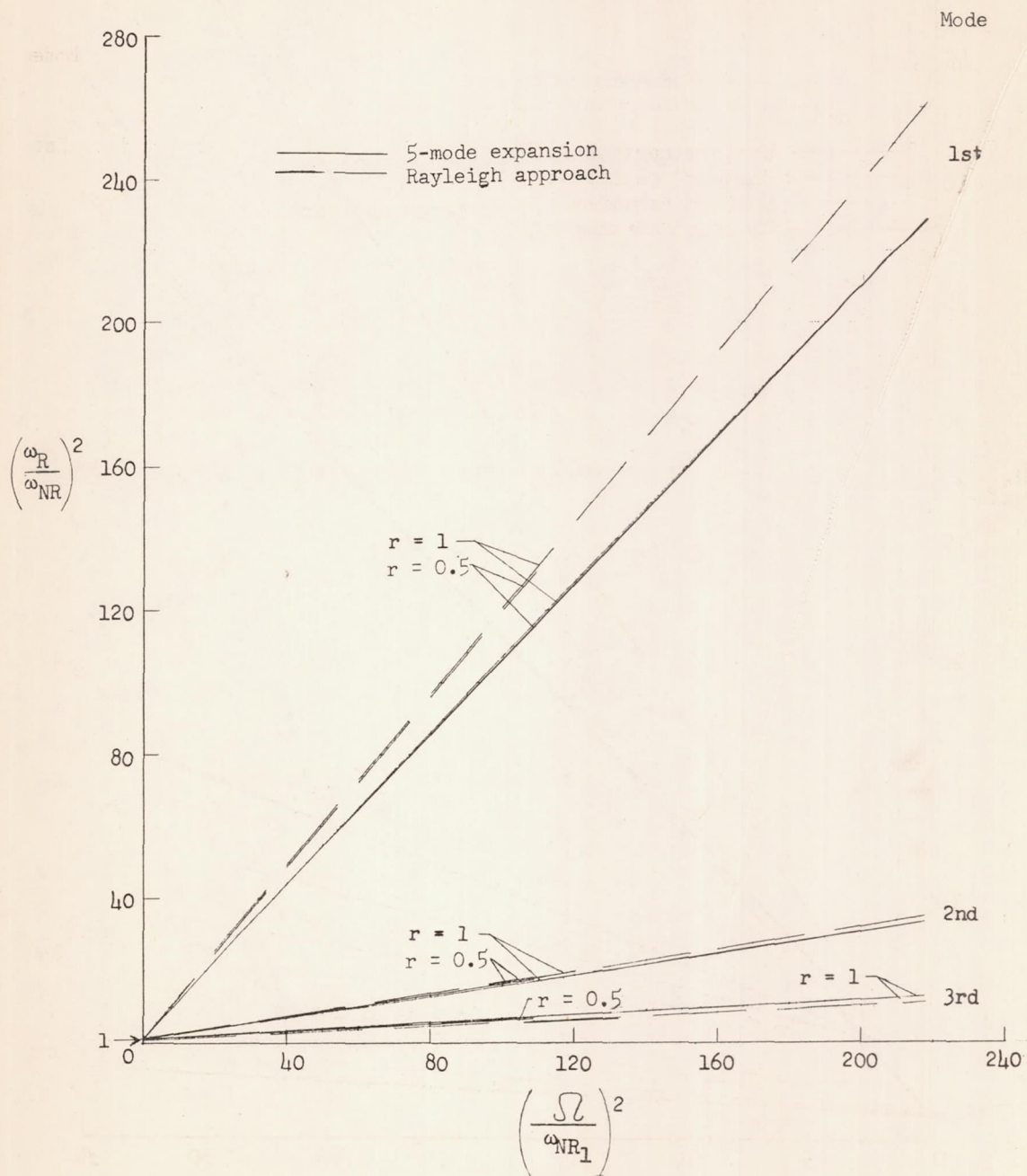
Figure 8.- Bending frequencies of a uniform cantilever beam with a mass at the tip and with zero offset. $r = \dfrac{\text{Tip mass}}{\text{Beam mass}}$.
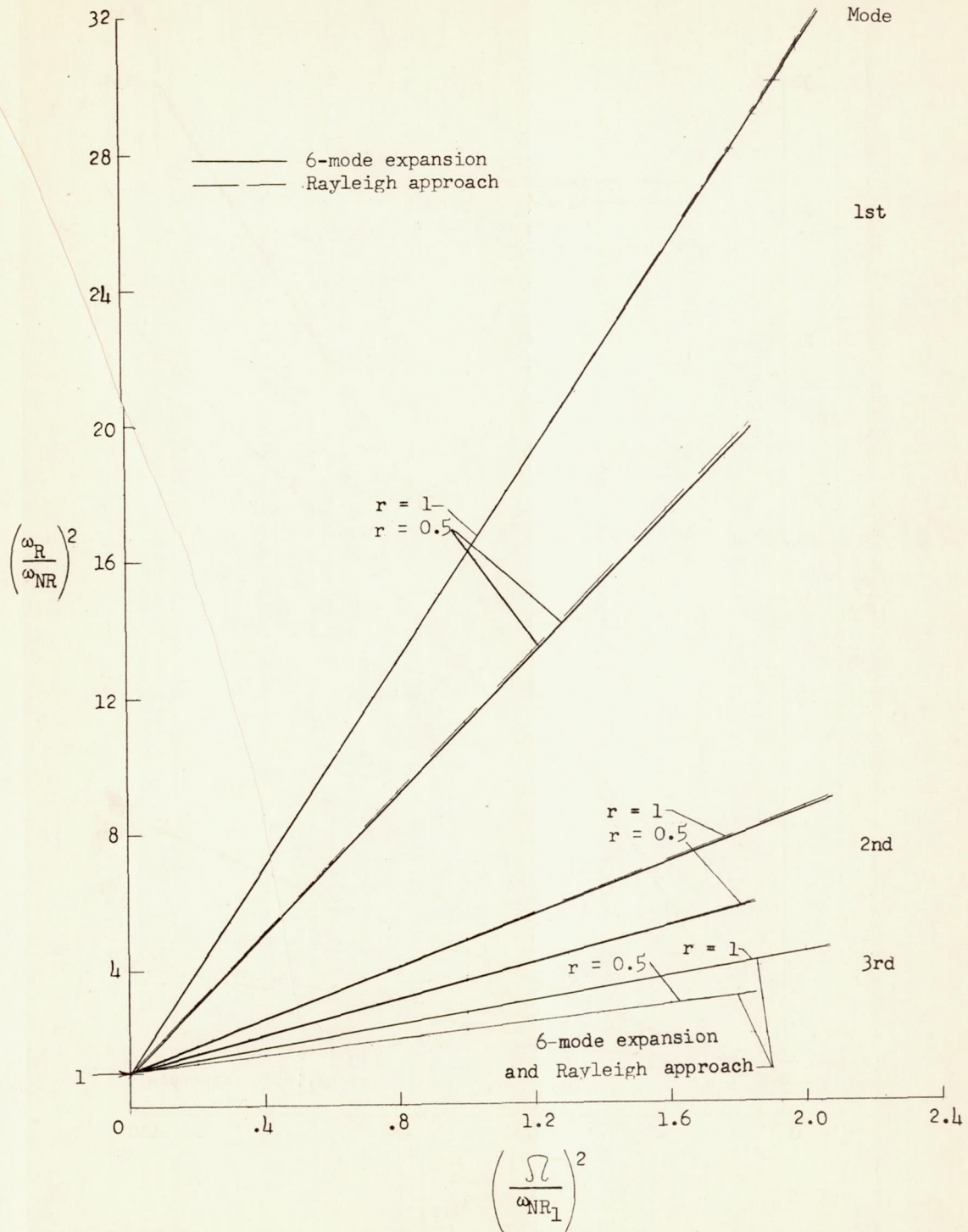
Figure 9.- Bending frequencies of a uniform hinged beam with a mass at the tip and with zero offset. $r = \dfrac{\text{Tip mass}}{\text{Beam mass}}$.
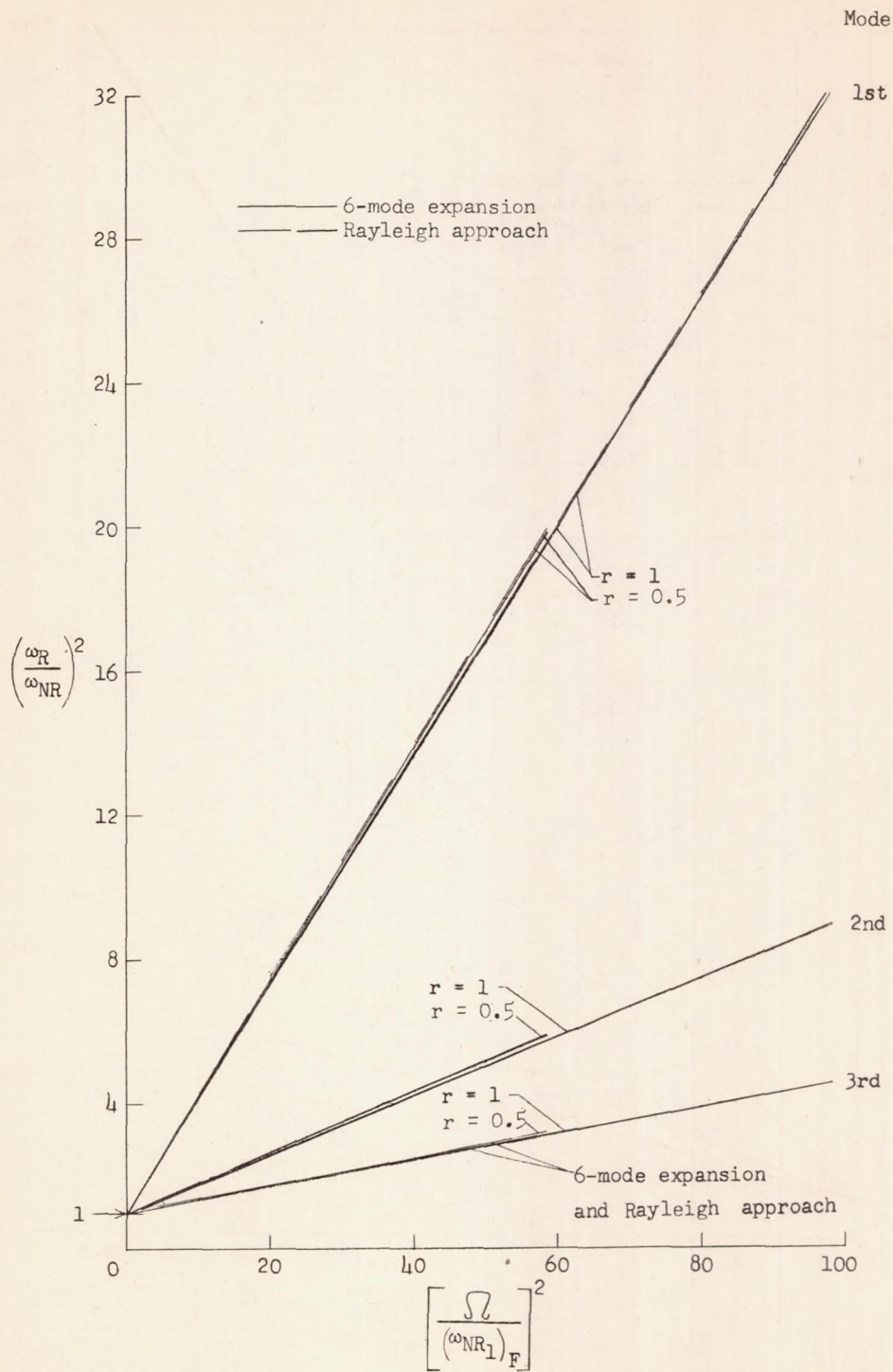
Figure 10.- Bending frequencies of a uniform hinged beam with a mass at the tip and with zero offset as a function of cantilever-beam rotational-speed parameter. $r = \dfrac{\text{Tip mass}}{\text{Beam mass}}$.
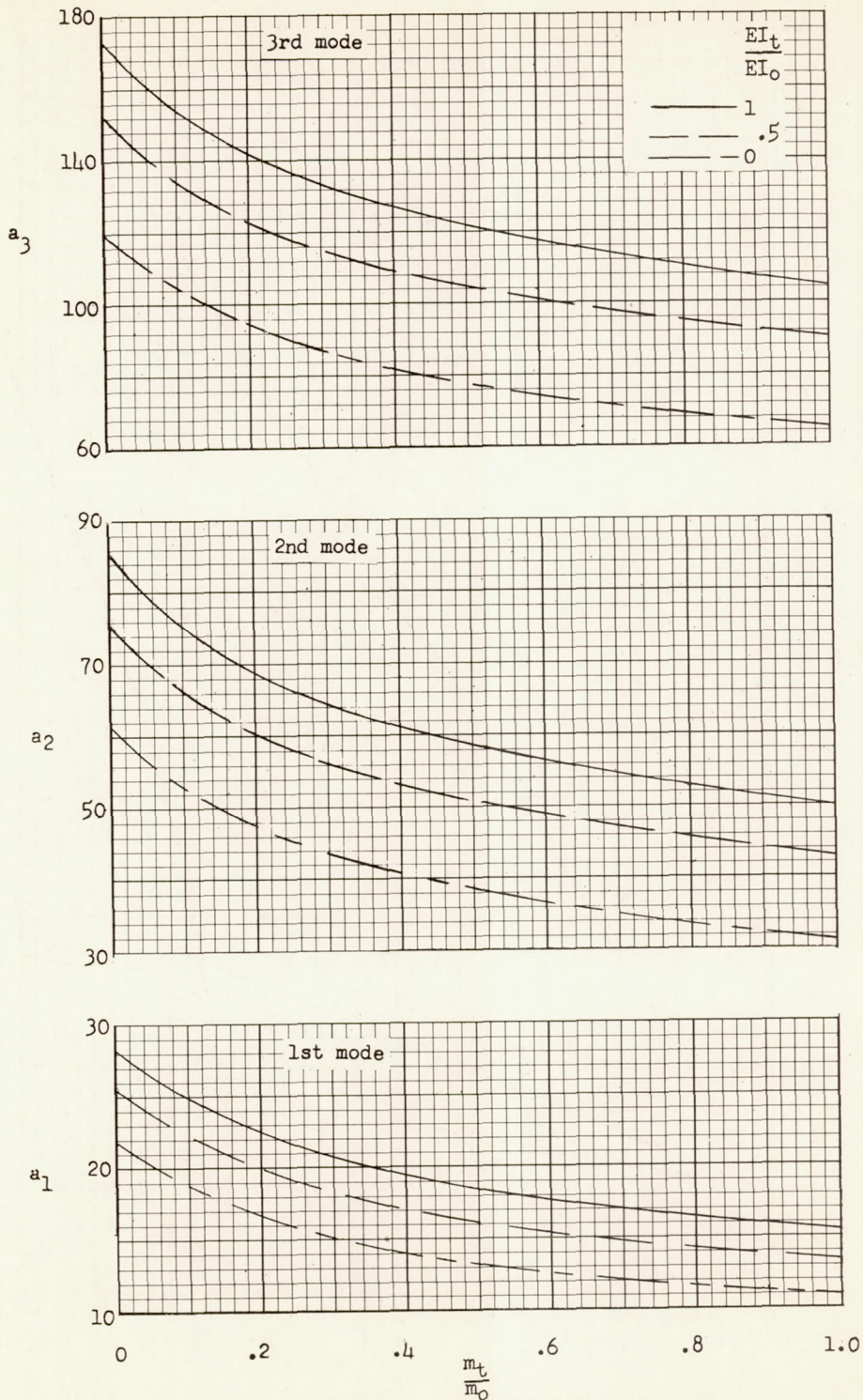
Figure 11.- Bending frequency coefficients a_n for hinged beams with linear mass and stiffness distributions.
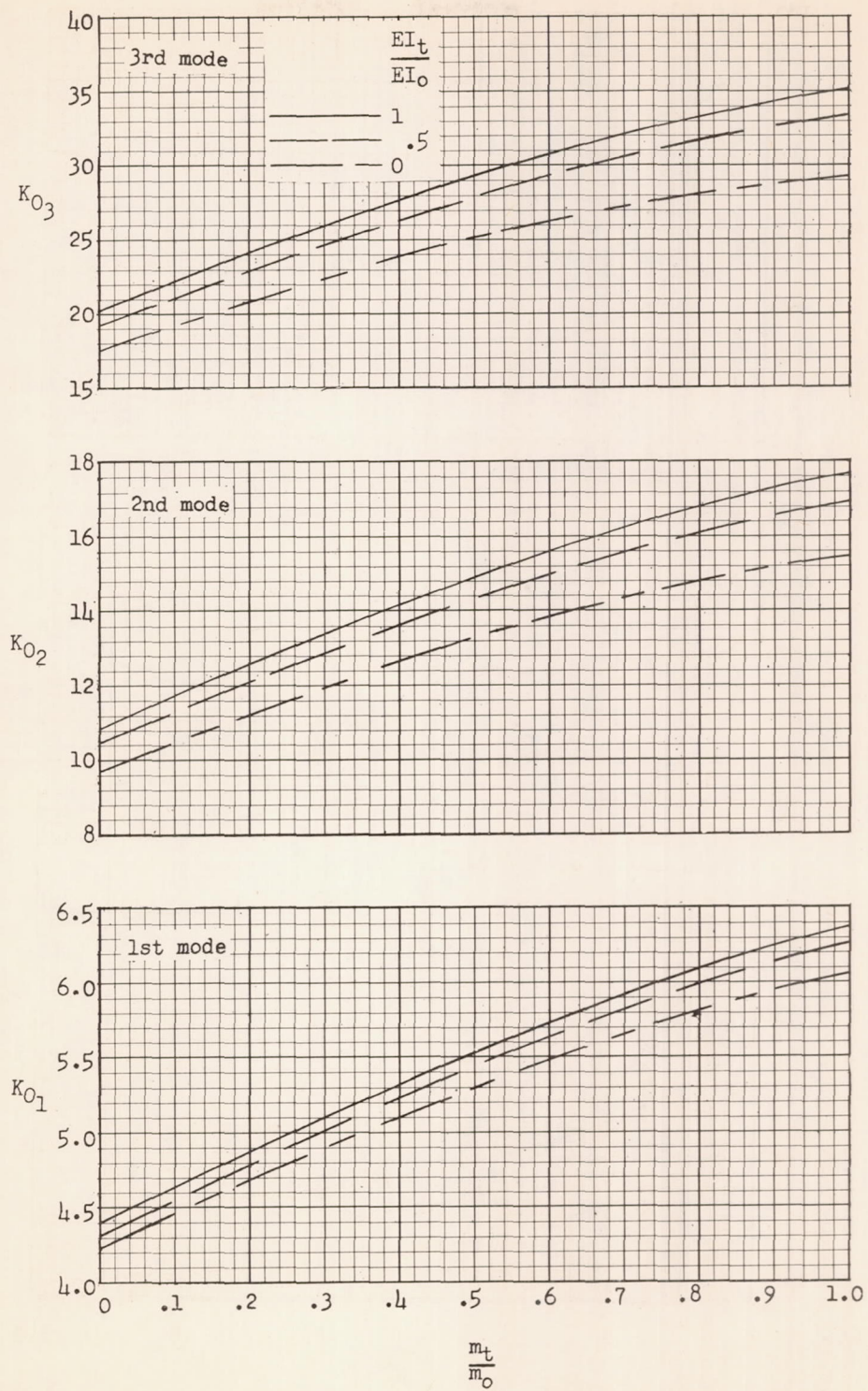
Figure 12.- Zero-offset Southwell coefficient K_{O_n} for hinged beams with linear mass and stiffness distributions.
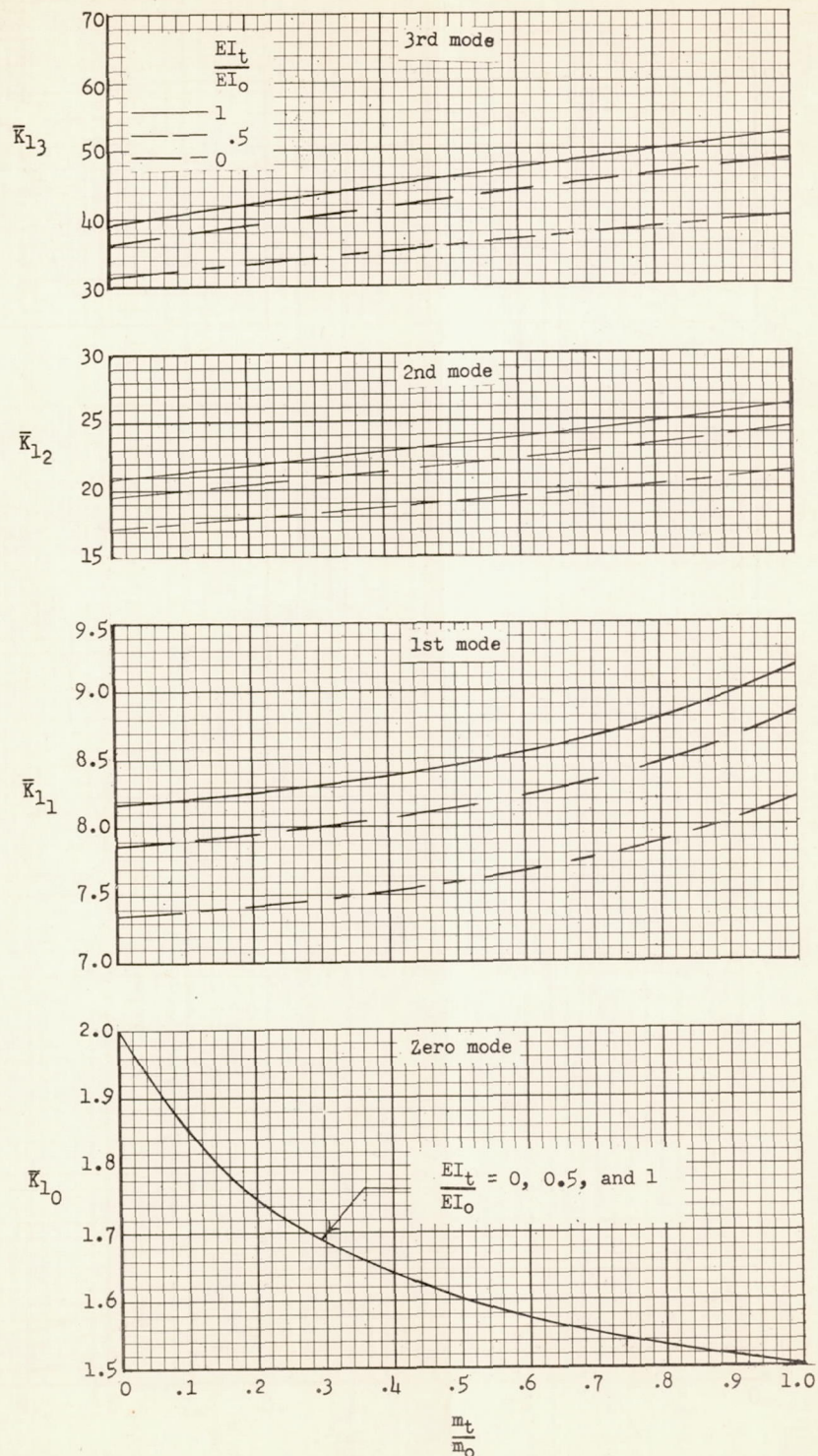
Figure 13.- Offset-correction factors for Southwell coefficients $\bar{K}_{1_n}$ for hinged beams with linear mass and stiffness distributions.
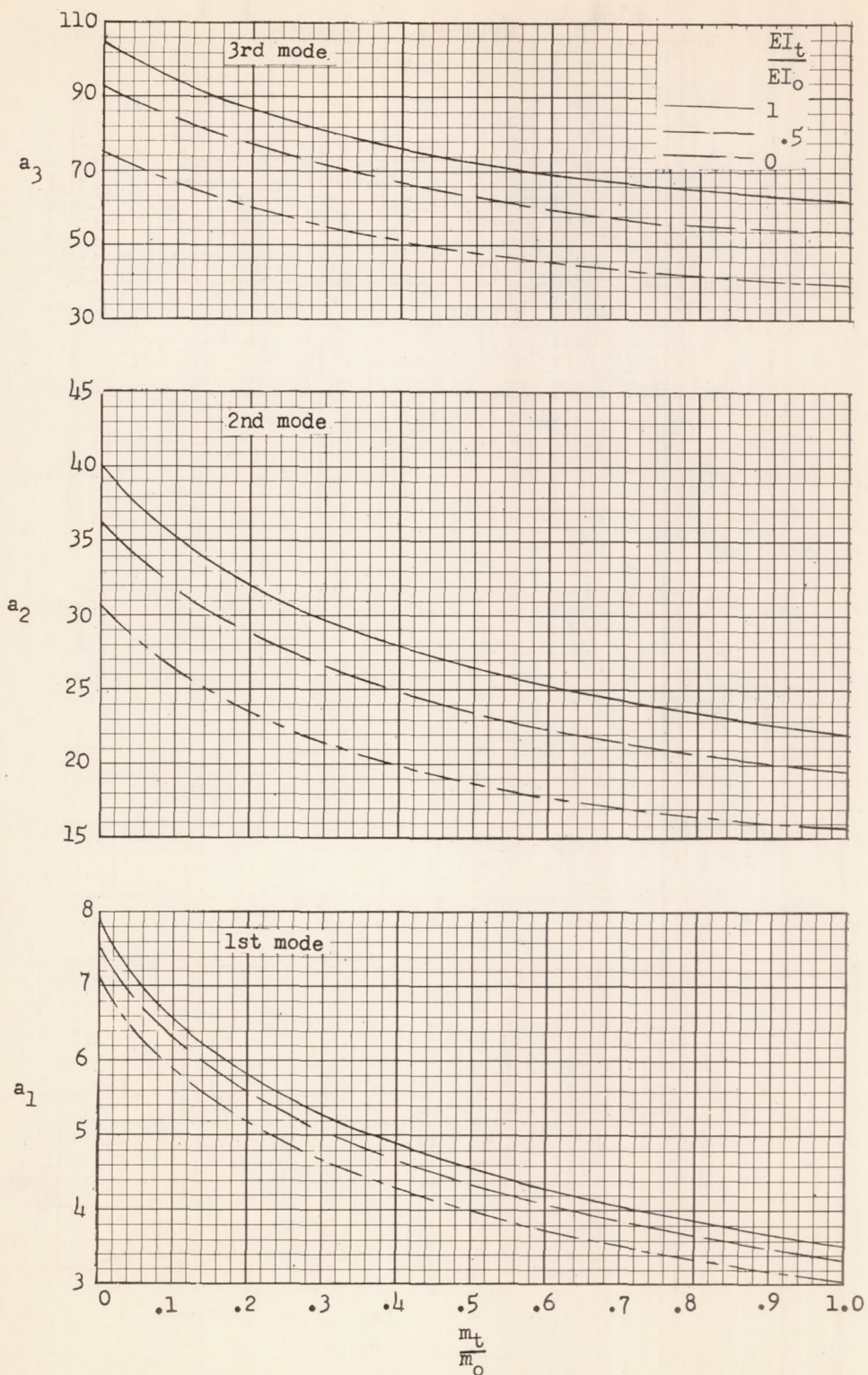
Figure 14.- Bending frequency coefficients a_n for cantilever beams with linear mass and stiffness distributions.
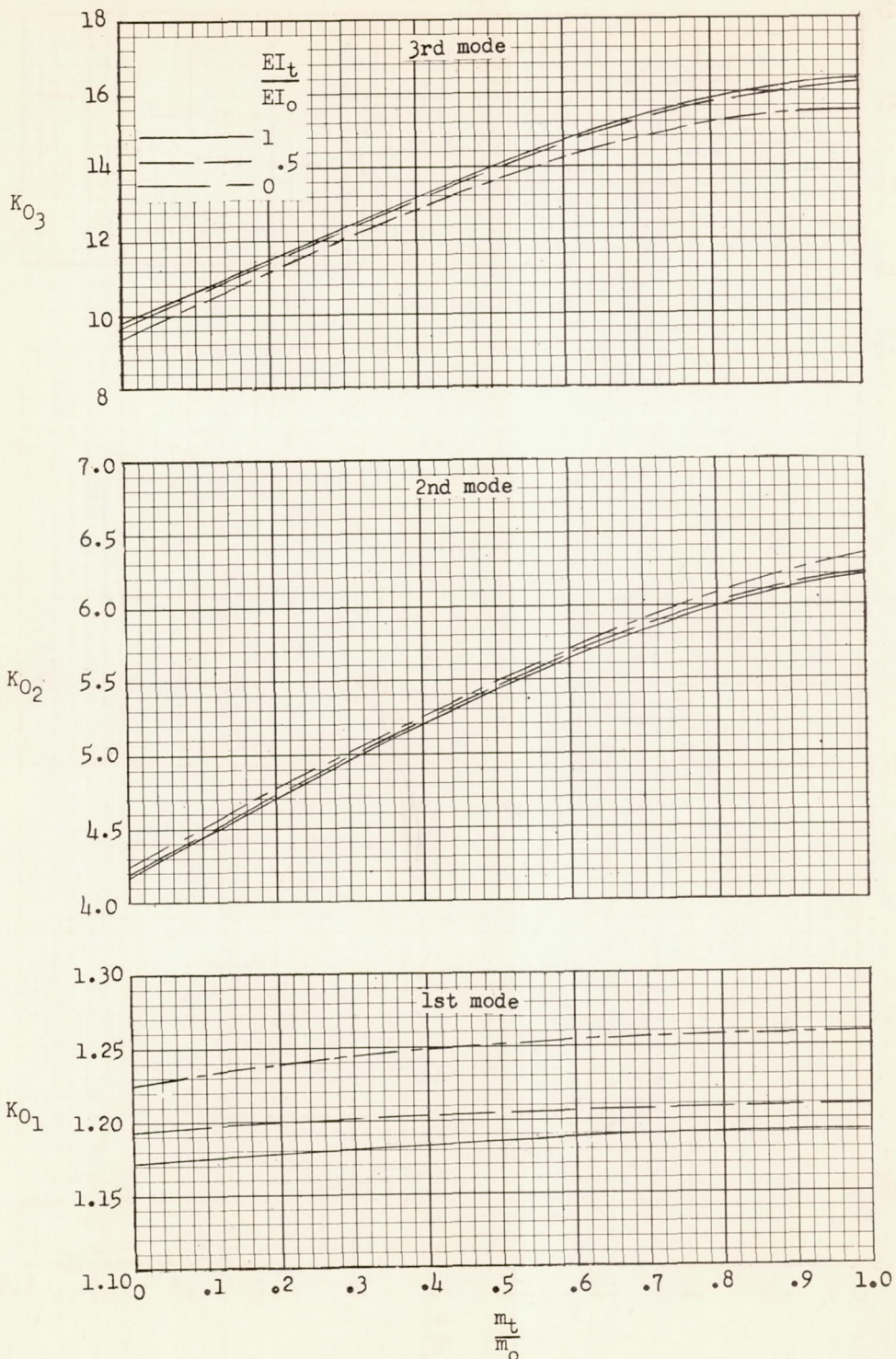
Figure 15.- Zero-offset Southwell coefficients K_{O_n} for cantilever beams
with linear mass and stiffness distributions.
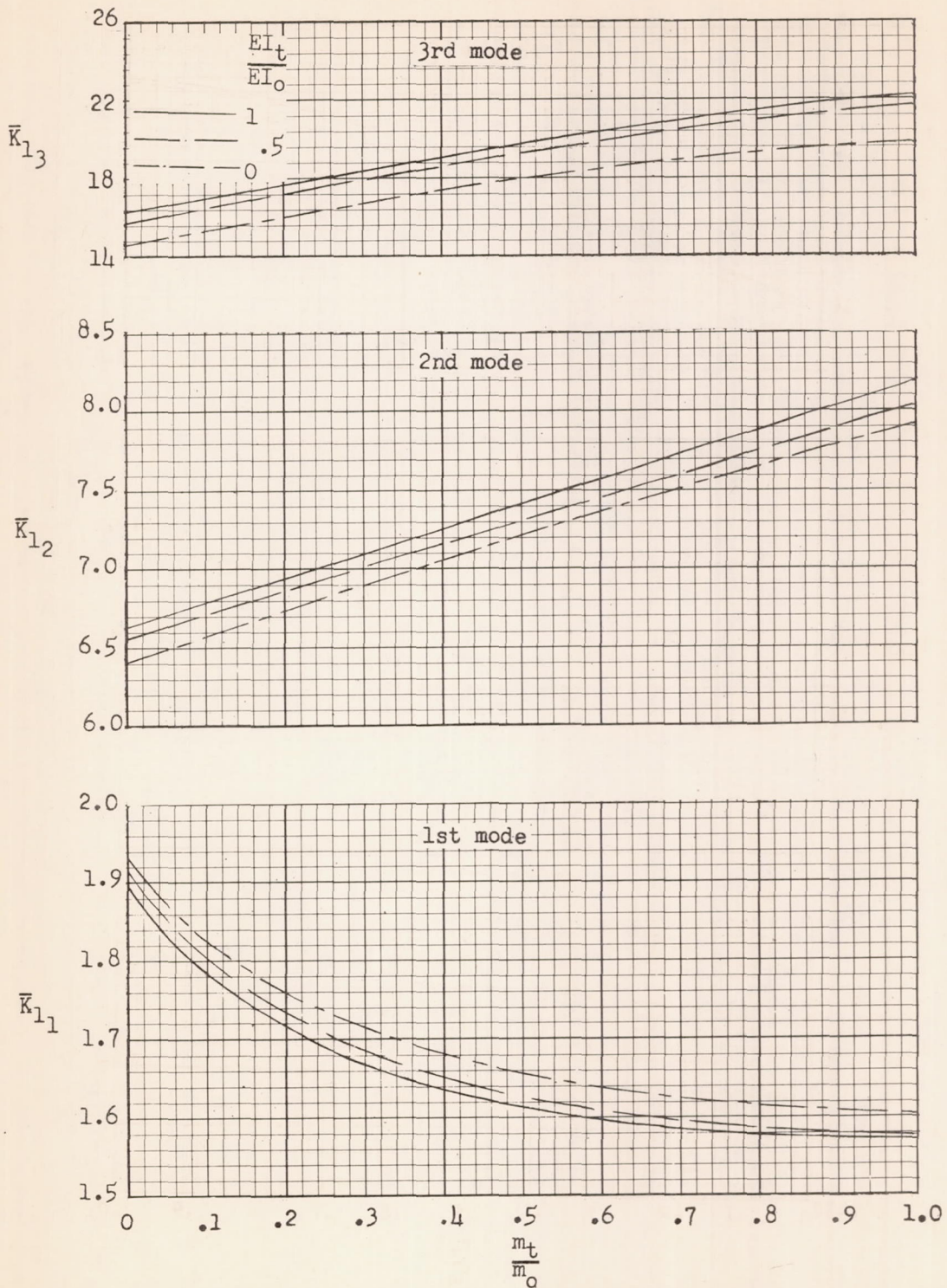
Figure 16.- Offset-correction factors for Southwell coefficients $\bar{K}_{l_n}$ for cantilever beams with linear mass and stiffness distributions.
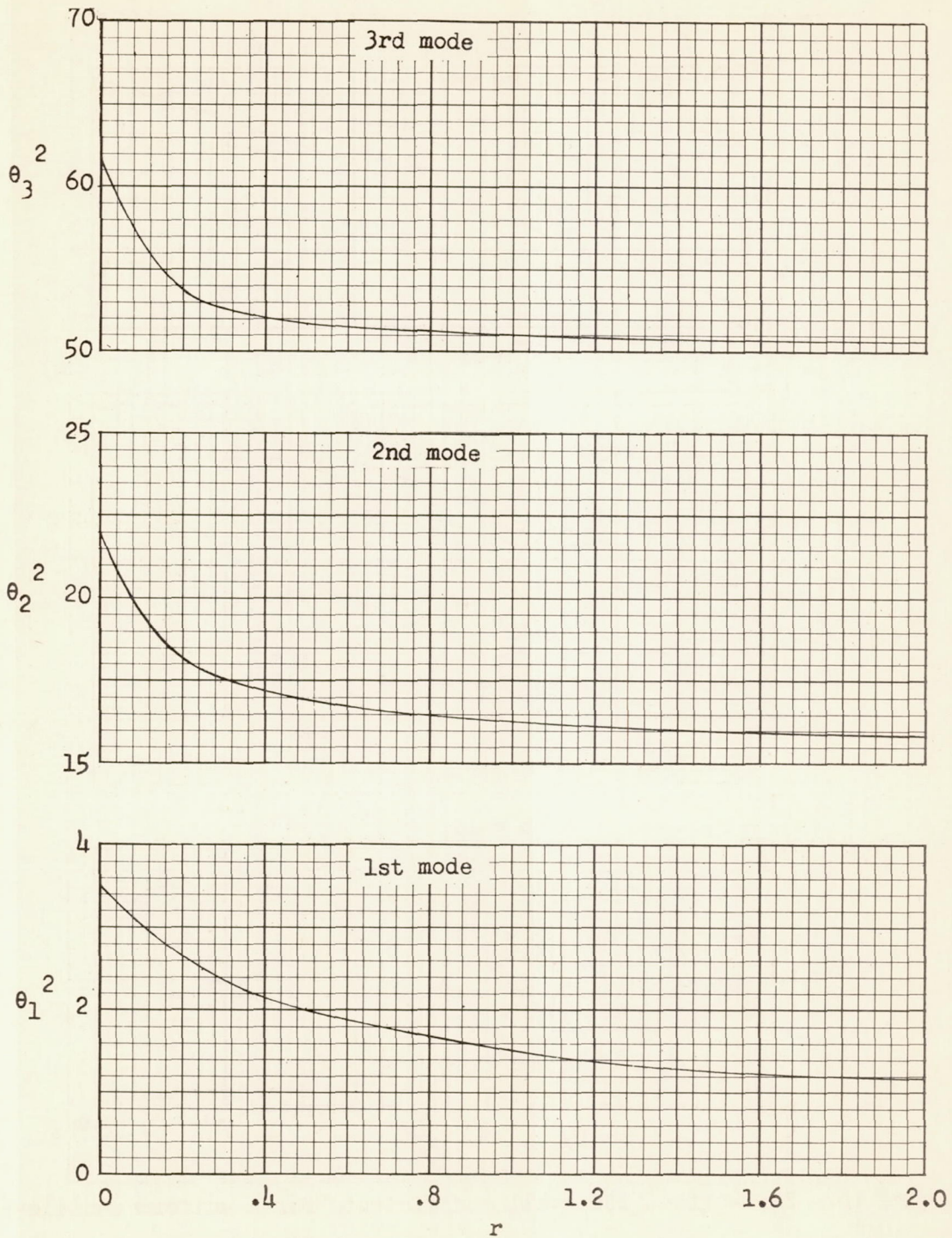
Figure 17.- Bending frequency coefficients for nonrotating uniform cantilever beams with a mass at the tip. $r = \dfrac{\text{Tip mass}}{\text{Beam mass}}$.
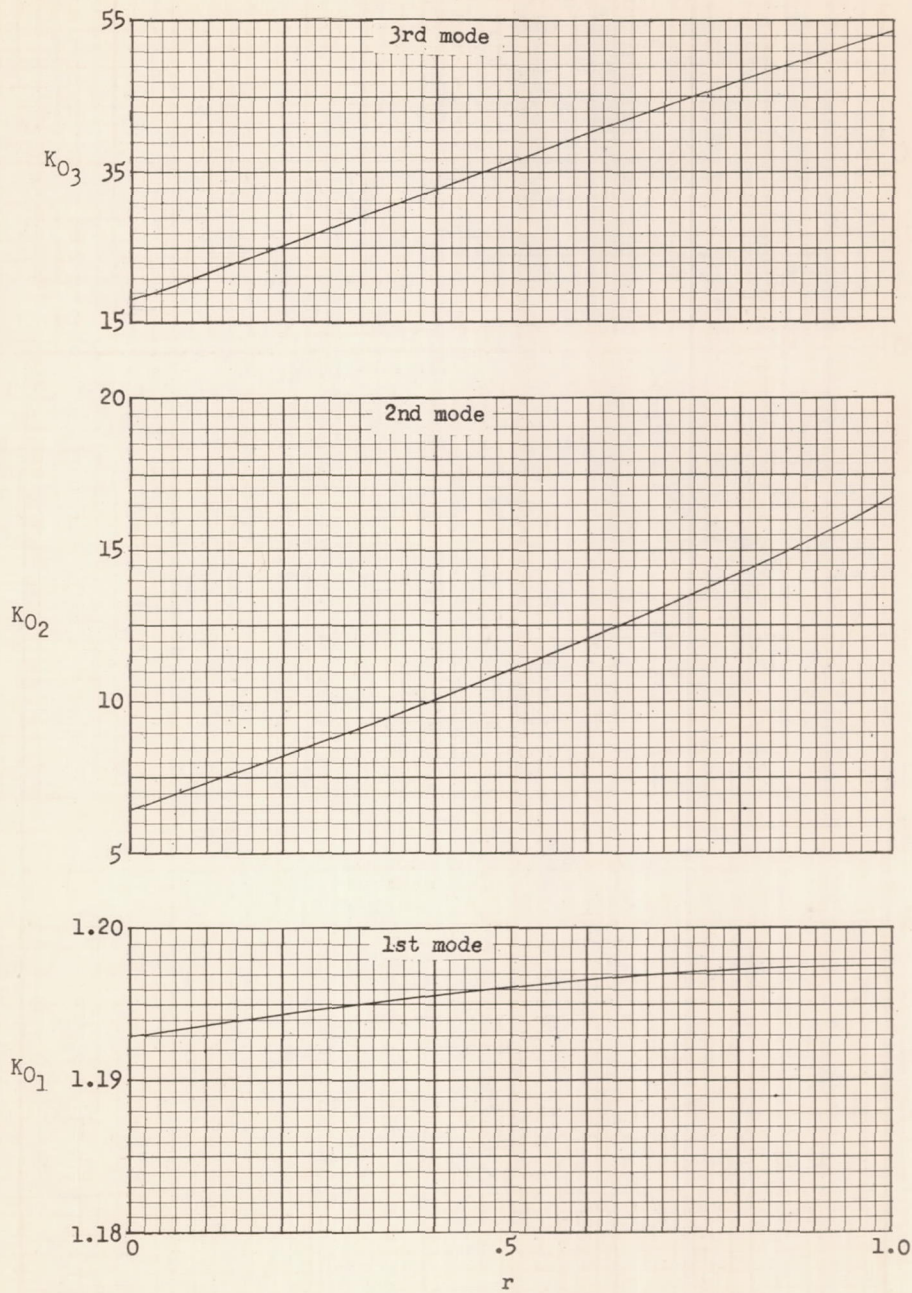
Figure 18.- Zero-offset Southwell coefficients for a uniform cantilever beam with a mass at the tip. $r = \dfrac{\text{Tip mass}}{\text{Beam mass}}$.
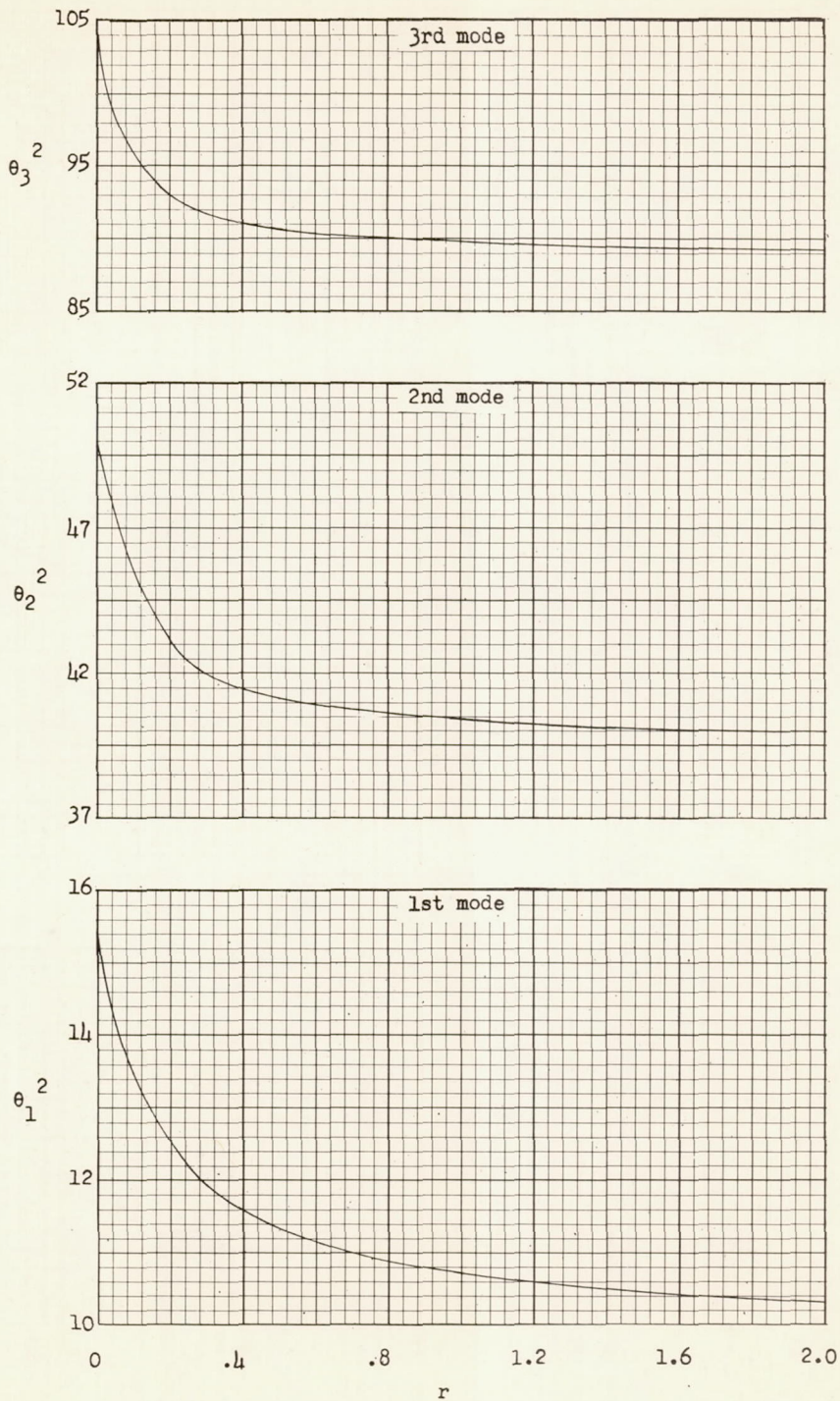
Figure 19.- Bending frequency coefficients for nonrotating uniform canti-
lever beams with a mass at the tip. $r = \dfrac{\text{Tip mass}}{\text{Beam mass}}$.
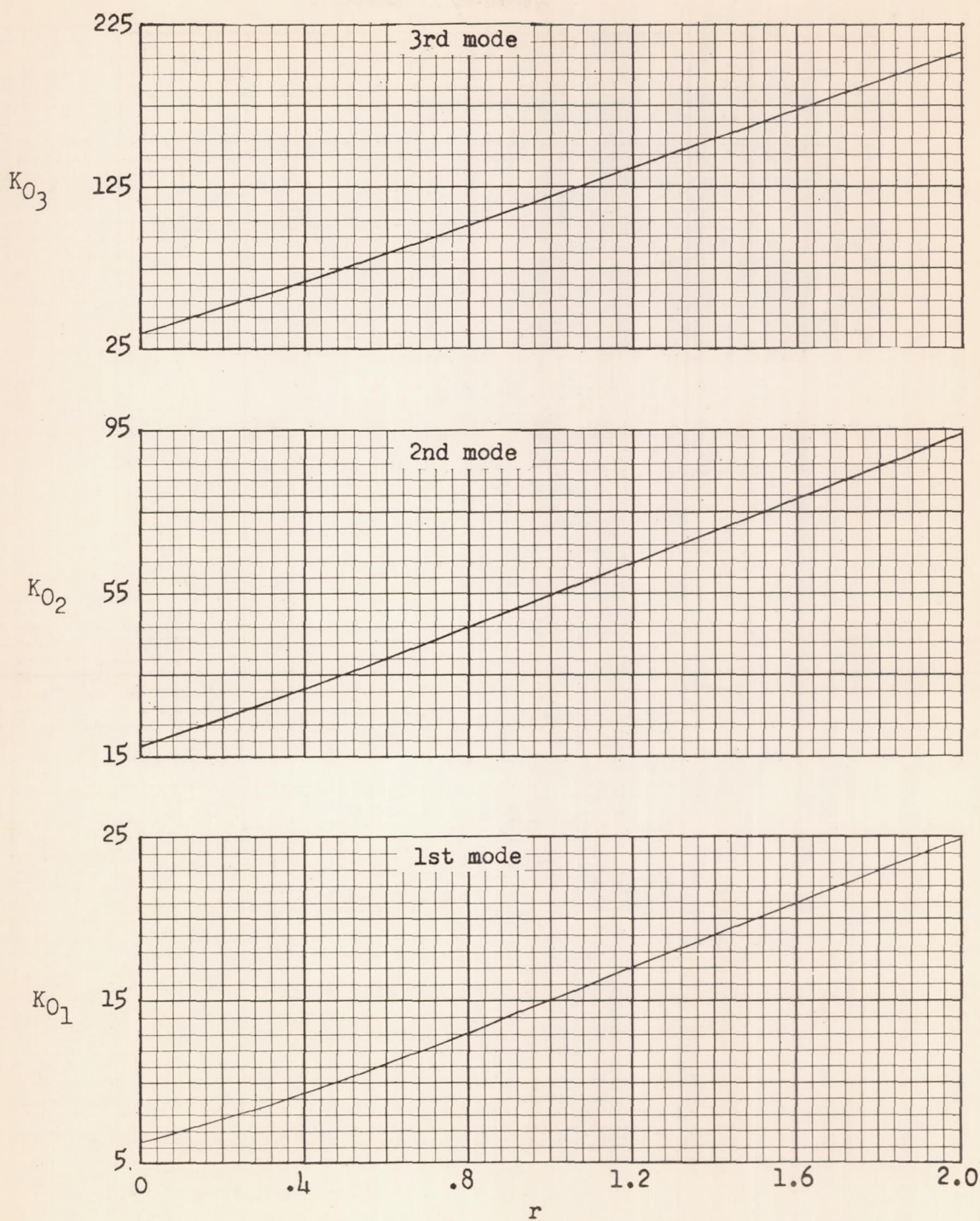
Figure 20.- Zero-offset Southwell coefficients for a uniform hinged beam with a mass at the tip. $r = \dfrac{\text{Tip mass}}{\text{Beam mass}}$.
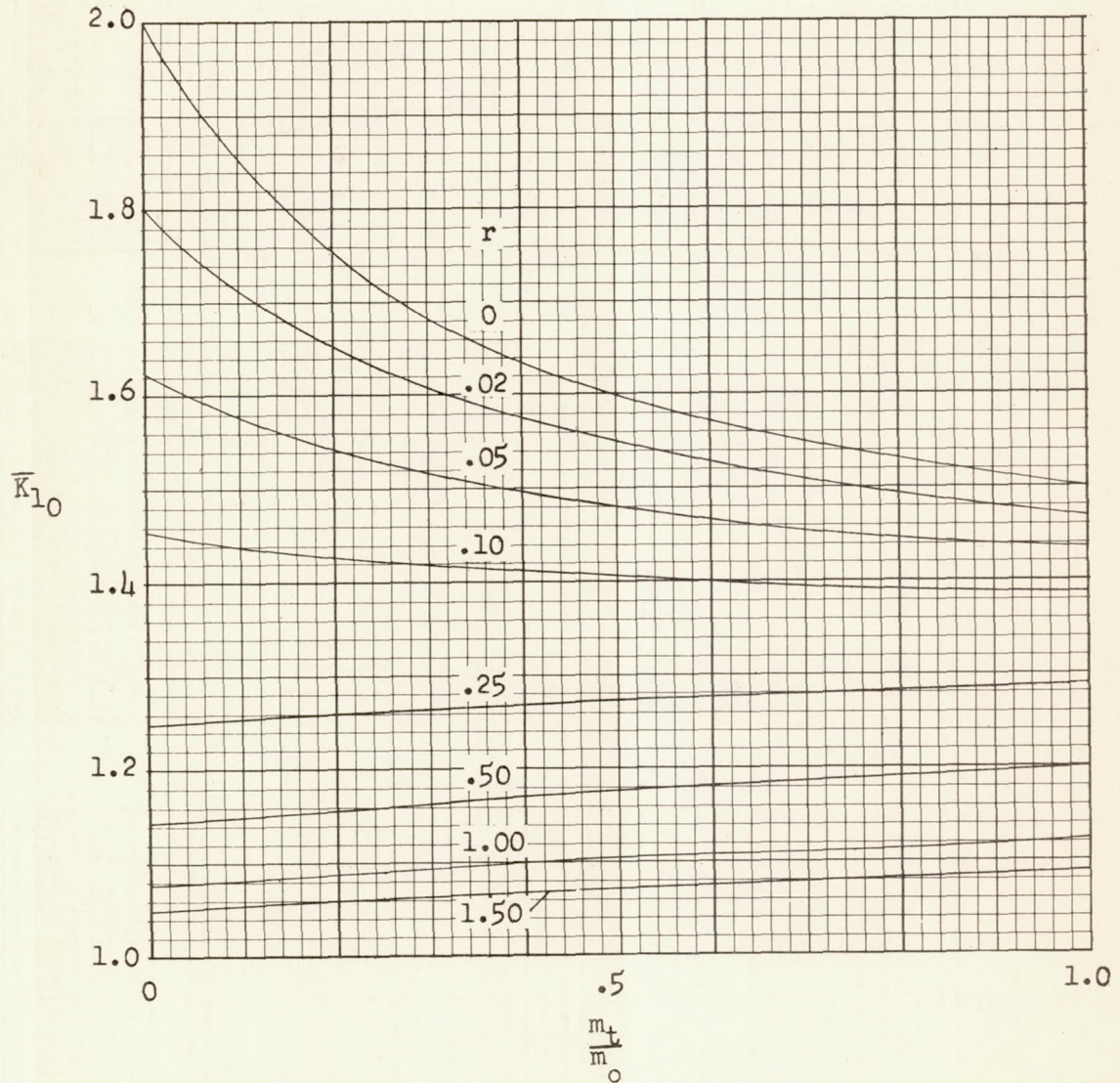
Figure 21.- Offset-correction factors for Southwell coefficients for the
pendulum mode of hinged beams with linear mass distribution plus a
mass at the tip.

3rd mode

$\frac{m_t}{m_o}$　　r

○　　1　　0
○○　1　　.5
○○　1　　1.0
△　　.5　　1.0
□　　0　　0

K_{03}'　.07

.05

.03

2nd mode

K_{02}'　.16

.12

.08

1st mode

K_{01}'　.5

.4

.3

0　　　　　　.5　　　　　　1.0

$\dfrac{EI_t}{EI_o}$
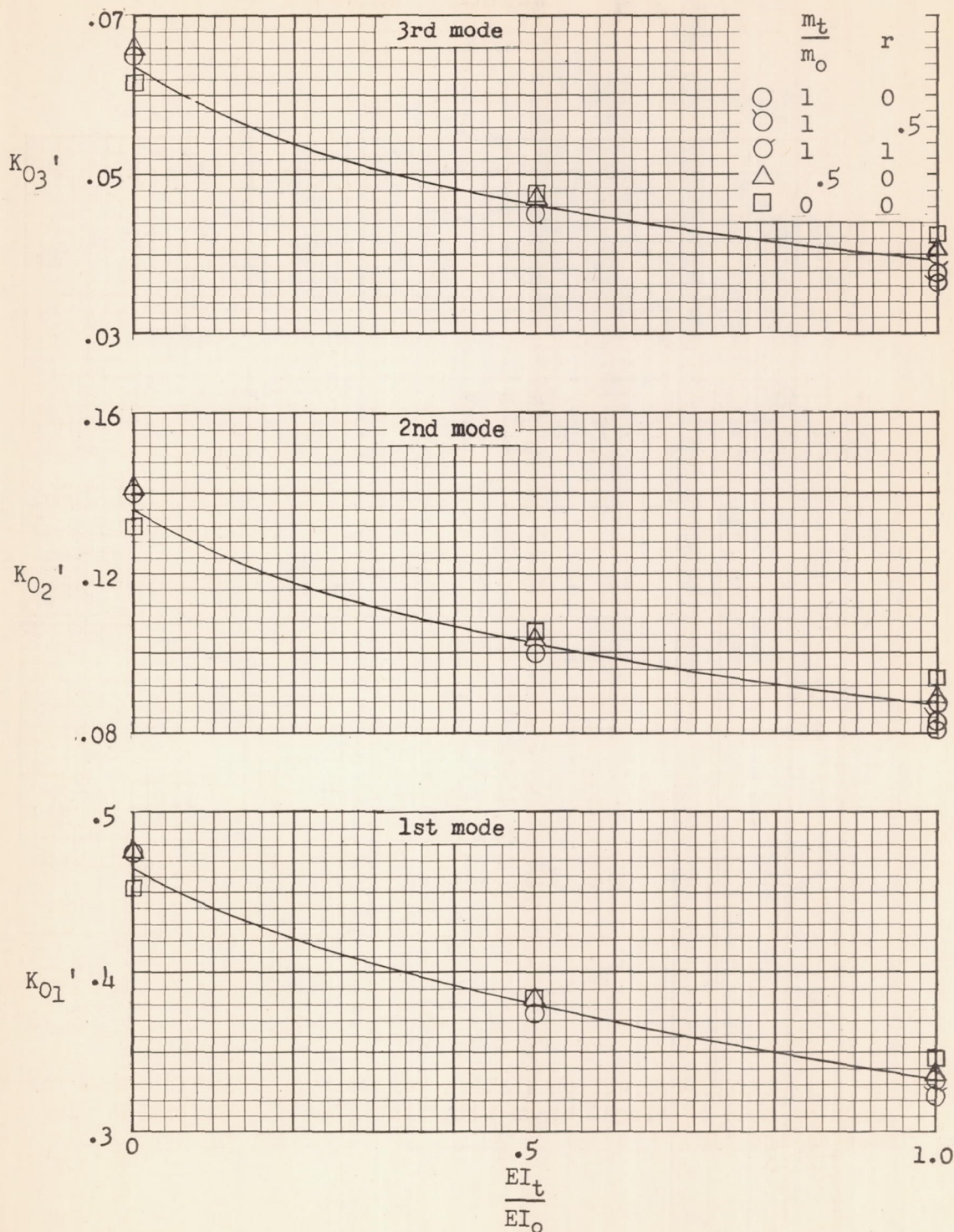
(a) Cantilever beams with linear stiffness distribution.

Figure 22.- A new rotating beam frequency coefficient which is essentially independent of beam mass distribution.
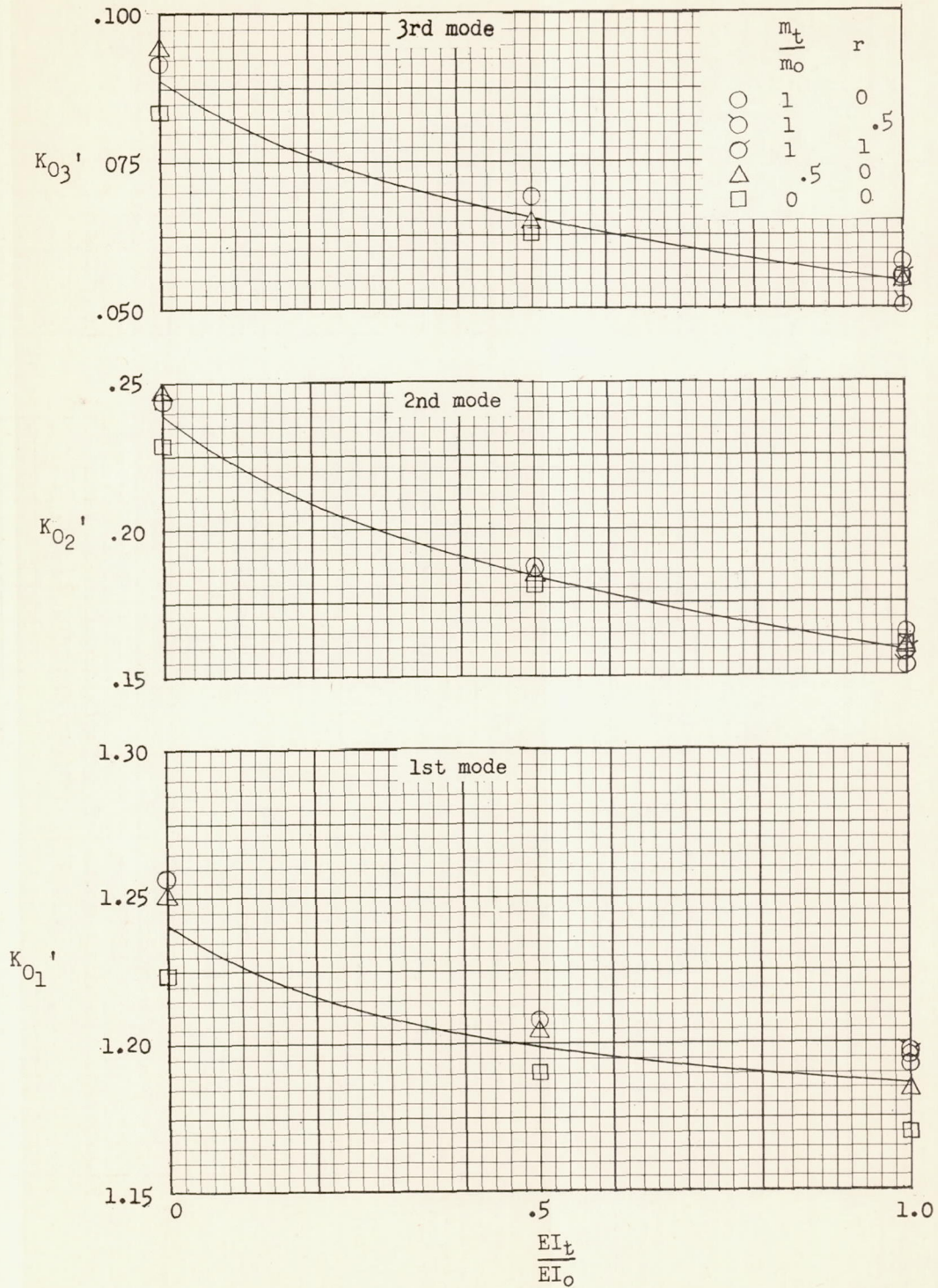
(b) Hinged beams with linear stiffness distribution.

Figure 22.- Concluded.
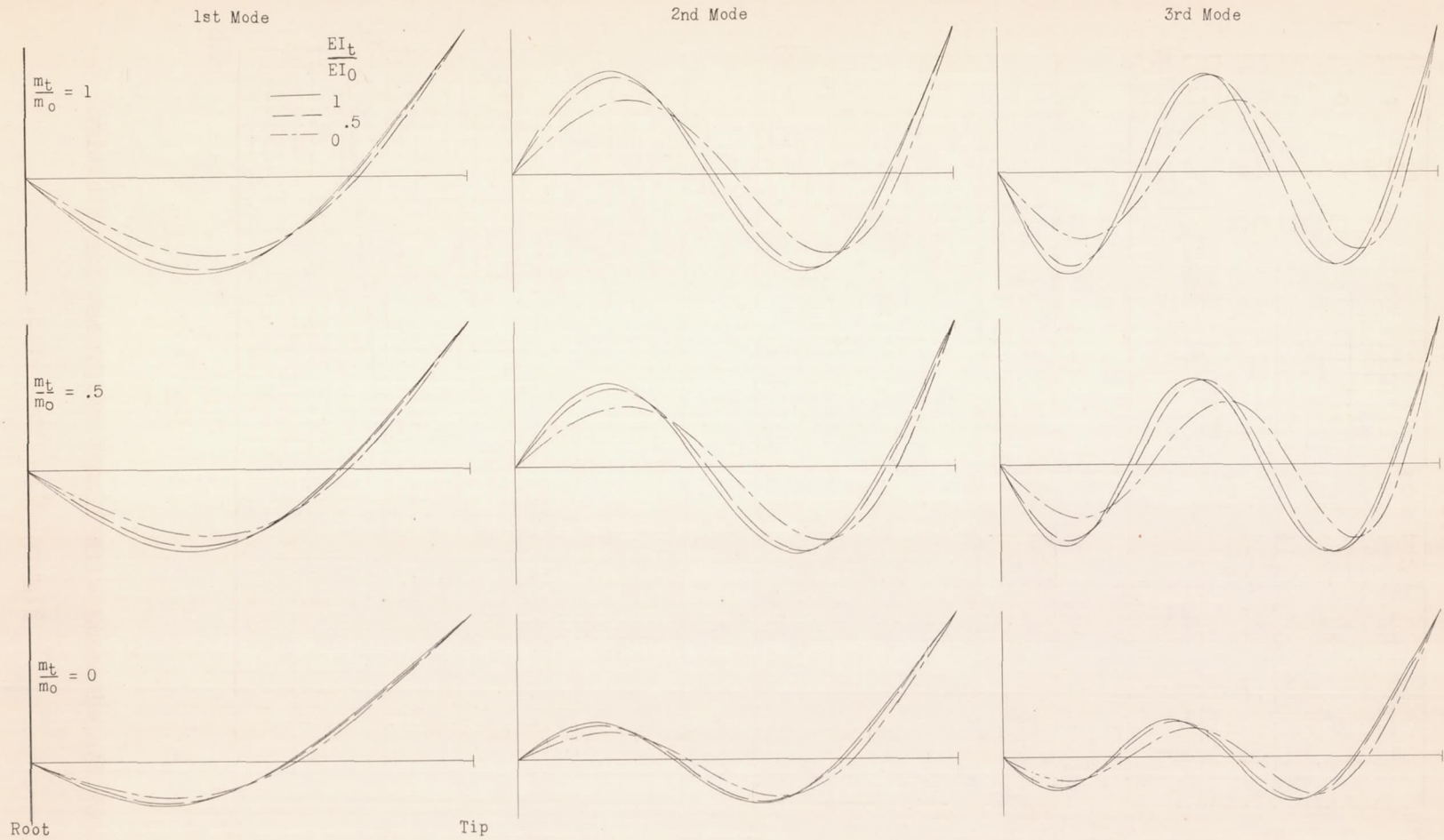
Figure 23.- Bending modes of nonrotating hinged beams with linear mass and stiffness distributions.
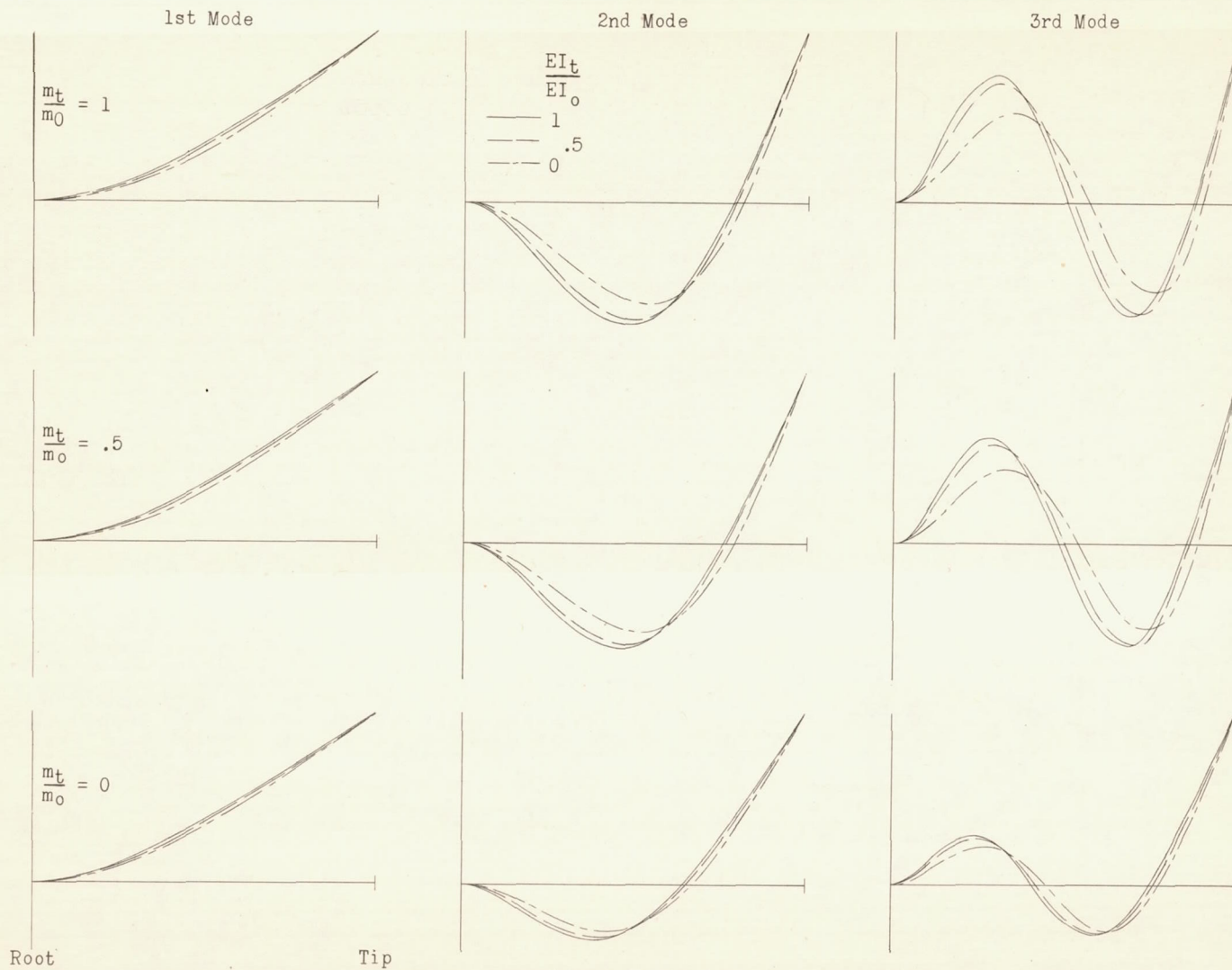
Figure 24.- Bending modes of nonrotating cantilever beams with linear
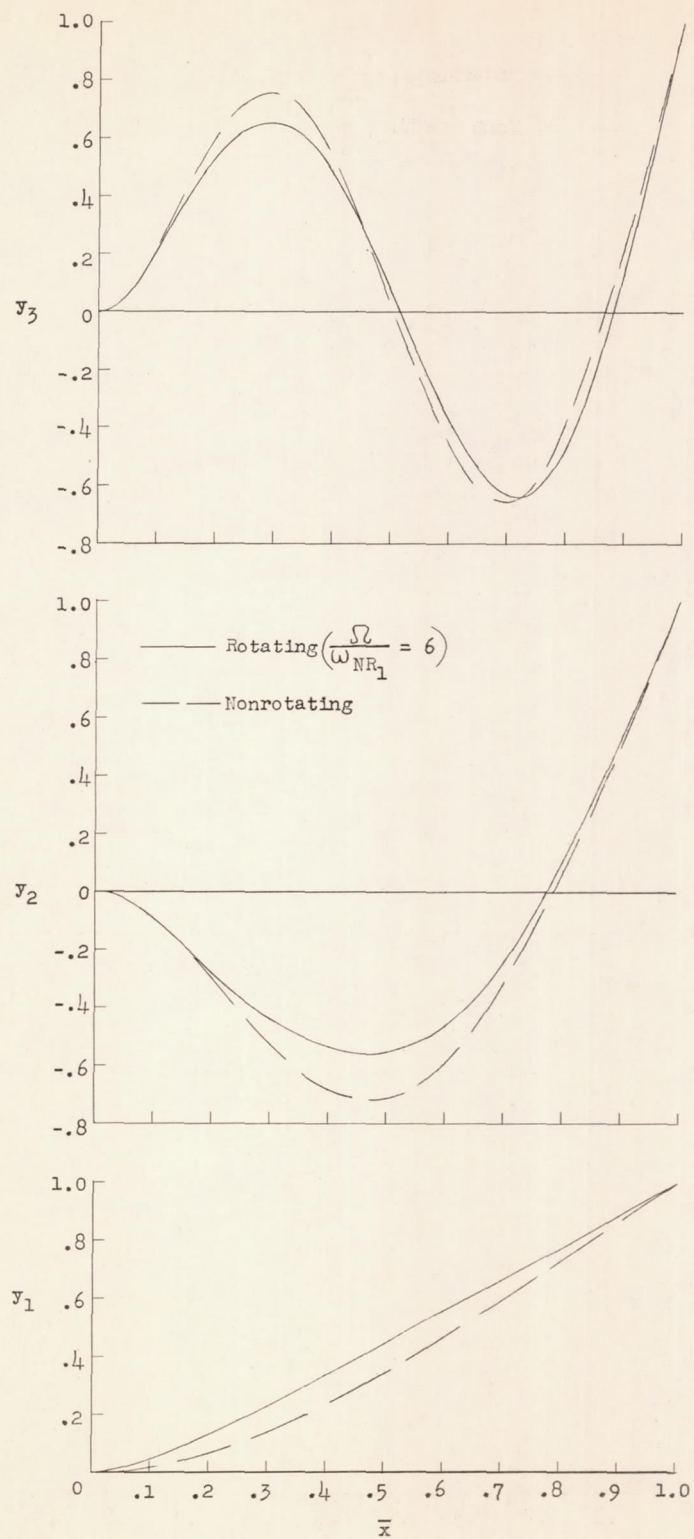mass and stiffness distributions.
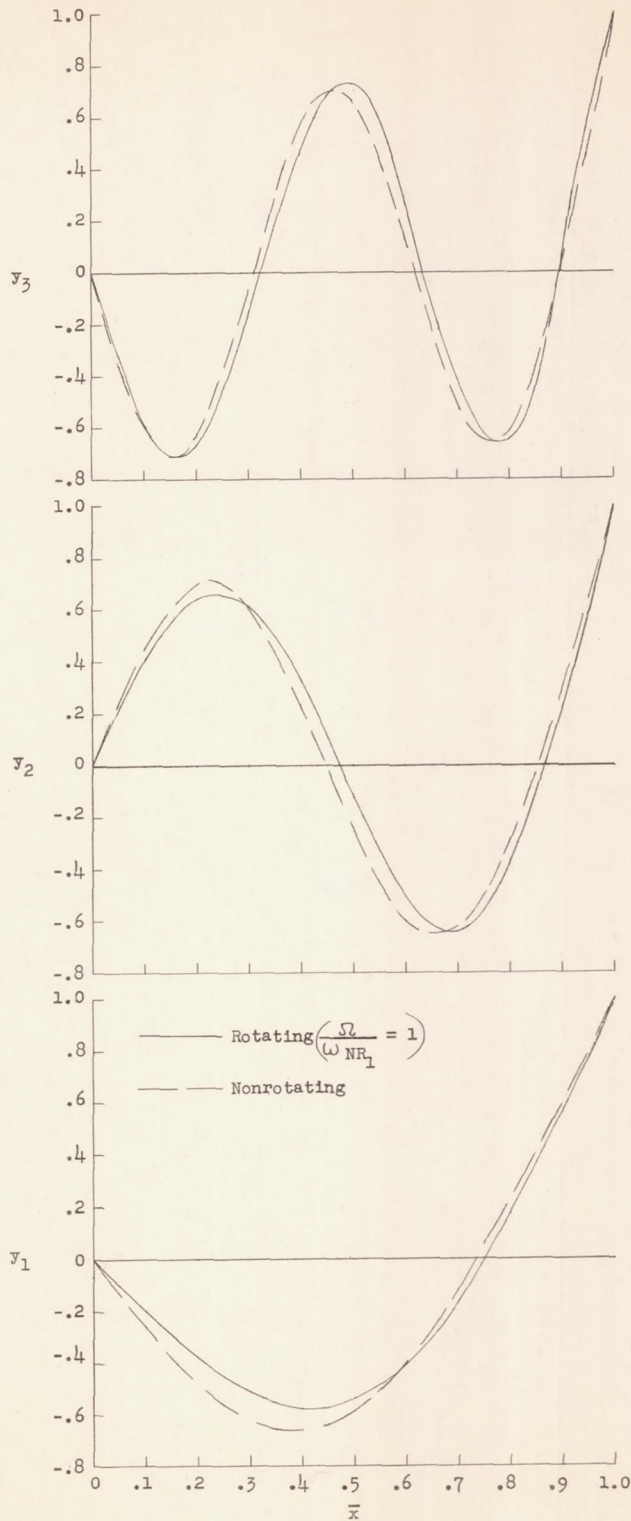
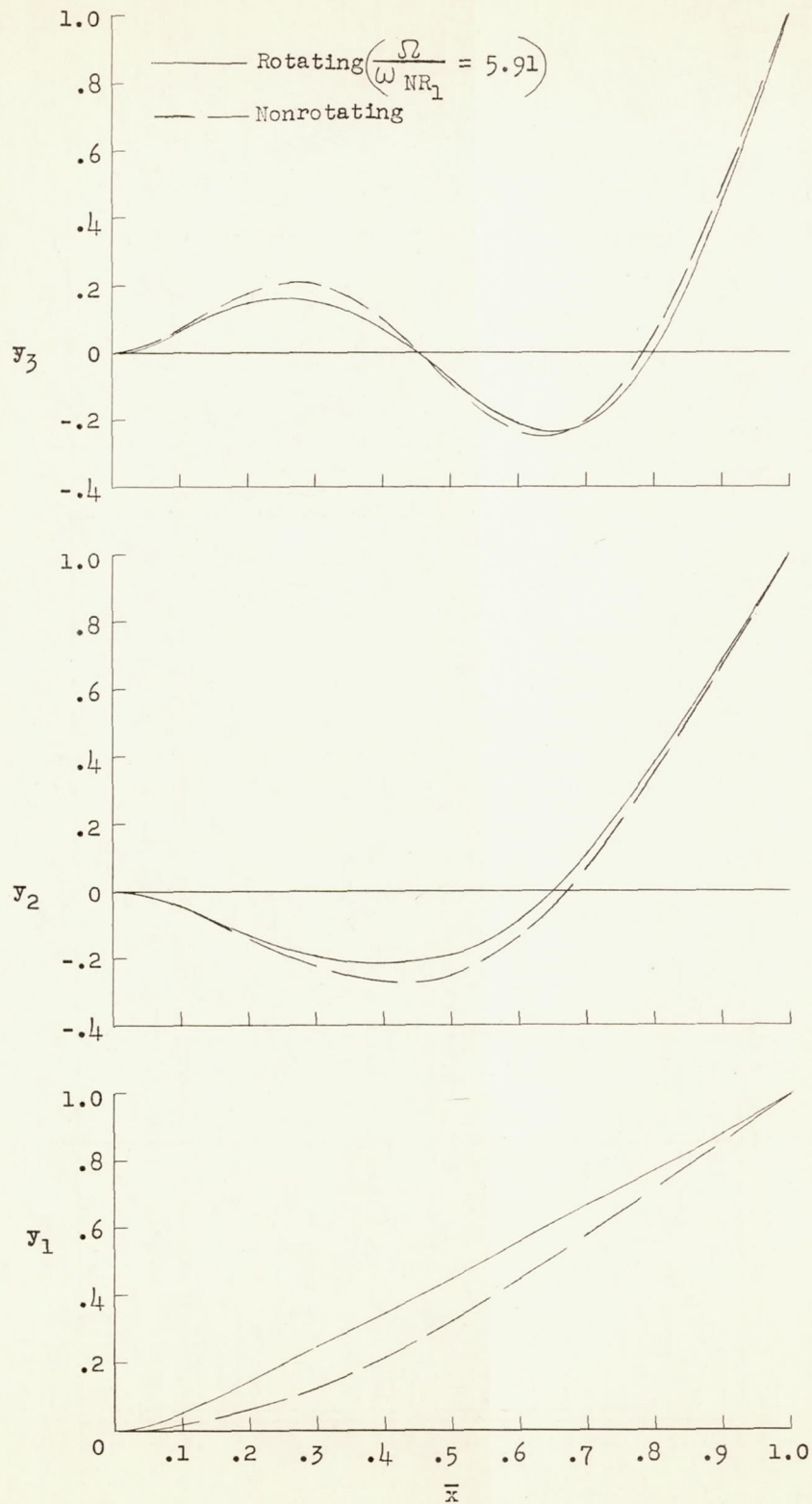Figure 25.- Comparison of bending modes of a rotating and nonrotating uniform hinged beam.
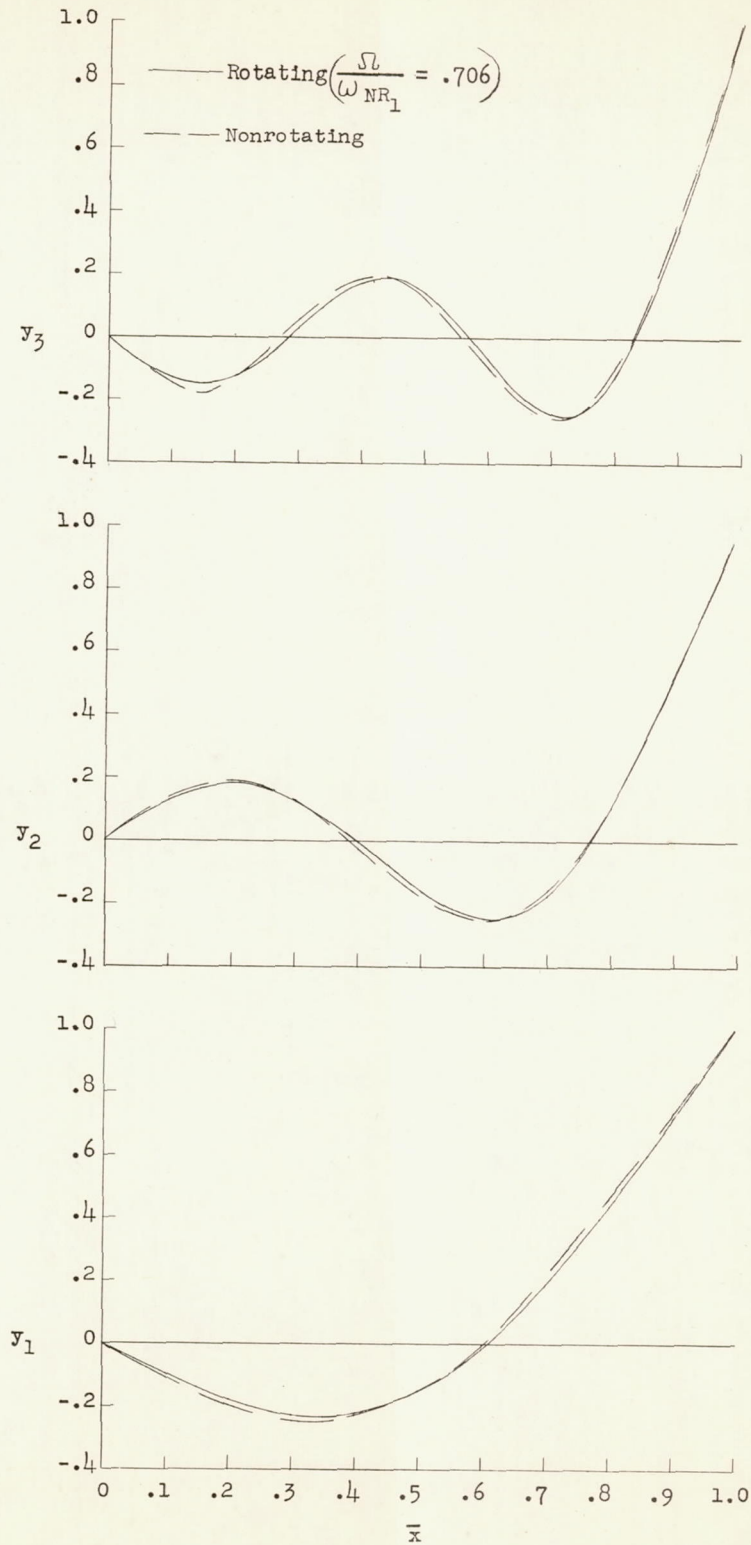
Figure 26.- Comparison of bending modes for a rotating and nonrotating
hinged beam with linear mass and stiffness distribution.

Figure 27.- Comparison of bending modes of a rotating and nonrotating uniform cantilever beam.

Figure 28.- Comparison of bending modes of a rotating and nonrotating cantilever beam with linear mass and stiffness distribution.
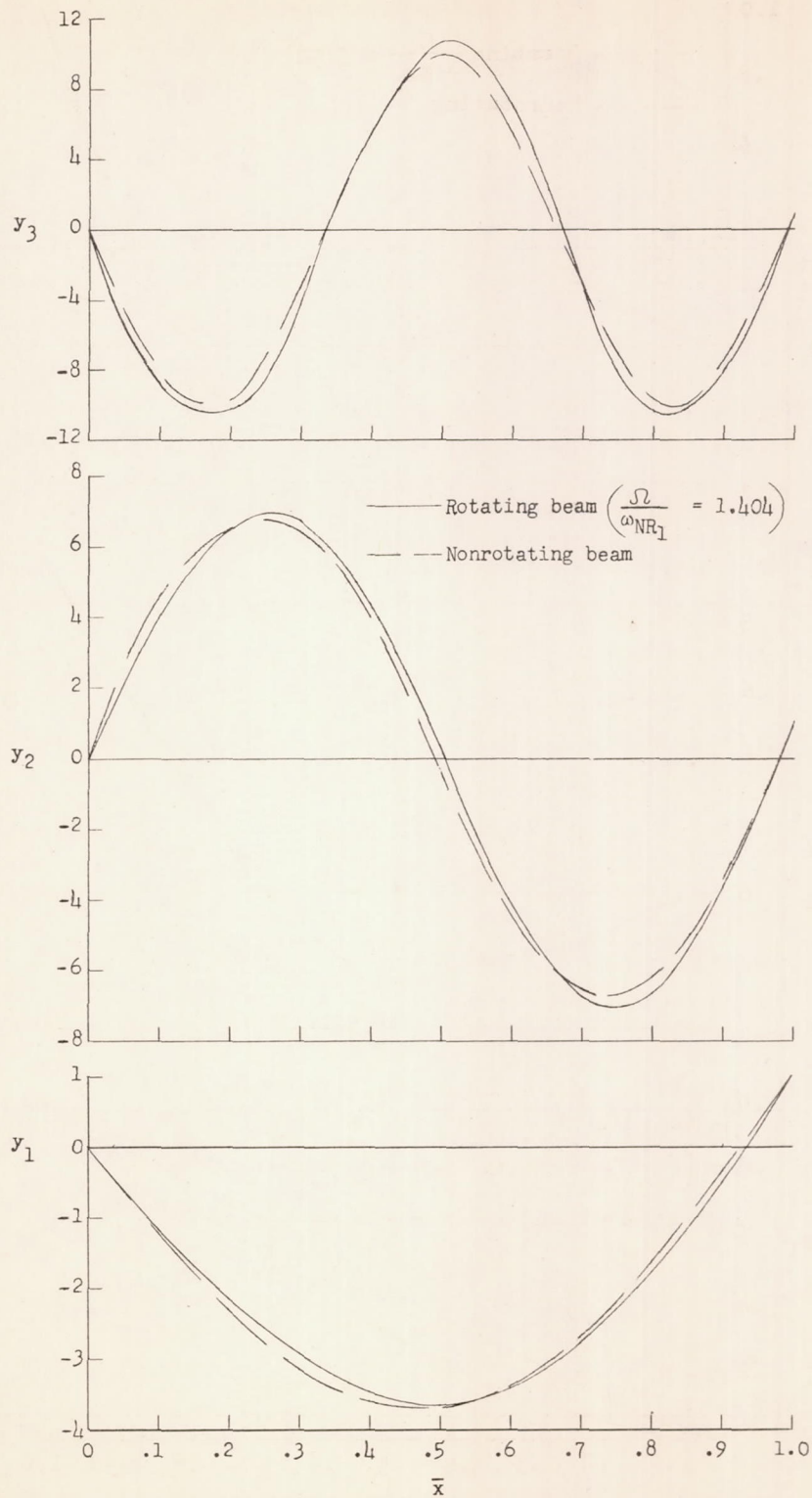
Figure 29.- Comparison of bending modes of a rotating and nonrotating
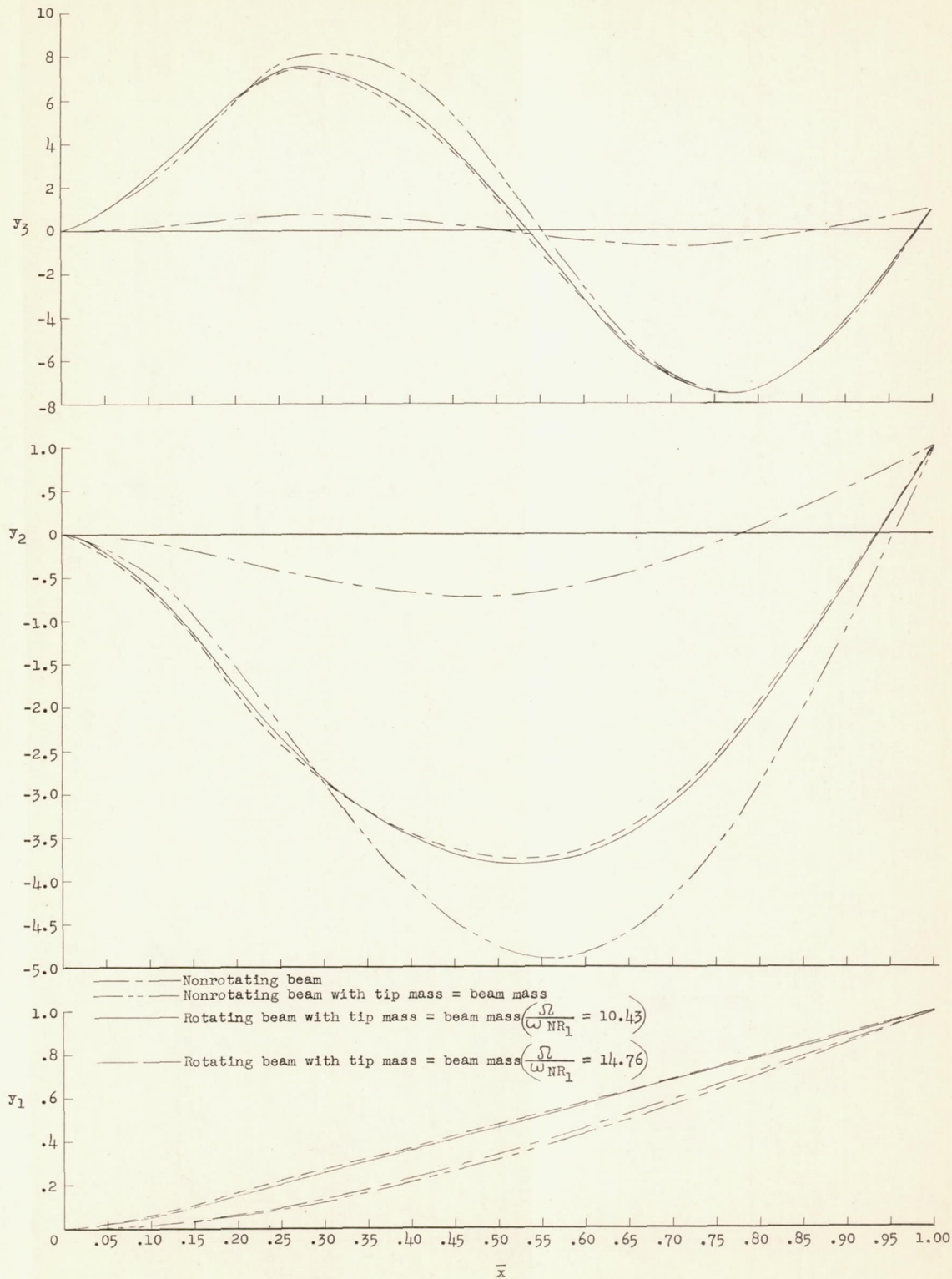uniform hinged beam with a tip mass equal to the mass of the beam.

Figure 30.- Comparison of bending modes of a rotating and nonrotating uniform cantilever beam with a mass at the tip.